

**Experimental investigation and theoretical analysis on the
effects of nanolayer on nanofluids' thermo-physical
properties**

by

Saboura Yousefiaboksari

Submitted in partial fulfilment of the requirements for the degree

MSc (Applied Science) Mechanical Engineering

in the

Faculty of Engineering, Built Environment and Information Technology

University of Pretoria

2016

ABSTRACT

Title: Experimental investigation and theoretical analysis on the effects of nanolayer on nanofluids' thermo-physical properties

Student: Saboura Yousefiaboksari

Supervisors: Dr Mohsen Sharifpur and Prof Josua P Meyer

Department: Mechanical and Aeronautical Engineering

University: University of Pretoria

Degree: Master of Science

Nanofluids, which are suspensions of nanoparticles in conventional heat transfer fluids, attracted research studies on different heat transfer applications, while they enhance thermal transport properties in comparison with conventional base fluids.

Recently, the use of these new fluids has been growing increasingly. However, the ambiguities of their thermo-physical properties cause them to function inefficiently in industrial design. The recognised important parameters that affect the properties of nanofluids include the volume fraction of the nanoparticles, temperature, nanoparticle size, nanolayer, thermal conductivity of the base fluid, pH of the nanofluid and the thermal conductivity of the nanoparticles. However, there is a distinct lack of investigation and reported research on the nanolayer and its properties.

In this study, the effect of uncertainty of the nanolayer properties on the effective thermal conductivity and viscosity of nanofluids, and heat transfer are discussed in detail. The results show that the uncertainties can cause 20% error in the calculation of the Nusselt number and 24% for the Reynolds number. Therefore, more research needs to be conducted on nanolayer properties in order to identify them accurately.

The density of some nanofluids, such as SiO₂-water, SiO_x-EG-water, CuO-glycerol and MgO-glycerol, has also been investigated experimentally. Therefore, the effects of nanolayer thickness and density on nanofluid properties are discussed in detail. The results show that nanolayer density and thickness have a significant effect on nanofluid

density, and nanolayer density is found to be between void and base fluid density. Consequently, by analysing experimental results and performing a theoretical analysis, a model has been derived to calculate the density of nanofluids.

Specific heat capacity is the other nanofluid property that is discussed in this study. Experimental data from literature, available formulae and the presented model for nanofluid density have been used to identify nanofluid-specific heat capacity, while nanofluid density is one of the parameters in calculating specific heat capacity. This investigation was performed using a model – used by different authors – that also considers the nanolayer. The specific heat capacity of nanofluids that resulted from two methods of calculation has been compared with available experimental data. This investigation shows that the proposed model for the density of nanofluids provides better agreement for specific heat capacity in comparison to experimental data.

Keywords: *Nanofluids, nanoparticle, nanolayer, thermal conductivity, viscosity, specific heat capacity*

DEDICATION

To my husband, Danial Tanhaemami, and
my parents, Freshteh and Mohammadreza Yousefi

ACKNOWLEDGEMENTS

I would like to sincerely thank my advisor, Dr Mohsen Sharifpur, for his continuous support, understanding, immense knowledge and patience during my master's degree study at the University of Pretoria. His guidance helped me throughout the process of conducting research and writing this dissertation. It has been a privilege to work with him.

Besides my advisor, I would like to thank the Head of the Department of Mechanical and Aeronautical Engineering at the University of Pretoria, Prof Josua P. Meyer, who co-supervised my dissertation. It has been an honour to work under his supervision.

I am grateful for the help that I received from Hadi Ghodsinejad during the experimental work.

Lastly, I would like to thank my husband for his love, encouragement and support during my study.

TABLE OF CONTENTS

ABSTRACT	ii
DEDICATION.....	iv
ACKNOWLEDGEMENTS.....	v
TABLE OF CONTENTS.....	vi
LIST OF FIGURES	viii
LIST OF TABLES	x
NOMENCLATURE.....	xi
PUBLICATIONS IN JOURNALS AND CONFERENCE PROCEEDINGS.....	xiii
CHAPTER 1: INTRODUCTION.....	1
1.1 Background.....	1
1.2 Motivation.....	2
1.3 Objectives of the present research.....	2
1.4 Organisation of the dissertation.....	2
CHAPTER 2: LITERATURE REVIEW	4
2.1. Introduction.....	4
2.2. Solid-liquid interfacial layer physics	4
2.3. Nanofluid thermal conductivity	7
2.4. Nanofluid viscosity	24
2.5. Nanofluid density.....	28
2.6. Nanofluid’s specific heat capacity.....	29
2.7. Conclusion.....	31
CHAPTER 3: EXPERIMENTAL MEASUREMENT	32
3.1. Introduction.....	32
3.2. Nanofluid density measurement	32
3.3. Density measurement uncertainty analysis.....	38
3.4. Conclusion.....	40
CHAPTER 4: THEORETICAL ANALYSIS AND MODEL DEVELOPMENT	41
4.1. Introduction.....	45
4.2. The effects of the nanolayer on the nanofluid properties and heat transfer.....	45
4.3. Model development for measuring the density of nanofluids	50
4.4. Conclusion.....	53
CHAPTER 5: RESULTS AND DISCUSSIONS.....	55
5.1. Introduction.....	55
5.2. Nanofluid density results and discussion.....	55

5.3. Nanofluids' isobaric specific heat capacity results and discussions.....	69
5.4. Conclusion.....	72
CHAPTER 6: CONCLUSION.....	74
6.1. Summary.....	74
6.2. Conclusions	74
REFERENCES	77
Appendix A: Nanofluid Density Uncertainty Analysis	86

LIST OF FIGURES

Figure 1: Electron density distribution of the solid-liquid interface [12].....	7
Figure 2: Ratio of the outer and the inner radius of the nanolayer.....	23
Figure 3: Radwag AS220-R2 scale with a readability of 0.1 mg and an accuracy of 0.2 mg.....	33
Figure 4: Dispensette Organic dispenser with a readability of 0.01 ml and an accuracy of 0.005 ml	34
Figure 5: Q700 QSonica sonicator	35
Figure 6: Hielscher sonicator and Lauda thermostatic bath.....	35
Figure 7: ZnO-glycerol 4% nanofluid.....	36
Figure 8: SiO ₂ -water 4% nanofluid.....	36
Figure 9: Rudolph Research Analytical DDM 2911 digital density meter	37
Figure 10: (a) The thermal conductivity ratio of an Al ₂ O ₃ -water nanofluid, according to the Yu and Choi [25] model (kf = 0.604, kp = 46, rp=10). (b) The thermal conductivity ratio of an Al ₂ O ₃ -water nanofluid, according to the model of Xue and Xu [29] (kf = 0.604, kp = 46, rp=10).	46
Figure 11: (a) The thermal conductivity ratio of an Al ₂ O ₃ -water nanofluid, according to the model of Xie et al. [30] (kf = 0.604, kp = 46, rp=10). (b) The thermal conductivity ratio of an Al ₂ O ₃ -water nanofluid according to the model of Feng et al. [35] (kf = 0.604, kp = 46, rp=10).	47
Figure 12: (a) The viscosity ratio of an Al ₂ O ₃ -water nanofluid according to the model of Avsec and Oblak [50]. (b) The viscosity ratio of an Al ₂ O ₃ -water nanofluid according to the model of Yang et al. [49].....	48
Figure 13: The nanofluid density of SiO ₂ -water at 10 °C	56
Figure 14: The nanofluid density of SiO ₂ -water at 20 °C	57
Figure 15: The nanofluid density of SiO ₂ -water at 30 °C	57
Figure 16: The nanofluid density of SiO ₂ -water at 40 °C	58
Figure 17: The nanofluid density of SiO _x -EG-water at 10 °C.....	59
Figure 18: The nanofluid density of SiO _x -EG-water at 20 °C.....	59
Figure 19: The nanofluid density of SiO _x -EG-water at 30 °C.....	60
Figure 20: The nanofluid density of SiO _x -EG-water at 40 °C	60
Figure 21: The nanofluid density of CuO-glycerol at 10 °C.....	61
Figure 22: The nanofluid density of CuO-glycerol at 20 °C.....	62
Figure 23: The nanofluid density of CuO-glycerol at 30 °C.....	62

Figure 24: The nanofluid density of CuO-glycerol at 40 °C	63
Figure 25: The nanofluid density of MgO-glycerol at 10 °C	64
Figure 26: The nanofluid density of MgO-glycerol at 20 °C	64
Figure 27: The nanofluid density of MgO-glycerol at 30 °C	65
Figure 28: The nanofluid density of MgO-glycerol at 40 °C	65
Figure 29a-c: The specific heat capacity of SiO ₂ -water in the range of a volume fraction of 1 to 6%, at temperatures 60, 70 and 80 °C	71

LIST OF TABLES

Table 1: Nanopowder properties	34
Table 2: Nanofluid samples and measuring ranges	37
Table 3: Most common expressions for the thermal conductivity of nanofluids	42
Table 4: Most common expressions for the viscosity of nanofluids	44
Table 5: Nanolayer thickness ranges were used in some studies	53
Table 6: Nanofluid density model constants	56
Table 7: The nanofluid density of SiO ₂ -water.....	58
Table 8: The nanofluid density of SiO _x -EG-water	61
Table 9: The nanofluid density of CuO-glycerol	63
Table 10: The nanofluid density of MgO-glycerol.....	66
Table 11: The results of nanolayer thickness calculations for SiO ₂ -water nanofluid.....	67
Table 12: The results of nanolayer thickness calculations for SiO _x -EG-water nanofluid.....	68
Table 13: The results of nanolayer thickness calculations for CuO-glycerol nanofluid.....	68
Table 14: Specific heat capacity of SiO ₂ nanofluid in a volume fraction ranging from 1 to 6%, at temperatures of 60, 70 and 80 °C	70
Table 15: The specific heat capacity of equivalent SiO ₂ nanoparticles in water from Equation 102	72
Table 16: The specific heat capacity of SiO ₂ -water comparisons	73
Table A1: Uncertainty analysis data.....	86
Table A2: Uncertainty analysis data.....	87

NOMENCLATURE

c_p	Specific heat at constant pressure
d	Nanoparticle diameter
D	Diameter of complex nanotube
EG	Ethylene glycol
h	Convection heat transfer coefficient
Gr_L	Grashof number
H	Inter-particle spacing
k	Thermal conductivity
L_c	Characteristic length of the geometry
m	Mass
M_w	Molecular weight of liquid
Nu	Nusselt number
N_A	Avogadro's constant
Pe	Peclet number
Pr	Prandtl number
r_p	Nanoparticle radius
Ra_L	Reyleigh number
s	Thickness of the surfactant adsorption monolayer
SSA	Specific surface areas
t_l	Nanolayer thickness
T	Temperature
T_∞	Temperature of the fluid
TEHOS	Tetrakis(2-ethylhexoxy)silane
V	Volume
V	Fluid velocity
V_B	Brownian velocity

Greek symbols

β	Coefficient of volume expansion
γ	Ratio of nanolayer thickness to particle radius
δ	Ratio of the radius of the outer interface to the inner interface of the nanolayer
ε_p	Particle and fluid thermal conductivity ratio



μ	Fluid dynamic viscosity
μ_r	Nanofluid viscosity ratio to base fluid
ρ	Density
m	Nanoparticle mass concentration
τ	Particle shape factor
γ	Nanoparticle volumetric concentration
φ	Particle volume fraction
φ_e	Equivalent volume fraction
φ_h	Hydrodynamic volume fraction
ψ	Particle sphericity

Subscripts

l	Nanolayer
f	Fluid
p	Particle
nf	Nanofluid
eff	Effective
pe	Equivalent nanoparticle

Abbreviations

EG	Ethylene Glycol
GO	Gear Oil
Al	Aluminium
SSA	Specific Surface Area
Cu	Copper

PUBLICATIONS IN JOURNALS AND CONFERENCE PROCEEDINGS

Article in peer-reviewed journal:

1. M Sharifpur, Saboura Yousefi and JP Meyer, A New Model for Density of Nanofluids Including Nanolayer, Submitted to *International Communications in Heat and Mass Transfer*, manuscript number: CJ16/7120.

Conference papers:

1. S.A. Yousefi, M. Sharifpur and J.P. Meyer, The effects of uncertainty of nanolayer thickness on the heat transfer through nanofluids, *Proceedings of the 10th International Conference on Heat Transfer, Fluid Mechanics and Thermodynamics (HEFAT 2014)*, July 14–16, 2014, Orlando, Florida, USA.

CHAPTER 1: INTRODUCTION

1.1 Background

Conventional heat transfer fluids like water, engine oil and ethylene glycol (EG) have limitations on heat transport. On the other hand, the rapid development of technology and methods to generate an enormous amount of heat in new heat transfer systems, such as micro electromechanical machines and high efficiency heat exchangers, require an enhanced heat transfer fluid.

The main factor in the efficiency of the thermal transport ability of a heat transfer fluid is its thermal conductivity. However, conventional heat transfer fluids have poor thermal properties compared to solids. A way to improve the thermal conductivity of conventional fluids is to disperse solid particles in them.

The idea of dispersing micrometre- or millimetre-sized solid particles in fluids can be traced back to the theoretical work of Maxwell [17] in 1873. Numerous theoretical and experimental studies have been performed to increase the thermal conductivity properties of fluids by dispersing millimetre- or micrometre-sized particles in fluids. Although adding these solid particles may improve the thermal conductivity properties of conventional fluids, they could cause stability, rheological, sedimentation, clogging and pressure drop problems.

Choi [1] proposed using nanofluids, which are solid-liquid composite materials that consist of nanometre-sized solid particles (1 to 100 nm), fibres, rods or tubes suspended in different base fluids. The thermo-physical properties of fluids play a vital role in developing heat transfer equipment with a high efficiency. Numerous studies have been performed for calculating the effective thermal conductivity and viscosity of nanofluids as key factors in order to introduce nanofluids into industrial design and applications. Several authors have introduced the volume fraction of nanoparticles, temperature, nanoparticle size, nanolayer, thermal conductivity of the base fluid, pH of the nanofluid and the thermal conductivity of the nanoparticles as important parameters that affect the properties of nanofluids [2] [3].

Even nanofluids can enhance heat transfer, but the density of nanofluids has not been investigated in much detail.

1.2 Motivation

In view of industry's interest in nanofluids, especially their heat transfer applications, it was deemed necessary to study the thermo-physical properties of nanofluids. For a better understanding of nanofluid properties, it is necessary to consider solid-liquid interfacial layer, nanolayers, and their characteristics like thickness, thermal conductivity, density and specific heat capacity.

The aim of this dissertation is to study the effects of nanolayers on the other characteristics of nanofluids, which can be able to measure.

The next chapter reveals the lack of reported data and formulae on the thermo-physical properties of nanofluids with regard to nanolayers. Therefore, this research explains nanolayers and their influence on nanofluid properties.

1.3 Objectives of the present research

The research presented in this dissertation aims to achieve the following goals:

- To analyse effects of nanolayers on nanofluids' thermo-physical properties
- To measure the density of SiO₂-water, SiO_x-EG-Water, CuO-glycerol and MgO-Glycerol nanofluids from 10 to 40 °C at volume fractions ranging from 1 to 6%
- To develop a correlation for nanofluid density with measurable variables
- To use data from developed nanofluid density correlations for optimising nanofluids' heat capacity data

1.4 Organisation of the dissertation

The dissertation consists of six chapters. Chapter 1 presents the background, objectives, motivation and organisation of the study. Chapter 2 comprises the literature review

relevant to the nanolayers' effects on the thermal conductivity, viscosity, density and heat capacity of nanofluids. It also presents the available experimental correlations for and models of the thermal conductivity, viscosity, density and heat capacity of nanofluids.

Chapter 3 shows the experimental work for measuring SiO₂-water, SiO_x-EG-water, CuO-glycerol and MgO-glycerol nanofluid density and presents an uncertainty analysis. Chapter 4 discusses the effects of nanolayers on nanofluid properties and develops a model for nanofluid density and optimising the nanofluid heat capacity model. Chapter 5 deals with the results of the analysis, and the experiments that have been done are presented in Chapter 4. Chapter 6 presents a summary of the previous chapters and a conclusion.

CHAPTER 2: LITERATURE REVIEW

2.1. Introduction

This chapter reviews the literature that is relevant to the solid-liquid interfacial layer. It also explains the thermal conductivity, viscosity, density and heat capacity of nanofluids. The chapter presents the literature that considers the effects of nanolayers on the thermal conductivity, viscosity, density and heat capacity properties of nanofluids. This chapter also presents the available experimental correlations for and models of the thermal conductivity, viscosity, density and heat capacity of nanofluids.

2.2. Solid-liquid interfacial layer physics

Many theoretical analyses and molecular simulations have been performed to investigate the properties of layers at solid-liquid interfaces. Probing the structure of these interfaces was difficult and the theoretical analyses were not verified experimentally.

Broughton and Abraham [4] used molecular dynamics simulation to study the influence of crystal orientation on the structure of the liquid neighbouring the crystal face. In their study, density oscillations were also observed for the liquid close to the solid interface. These oscillations occurred in five or six layers of liquid neighbouring the crystal face, which shows the ordering of liquid molecules close to the solid interface.

Henderson and Van Swol [5] analysed the properties of a fluid in the presence of a hard wall. They performed theoretical analysis and used the results of the molecular dynamic simulation of hard sphere fluid bounded by a pair of planar walls. They predicted the density oscillation of molecules close to the solid-liquid interface from the simulation results. They also discussed the presence of layered fluid molecules in the interface of the planar wall and fluid.

Thompson and Robbins [6] worked on the epitaxial order of fluids near solids. They showed that the degree of slip on the solid is directly related to wall-fluid interaction. They indicated that substantial epitaxial ordering occurs at large interactions, and that the first of two fluid layers becomes locked to the wall. Additionally, as wall-fluid interactions increased further, the density of the first layer increased to that of the solid.

Han and Hunt [7] measured the number of particles in the fluid that attach to artificial interfaces under different flow conditions. They divided the process of particle pushing by a freezing front into three steps. The first step is the presence of particles at the solid-liquid interface, the second is the attachment of particles to the interface, and the third is the interaction of the particles with the growing solid. In their investigation, they discussed the second step. Particles pushing to the solid surface were measured in vertical and horizontal flow for different particle sizes, densities and interface surfaces in lamina and turbulent flows. Their results showed that more particles pushed to the interface in turbulent and rough surfaces. They also found that particle size and density influence the results.

Liu, Bennema, Meijer and Couto [8] used self-consistent field lattice models to study the structure of molecules in the solid-liquid interface. Oscillation of segmental density profiles, which depend on the structure of the chain-like molecules at the solid-fluid interface, has been developed. Rigid molecules show a tendency towards ordering and adsorption in the solid-liquid interface to achieve maximum adsorption energy.

Teramoto and Nakanishi [9] studied molecular orientation by using the density-functional method and compared the results with Monte Carlo simulation. In both methods, the density profile close to the solid surface showed a higher density compared to that of the liquid.

Steitz, Braun, Lang, Reiss and Findenegg [10] used neutron reflection analysis to study the solid-liquid interface and supported the conjecture of ordering liquids at the interface.

Huisman, Peters, Derks, Abernathy and Van der Veen [11] investigated the structure of the solid-liquid interface with a synchrotron X-ray diffraction method. This method can be used because of the X-ray's deep penetration into matter. The specular reflectivity was measured in the Ga/diamond (111)-2x1 interface. They reported exponentially decaying density oscillation in the Ga/diamond interface. In the experiment, liquid gallium was super cooled so that the layering could be the consequence of local freezing.

In 1998, Huisman and Van der Veen [12] introduced a model for the density profile in the solid-liquid interface. Figure 1 shows the electron density distribution of the solid-liquid interface. The solid line in the graph is the electron density distribution in the Ga/diamond (111)-2x1 interface, which is calculated from their model, and the dashed line curves are the solid and liquid distributions. As shown in the graph and schematic, the model for the interface structure of gallium atoms close to the solid surface forms a solid-like layer with a high electron density. The gallium atom structure close to the diamond surface is Ga₂ dimer, which is a stable solid phase of gallium at low temperature and ambient pressure.

Doerr, Tolan, Seydel and Press [13] studied thin liquid hexane films on silicon with specular and off-specular X-ray scattering. Their experimental results show one solid-liquid interfacial layer extended to 4 nm from the interface. They concluded that the ordering of an interfacial layer in the solid-liquid interface is independent of the thickness of the liquid film.

Yu, Richter, Datta, Durbin and Dutta [14] studied the interfacial properties of thin liquid film of tetrakis(2-ethylhexoxy)silane (TEHOS) on silicon (111) substrate with X-ray reflectivity. They showed three electron density oscillations near the interface with a period of ~1 nm, which is consistent with the molecular density.

In 2000, Yu, Richter, Datta, Durbin and Datta [15] studied the interface layering of TEHOS as a normal liquid at room temperature that was higher than freezing point. Samples of various thicknesses were tested and density oscillations of a period of 1 nm independent of film thicknesses was reported.

Yu, Richter, Kmetko, Dugan, Datta and Datta [16] used synchrotron X-rays to study the solid-liquid interface of three different liquids on silicon substrates. They studied ultrathin (45 to 90 Å) and thick (5 000 Å) liquid films. They found that the liquid molecules form three to six layers at the interface with the plane close to molecular dimensions.

According to the abovementioned studies, there is no doubt of the presence of liquid ordering in the solid-liquid interfaces. However, there are no certain models for predicting the interfacial layer properties.

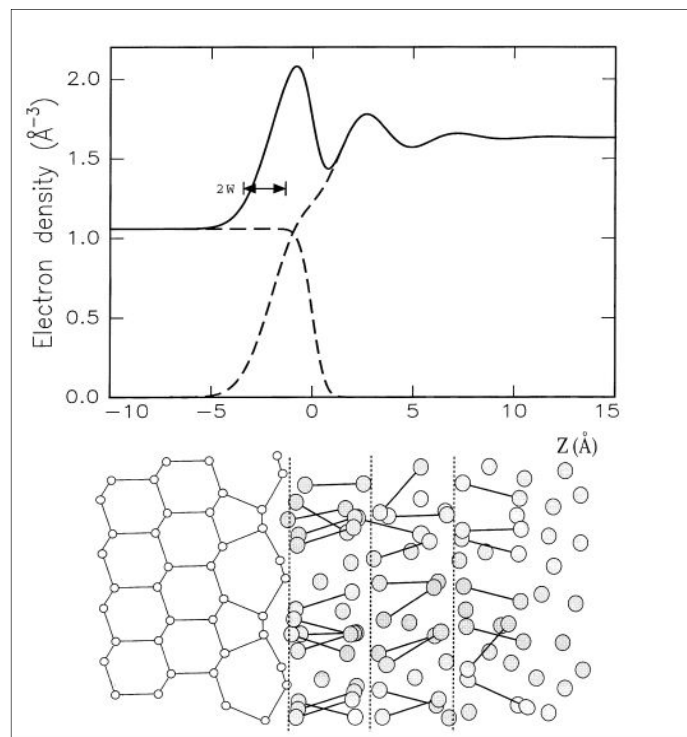


Figure 1: Electron density distribution of the solid-liquid interface [12]

2.3. Nanofluid thermal conductivity

After Choi [1] dispersed nano-sized particles in conventional fluids, many experimental studies have been done to determine the effective thermal conductivity of nanofluids.

The model of Maxwell [17], which calculates the effective thermal conductivity of fluids with suspended particles, is based on some of the models for calculating the effective thermal conductivity of nanofluids. This model considers particle and base fluid thermal conductivities and particle volume fraction:

$$k_{Maxwell} = \frac{k_p + 2k_f + 2(k_p - k_f)\varphi}{k_p + 2k_f - (k_p - k_f)\varphi} k_f \quad (1)$$

In 1935 Bruggeman, as reported in [18], presented a model that was valid in a wider range of concentration.

The factors that play a role in this model are the same as in Maxwell's model:

$$k_{eff} = (3\varphi - 1) + [3(1 - \varphi) - 1]k_f + \sqrt{\Delta} \quad (2)$$

$$\sqrt{\Delta} = (3\varphi - 1)^2 k_p^2 + [3(1 - \varphi) - 1]^2 k_f^2 + 2\varphi k_p k_f \quad (3)$$

Hamilton and Crosser [19] developed a model by considering shape factor influences on the effective thermal conductivity of fluids with suspended particles as:

$$\frac{k_{eff}}{k_f} = \frac{\varepsilon_p + (\tau - 1) - (\tau - 1)(1 - \varepsilon_p)\varphi}{\varepsilon_p + (\tau - 1) + (1 - \varepsilon_p)\varphi} \quad (4)$$

$$\varepsilon_p = \frac{k_p}{k_f} \quad (5)$$

Where τ is the empirical shape factor, and calculating from the equation below:

$$\tau = 3/\psi \quad (6)$$

ψ is particle sphericity, and in the case of spherical particles, is equal to 1.

In 1973, Jeffrey [20] extended Maxwell's model by considering interactions between pairs of spheres as:

$$\frac{k_{eff}}{k_f} = 1 + 3\partial\varphi + \left(3\partial^2 + \frac{3\partial^2}{4} + \frac{9\partial^3}{16} \frac{\varepsilon_p+2}{2\varepsilon_p+3}\right)\varphi^2 \quad (7)$$

$$\partial = \frac{\varepsilon_p-1}{\varepsilon_p+2} \quad (8)$$

Davis [21] worked on the effective thermal conductivity of composite material with spherical inclusions and presented a model slightly different from that of Jeffrey.

$$\frac{k_{eff}}{k_f} = 1 + \frac{3(\varepsilon_p-1)}{(\varepsilon_p+2)-(\varepsilon_p-1)\varphi} [\varphi + f(\varepsilon_p)\varphi^2 + 0(\varphi^3)] \quad (9)$$

$$f(\varepsilon_p) = \sum_{p=6}^{\infty} [(B_p - 3A_p)/(p-3) 2^{p-3}], \quad (10)$$

where B_p and A_p are functions of ε_p .

Independent experimental results show that the effective thermal conductivity of nanofluids is an order of magnitude larger than the calculated amount from developed models. Many studies have been performed to find the factors that enhance the effective thermal conductivity of nanofluids, and a variety of assumptions have been made to explain the mechanisms that cause the enhanced thermal conductivity of nanofluids, which will be discussed in detail in the following sections.

Eastman, Choi, Li, Yu and Thompson [22] indicated that the dramatic enhancement in the thermal conductivity of nanofluids occurs because of increasing surface area to volume ratio. This enhancement can be improved by decreasing particle size. They also compared experimental results with theoretical predictions and recounted the weaknesses of the Hamilton-Crosser model in terms of particle size in predicting the effective thermal conductivity of nanofluids.

On the other hand, some studies [5] showed that molecules of liquids close to a solid surface form a solid-like layer. This layer was more ordered than bulk liquid, so should have better thermal properties than liquid [15].

Some researchers tried to determine the effects of this interfacial nanolayer on the effective thermal conductivity of nanofluids, which will be discussed in the following paragraphs.

Keblinski, Phillpot, Choi and Eastman [23] explored possible solutions to the challenge of anomalous effective thermal conductivity enhancement, namely the Brownian motion of particles, interfacial nanolayer, ballistic conduction and particle clustering.

In the case of Brownian motion, the analysis showed that the movement of nanoparticles could not transport a significant amount of heat. Keblinski et al. [23] concluded that there should be other reasons for such enhancement.

They conducted an analysis and a computer simulation that demonstrated the important role of the nanolayer in the effective thermal conductivity of nanofluids, because this liquid layer is more ordered than bulk liquid. This layer also increases the effective volume fraction of nanoparticles.

In their analysis, the nanolayer's thermal conductivity was assumed equal to k_p to estimate upper limit of the nanolayer that enhances thermal conductivity. Keblinski et al. [23] mentioned that, if a double effective volume fraction is required for an amount of enhancement, the nanolayer should have a thickness of 10 nm, which is larger than the experimental and simulation data for liquid layering on solid surfaces. They concluded that the forming nanolayer could not have such a big effect on effective thermal conductivity as was shown in experiment results.

They also concluded that ballistic conductivity and particle clustering do not support such an enhancement in effective thermal conductivity.

Xue [24] derived a model for predicting the effective thermal conductivity of nanofluids based on Maxwell's model and average polarisation theories. He considered the particle and nanolayer as a "complex particle" and derived an equation for this complex particle.

A flaw of his analysis is that he selected nanolayer thickness and thermal conductivity to fit experimental results. The size of the carbon nanotube used in the experiments had a mean diameter of 25 nm and 50 μm . In this analysis, nanolayer thickness and thermal conductivity were fitted as 1, 2, 3 and 5 nm and 20 W/mK respectively.

The Al_2O_3 particle size was 60.4 nm in diameter, and for Al_2O_3 -water, nanolayer thicknesses were fitted as 1, 2 and 5 nm, and 10 and 21 W/mK for thermal conductivity. Xue [24] did not mention any reason for these selections.

Yu and Choi [25] renovated Maxwell's model and considered the effects of the interfacial layer on the effective thermal conductivity of nanofluids. They used the theory of formation of the layered structure of liquid molecules on solid surfaces, and proposed that this solid-like nanolayer around the nanoparticle plays a key role in enhancing the thermal conductivity of nanofluids that act as a thermal bridge. The nanoparticle and surrounding nanolayer assumed an equivalent nanoparticle and defined an increased volume concentration as indicated below:

$$\varphi_e = \frac{4}{3}\pi(r_p + t_l)^3 n = \frac{4}{3}\pi r_p^3 n \left(1 + \frac{t_l}{r_p}\right)^3 = \varphi(1 + \gamma)^3, \quad (11)$$

$$\gamma = \frac{t_l}{r_p}, \quad (12)$$

where n is the particle number per unit volume. Based on the effective medium theory of Schwartz et al. [25], they calculated the equivalent nanoparticle thermal conductivity as indicated below:

$$k_{pe} = \frac{[2(1-\vartheta) + (1+\gamma)^3(1+2\vartheta)]\vartheta}{-(1-\vartheta) + (1+\gamma)^3(1+2\vartheta)} k_p \quad (13)$$

$$\vartheta = \frac{k_l}{k_p} \quad (14)$$

Then they modified Maxwell's model for the thermal conductivity of nanofluid as indicated below:

$$k_{eff} = \frac{k_{pe} + 2k_f + 2(k_{pe} - k_f)(1 + \gamma)^3 \varphi}{k_{pe} + 2k_f - (k_{pe} - k_f)(1 + \gamma)^3 \varphi} k_f \quad (15)$$

Therefore, they compared their model with the classic Maxwell model for Cu-EG nanofluid and concluded that the effects of nanolayer are significant when nanoparticles are smaller than 5nm ($r_p \sim t_l$). Their modified model results will reduce to the original Maxwell equation when $r_p \gg t_l$.

The effects of the thickness and thermal conductivity of the nanolayer on thermal conductivity enhancement for a nanofluid were discussed. According to Schwartz et al. [25], thermal conductivity enhancement is strongly dependent on the thickness of the nanolayer, but it is almost invariant to the thermal conductivity of the nanolayer when $k_l > 10k_f$. They concluded that the nanolayer thickness is crucial to thermal conductivity enhancement.

They compared the results from their model with the results from Maxwell's model and some experimental results from previous studies for Cu-EG (with surfactant and without surfactant) and CuO-EG nanofluids.

They concluded that thermal conductivity enhancement is strongly dependent on the thickness of the nanolayer, but it is almost invariant to the thermal conductivity of the nanolayer when $k_l > 10k_f$, and nanolayer thickness is crucial to thermal conductivity enhancement. They assumed intermediate thermal conductivity between the nanoparticle and base fluid thermal conductivities for the nanolayer, and nanolayer conductivity is considered to be constant over the nanolayer. Drawbacks to their model are the nanolayer thickness and thermal conductivity amount, which has been adjusted to match experimental data.

Yu and Choi [26] renovated the model of Hamilton-Crosser to include the solid-liquid interface effects on effective thermal conductivity for non-spherical particles. Particles are assumed to be elliptical. The particle and the nanolayer are considered as a complex particle.

Equivalent thermal conductivity and volume fraction were calculated for these elliptical particles. In order to analyse the model, they selected an unknown in their equation to fit a nanolayer thickness of 2 nm.

Their investigation included k_l equal to $10k_f$, $100k_f$ and k_p . Therefore, they found that the effective thermal conductivity is less than the case of $k_l=k_f$ when $k_l=10k_f$, in contrast with nanofluids with spherical particles. This is because the nanolayer increases sphericity and reduces the empirical shape factor, which reduces the effectivity of the thermal conductivity of nanofluids. However, if the thermal conductivity is large enough, the effective thermal conductivity will increase. Yu and Choi claim that their model is in good agreement with the experiment, but it is unable to predict effective thermal conductivity in non-linear behaviour.

Xue, Keblinski, Phillpot and Choi [27] conducted a molecular dynamic simulation on a simple (mono-atomic) liquid to discover the effects of ordered interfacial liquid layers on thermal transport. They proved that this interfacial layer does not have any significant effect on the thermal transport properties of nanofluids. Nevertheless, they stated that this result is for a simple liquid and that the effects of ordered layers could be more significant in more complex liquids.

Jang and Choi [28] considered the dynamic nanoparticles in nanofluid and derived an equation for effective thermal conductivity by considering the effects of Brownian motion. They concluded that Brownian motion has fewer effects than other heat transfer mechanisms and that it can be neglected.

In a part of their theoretical analysis, the hydrodynamic boundary layer thickness around nanoparticles should be calculated, and they assumed that nanolayer thickness is equal to the thickness of this boundary layer. The selected nanolayer thickness is 3 nm; refer to the theory of Yu et al. [15].

Xue and Xu [29] assumed the nanoparticle in the nanolayer as a complex particle. They solved the temperature distribution equation in the complex nanoparticle and presented a model for the effective thermal conductivity of this complex nanoparticle.

They used Bruggmen's effective media theory for two composite phases to derive the following equation for the effective thermal conductivity of nanofluids:

$$(1 - \varphi_e) \frac{K_{eff} - K_f}{2K_{eff} + K_f} + \varphi_e \frac{(K_{eff} - K_l)(2K_l + K_p) - \alpha(K_p - K_l)(2K_l + K_{eff})}{(2K_{eff} + K_l)(2K_l + K_p) + 2\alpha(K_p - K_l)(K_l - K_{eff})} = 0 \quad (16)$$

$$\alpha = \left(\frac{r_p}{r_p + t_l} \right)^3 \quad (17)$$

They also compared the results from their proposed equation with experimental data. Drawbacks of their model are selecting a nanolayer thickness equal to 3 nm and a nanolayer thermal conductivity $5 \text{ W m}^{-1} \text{ K}^{-1}$ in Al_2O_3 -water, $10 \text{ W m}^{-1} \text{ K}^{-1}$ in CuO-EG and $1.2 \text{ W m}^{-1} \text{ K}^{-1}$ in CuO-water nanofluids to fit experimental results. In order to select a nanolayer thickness equal to 3 nm, they refer to Yu et al. [15] who concluded that the thickness of liquid layering on solids is several nanometres.

Xie, Fujii and Zhang [30] discussed the role of particle size, nanolayer thickness, volume fraction and the thermal conductivity particle-to-base ratio of the fluid on enhanced thermal conductivity. They derived a model by investigating the contribution of nanoparticles, base fluids and nanolayers to the thermal conductivity of the nanofluid, as well as following the study of Lu [31]:

$$\frac{k_{eff} - k_f}{k_f} = 3\theta\varphi_e + \frac{3\theta^2\varphi_e^2}{1 - \theta\varphi_e} \quad (18)$$

$$\theta = \frac{\vartheta_{lf}[(1+\gamma)^3 - (\vartheta_{pl}/\vartheta_{fl})]}{(1+\gamma)^3 + 2\vartheta_{lf}\vartheta_{pl}} \quad (19)$$

Where,

$$\vartheta_{lf} = \frac{k_l - k_f}{k_l + 2k_f} \quad (20)$$

$$\vartheta_{pl} = \frac{k_p - k_l}{k_p + 2k_l} \quad (21)$$

$$\vartheta_{fl} = \frac{k_f - k_l}{k_f + 2k_l} \quad (22)$$

They assumed that the thermal conductivity of the nanolayer in an intermediate physical state between nanoparticle and base fluid would have a leaner distribution, using Yu and Choi [25]:

$$k_l = \frac{k_f M^2}{(M-\gamma) \ln(1+M) + \gamma M} \quad (23)$$

$$M = \varepsilon_p (1 + \gamma) - 1 \quad (24)$$

$$\varepsilon_p = k_p / k_f \quad (25)$$

Yu and Choi [25] also concluded that, with decreasing nanoparticle size, effective thermal conductivity will increase. The reason is the contribution of the nanolayer in small nanoparticles. The specific surface area (SSA) definition has been used to describe effects of the nanolayer on effective thermal conductivity. Therefore, they indicated that the SSA in micro-sized particles is so small and the effects of the nanolayer that formed on the surface is negligible, whereas the SSA for nanoparticles is large, so the nanolayer's effects could not be neglected.

By using the above expression for k_l and comparing thermal conductivity ratios, k_l/k_f , in Cu-EG nanofluid for different nanolayer thicknesses (0.5, 1.0 and 2.0 nm), Yu and Choi [25] concluded that k_l/k_f is strongly dependent on the particle size and thickness of the nanolayer. With an increase in the thickness of the nanolayer or a decrease in particle size, k_l/k_f increases and the impact of the nanolayer would be more effective when the particle is small and the nanolayer is thick.

Yu and Choi [25] used their developed model to investigate the effects of the nanolayer thickness and volume fraction of the nanoparticle in Cu-EG nanofluids with 10 nm-sized nanoparticles. Using the same nanofluid and a 5.0% volume fraction, they also discussed the effect of nanoparticle size on effective thermal conductivity. They concluded that when nanoparticle size decreases, the effective thermal conductivity increases. The reason is contribution of the nanolayer in small nanoparticles.

The model was compared with some available experimental data on Cu-EG, CuO-EG and Al₂O₃-water nanofluids. The results of the model of Yu and Choi [25] for Al₂O₃-water nanofluids, when $r_p=6.5$ nm and $k_l=5k_f$, were in good agreement with experiments. In their analyses, nanolayer thickness was selected as 2 nm and they validated their results again with only a few experimental results, which are drawbacks of their work.

Yajie, Xie and Cai [32] built up a model for the effective thermal conductivity of nanofluids. They assumed linear intermediate thermal conductivity for the nanolayer, nanoparticle and nanolayer as a complex nanoparticle, and identified four types of heat transfer in nanofluids: via the base fluid, via the nanoparticle, via the nanolayer and via micro convection. They used the model of Lu and Song [32] for heat conduction in suspension fluid and finally derived an equation for effective thermal conductivity:

$$k_{eff} = k_f \left[1 + F(\text{Pe}) + 3\theta\varphi_e + \frac{3\theta^2\varphi_e^2}{1-\theta\varphi_e} \right] \quad (26)$$

$$\theta = \frac{\vartheta_{lf}[(1+\gamma)^3 - (\vartheta_{pl}/\vartheta_{fl})]}{(1+\gamma)^3 + 2\vartheta_{lf}\vartheta_{pl}} \quad (27)$$

F is a function of the Peclet number and shows the micro convection heat transfer portion of effective thermal conductivity.

They assumed a nanolayer thickness of 2 nm based on the theory of magnitude of liquid layering on solids. They calculated the k_{eff} of a Cu-EG nanofluid with a 5% concentration and nanolayer thicknesses of 1, 2 and 3 nm, then concluded that the enhancement of effective thermal conductivity increases with a decreasing nanoparticle radius. An increase in nanolayer thickness leads to a larger enhancement. Lu and Song (1996) also compared the results of their model with some available experimental data for Cu-EG ($r_p=3.0$ nm), CuO-EG ($r_p=15.0$ nm) and Al₂O₃-H₂O ($r_p=6.5$ nm), and assumed a nanolayer thickness of 2 nm based on the theory of magnitude of liquid layering on solids.

A drawback of this comparison is that they validate their results with experiments using only nanoparticles smaller than 15 nm, and the nanolayer thickness is selected in this analysis.

Leong, Yang and Murshed [33] developed a model for the effective thermal conductivity of nanofluids. The proposed model considers the volume fraction, thickness and thermal conductivity of the interfacial layer and particle as:

$$k_{eff} = \left\{ k_f \frac{\varphi \varepsilon (k_p - \varepsilon k_f) [2\delta_1^3 - \delta^3 + 1] + (k_p + 2\varepsilon k_f) \delta_1^3 [\varphi \delta^3 (\varepsilon - 1) + 1]}{\delta_1^3 (k_p + 2\varepsilon k_f) - (k_p - \varepsilon k_f) \varphi [\delta_1^3 + \delta^3 - 1]} \right\} \quad (28)$$

Where, $\delta = \frac{r_p + d}{r_p}$

When comparing this model with experimental data, they used a nanolayer thickness of 1 nm and $k_l = (2 \sim 3) k_f$, but they did not consider the effects of nanolayer thickness in their model.

Sabbaghzadeh and Ebrahimi [34] used the model of Jang and Choi [28], and derived a theoretical model for explaining the effective thermal conductivity of nanofluids with cylindrical nanoparticles.

They discussed the following four mechanisms of heat transfer in nanofluids:

1. Collision between base fluid molecules
2. Thermal diffusion in nanoparticles
3. Thermal diffusion in nanolayers
4. The thermal interaction of dynamic complex nanoparticles (original nanoparticle and nanolayer)

Sabbaghzadeh and Ebrahimi [34] assumed an intermediate status for nanolayer thermal conductivity between the thermal conductivities of base fluids and nanoparticles. They also assumed a linear distribution for the thermal conductivity of the nanolayer. They referred to Yu and Choi [25] for both these assumptions.

$$k_l = \frac{k_f r_p (\varepsilon_p \delta - 1) \ln(\delta)}{\ln(\delta \varepsilon_p) d} \quad (29)$$

Where, $\varepsilon_p = k_p / k_f$

Sabbaghzadeh and Ebrahimi [34] finally derive an equation for effective thermal conductivity:

$$k_{eff} = k_f (1 - \varphi(1 + M')) + \varphi(k_p + k_l M') + \varphi(1 + M') \frac{d_f}{Pr_{f,D}} (0.35 + 0.56 Re_f^{0.52}) Pr_f^{0.3} k_f \quad (30)$$

$$M' = (\gamma + 1)^2 - 1, \quad (31)$$

where, D is the diameter of the complex particle:

$$D = 2(r_p + t_l) \quad (32)$$

Sabbaghzadeh and Ebrahimi [34] validate their model with carbon nanotubes in engine oil and distilled water and the results are in good agreement. They concluded that, by changing the nanolayer thickness in the calculations, effective thermal conductivity will change significantly when the nanoparticle diameter is less than 30 nm.

In these comparisons, they estimated nanolayer thicknesses of 1, 2 and 5 nm without any explanation of these assumptions. This was a shortcoming in their work.

Feng et al. [35] proposed a model for the effective thermal conductivity of nanofluids by considering nanolayer and nanoparticle aggregation effects. The model of Yu and Choi [25] was used to determine the effective thermal conductivity of non-aggregated particles:

$$k_{non-agg} = \frac{k_{pe} + 2k_f + 2(k_{pe} - k_f)(1 + \gamma)^3 \varphi}{k_{pe} + 2k_f - (k_{pe} - k_f)(1 + \gamma)^3 \varphi} k_f \quad (33)$$

$$k_{pe} = \frac{[2(1 - \beta) + (1 + \gamma)^3(1 + 2\beta)]\beta}{-(1 - \beta) + (1 + \gamma)^3(1 + 2\beta)} k_p \quad (34)$$

Feng et al. [35] proposed a model for the effective thermal conductivity of clusters, k_{agg} :

$$k_{agg} = \left[\left(1 - \frac{3}{2} \varphi_e \right) k_f + \frac{3k_f}{\omega} \varphi_e \left[\frac{1}{\omega} \ln \frac{(r_p+d)}{(r_p+d)(1-\omega)} - 1 \right] \right] \quad (35)$$

$$\omega = 1 - \frac{k_f}{k_{pe}} \quad (36)$$

$$k_{eff} = (1 - \varphi_e)k_{non-agg} + \varphi_e k_{agg} \quad (37)$$

In order to compare the model with experimental data, Feng et al. [35] selected a nanolayer thickness and thermal conductivity of 2 nm and $3k_f$ respectively. This nanolayer thickness was selected according to the model of Hashimoto et al. [36] to determine the electron density profile at the interface, as well as the model of Li et al. [37], which used $t_l = \sqrt{2\pi}\sigma$ to determine interfacial layer thickness, where σ has a value between 0.4 and 0.6 nm. Thus, the interfacial nanolayer thickness was expected to be 1 and 2 nm. Xue et al. [27] also performed a molecular dynamic simulation, which confirmed that the interfacial layer thickness is the order of magnitude of a few atomic distances. The reason for using $k_l = 3k_f$ was that several authors, including Yu and Choi [25] and Xie et al. [30] considered k_l equal to 2 or 3 k_f . Thus, they used $k_l = 3k_f$ in their calculations.

Results from the comparison of the experimental data of the models of Xue et al. [27] and Feng, Boming, Xu and Zou [35] showed that Feng's model under predicts effective thermal conductivity when thermal conductivity enhancement is more than 15%.

Kole and Dey [38] measured the thermal conductivity of CuO-GO nanofluid as a function of volume fraction and temperature. They performed this measurement at between 5 and 80 °C in different volume fractions (0.5 to 2.5%).

In their study, the roles of Brownian motion, the interfacial nanolayer and nanoparticle clustering in the enhanced effective thermal conductivity of CuO-GO nanofluids have been discussed. They compared the measurement results with the model of Feng et al. [35] and confirmed that thermal conductivity enhancement is within 15%. The Feng model excellently predicts the thermal conductivity of oxide-based nanofluids.

Hari, Joseph, Mathewa, Nithyaja, Nampoori and Radhakrishnan [39] investigated the thermal diffusivity of nanofluids with rod-shaped nanoparticles, and studied various factors like the shape of the nanoparticle, chemical environment, the interfacial layer around the particle surface and the thickness of the nanolayer.

They stated that thermal conductivity may vary with the thickness of the nanolayer, but further experimental investigation is required to study the influence of nanolayer thickness on thermal conductivity.

In this study, Hari et al. [39] found that rod-shaped nanoparticles improve heat diffusion in the base fluid more efficiently than spherical nanoparticles.

Kole and Dey [40] performed experimental investigations on Cu-GO nanofluids and measured the thermal conductivity and viscosity of Cu-GO for a volume concentration between 0.11 and 2% at different nanofluid temperatures (10 to 80 °C). They observed 24% thermal conductivity enhancement in 2% volume concentration of Cu at room temperature and believed that the interfacial liquid layering and ballistic transport of phonons across the percolating nanoparticle aggregated structures play a major role in enhancing thermal conductivity.

They examined these experimental results with the theoretical models of Maxwell [17], Hamilton and Crosser [19], Leong et al. [33], Chen, Ding, He and Tan [41] and Feng et al. [35]. They concluded that none of these models produces an acceptable prediction for Cu-EG nanofluid.

Ghosh and Mukherjee [42] considered the effects of nanolayers on the effective thermal conductivity of nanofluids, and developed an expression for the effective thermal conductivity of nanofluids.

They used the Langmuir formula of monolayer adsorption of molecules cited in Wang, Zhou and Peng [43].

$$t_l = \frac{1}{\sqrt{3}} \left[\frac{4M_w}{\rho_f N_A} \right]^{1/3} \quad (38)$$

By assuming linear intermediate thermal conductivity for the nanolayer between particles and fluid thermal conductivities, and solving the heat flow rate in spherical particles with interfacial layers, they proposed the equation below for the thermal conductivity of the nanolayer:

$$k_l = \frac{1}{r_p(r_p+t_l) \left[C \ln \left(1 + \frac{t_l}{r_p} \right) + \frac{J t_l}{r_p(r_p+t_l)} - \frac{E}{\lambda} \ln \left(1 - \frac{\lambda t_l}{k_p} \right) \right]} \quad (39)$$

$$\lambda = \frac{k_p - k_f}{t_l} \quad (40)$$

$$C = \frac{\lambda}{(k_p + \lambda r_p)^2} \quad (41)$$

$$J = \frac{1}{(k_p + \lambda r_p)} \quad (42)$$

$$E = \frac{\lambda^2}{(k_p + \lambda r_p)^2} \quad (43)$$

They used the proposed expression for thermal conductivity of equivalent particles developed by Xue and Xu [29] and Bruggeman's effective media theory, and offered their model as:

$$\left(1 - \frac{\varphi}{\alpha} \right) \frac{k_{eff} - k_f}{2k_{eff} + k_f} + \frac{\varphi}{\alpha} \frac{(k_{eff} - k_l)(2k_l + k_p) - \alpha(k_p - k_l)(2k_l + k_{eff})}{(2k_{eff} + k_l)(2k_l + k_p) + 2\alpha(k_p - k_l)(k_l - k_{eff})} = 0 \quad (44)$$

$$\alpha = \left(\frac{r_p}{r_p + t_l} \right)^3 \quad (45)$$

So far, the resulting thickness and conductivity of the nanolayer both have to be chosen to match the measured thermal conductivity of the nanofluid.

Tillman and Hill [44] tried to derive an equation for determining nanolayer thickness. In this study, a mathematical procedure was developed to determine nanolayer thickness for any thermal conductivity profile.

The thermal conductivity in the nanolayer was assumed to be known. Nanolayer thickness is then derived from the thermal conductivity equation in the solid-liquid interface.

They proposed three kinds of functions for $k(r)$:

$$k(r) = k_0(1 - ar)^m \quad (46)$$

$$k(r) = k_0(1 - a/r)^m \quad (47)$$

$$k(r) = k_0 e^{-\frac{a}{r^m}} \quad (48)$$

Tillman and Hill [44] successfully used Equation 46 and achieved results. They calculated k_0 and a from thermal conductivity continuity in nanolayer interfaces with the known nanoparticle and base fluid conductivities. Subsequently, they solved the steady thermal conduction equation by using an assumed function for thermal conductivity in the nanolayer $k(r)$:

$$\frac{1}{r^2} \frac{\partial}{\partial r} \left[r^2 k \frac{\partial T}{\partial r} \right] + \frac{1}{r^2 \sin \theta} \frac{\partial}{\partial \theta} \left[k \sin \theta \frac{\partial T}{\partial \theta} \right] = 0 \quad (49)$$

By using the first-order Legendre function for solving the temperature field in the nanolayer,

$$T(r, \theta) = A(r) \cos \theta \quad (50)$$

By substituting this equation in the thermal conduction equation,

$$\frac{d^2 A}{dr^2} + \left(\frac{2}{r} + \frac{k'}{k} \right) \frac{dA}{dr} - \frac{2}{r^2} A = 0 \quad (51)$$

The solution for the equation above is as follows:

$$T(r, \theta) = [Ey_1(r) + Fy_2(r)] \cos \theta \quad (52)$$

They derived Equation 53 for calculating δ by using temperature and conductivity boundary conditions in the nanolayer.

$$\frac{[y_1(r_p)/r_p]'}{[y_2(r_p)/r_p]'} = \frac{[(\delta r_p)^2 y_1(\delta r_p)]'}{[(\delta r_p)^2 y_2(\delta r_p)]'} \quad (53)$$

where $\delta = \frac{r_p+d}{r_p}$ is the ratio of the outer and inner radius of the nanolayer.

Mathematic analysis was done on the Al_2O_3 -EG nanofluid, which shows that δ approached 1.19 when m was increased. This indicates that the nanolayer thickness is 19% of the nanoparticle radius (Figure 2).

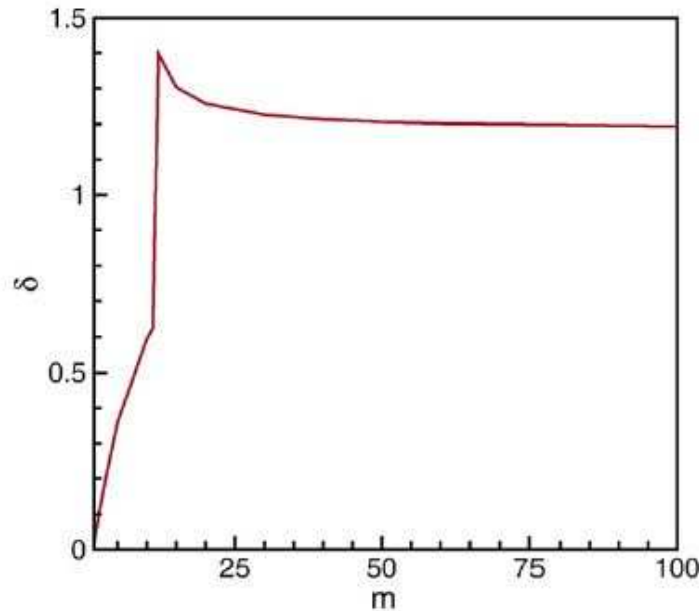


Figure 2: Ratio of the outer and the inner radius of the nanolayer

The results for $CuO-H_2O$ with the same analysis was $\delta=1.22$.

They tested their model for $k_f < 1 \text{ W m}^{-1} \text{ K}^{-1}$ and various equilibrium constants. They concluded that the nanolayer thickness for all nanofluids is between 19 and 22% of the nanoparticle radius.

The effects of bonding between the nanoparticle and the base fluid were not considered in their model. There is also no evidence that the equation that was used for the thermal conductivity of the nanolayer was accurate.

2.4. Nanofluid viscosity

In the heat transfer analysis, viscosity is as critical as thermal conductivity, while nanoparticles increase the base fluid's viscosity, which causes an increasing pressure drop. Therefore, recognising the factors that affect nanofluid viscosity and developing a model for predicting nanofluid viscosity is crucial in nanofluid applications. Consequently, in order to predict the flow and heat transfer rates in convective nanofluids, the viscosity and the correlation between viscosity and temperature should be considered.

The investigation of the rheological behaviour of fluid with dispersions can be traced back to Einstein's analysis of infinitely dilute suspensions of hard spheres in 1906 [45]. Most of the existing models are derived from Einstein's work. However, the model does not consider particle interactions and it is valid for a low particle volume concentration of about 2%.

$$\mu_r = \frac{\mu_{nf}}{\mu_f} = (1 + 2.5\varphi) \quad (54)$$

In 1952, Brikman, as reported in [45], extended Einstein's formula to a volume concentration of up to 4%:

$$\frac{\mu_{nf}}{\mu_f} = \frac{1}{(1-\varphi)^{2.5}} \quad (55)$$

Frankei and Acrivos [46] proposed the following equation:

$$\frac{\mu_{nf}}{\mu_f} = \frac{9}{8} \left[\frac{(\varphi/\varphi_m)^{1/3}}{1 - (\varphi/\varphi_m)^{1/3}} \right], \quad (56)$$

where φ_m is the maximum attainable volume fraction that must be determined experimentally.

Lundgren [45] proposed a model in the form of a Taylor series:

$$\frac{\mu_{nf}}{\mu_f} = \left[1 + 2.5\varphi + \frac{25}{4} \varphi^2 + O(\varphi^3) \right] \quad (57)$$

Batchelor [47] includes the effects of Brownian motion on viscosity of dispersion as:

$$\frac{\mu_{nf}}{\mu_f} = (1 + 2.5\varphi + 6.5 \varphi^2) \quad (58)$$

Graham [48] considered interparticle spacing on the viscosity of dispersion and then developed his model as:

$$\frac{\mu_{nf}}{\mu_f} = 1 + 2.5\varphi + 4.5 \left[1 / \left(\frac{H}{r_p} \right) \left(2 + \frac{H}{r_p} \right) \left(1 + \frac{H}{r_p} \right)^2 \right], \quad (59)$$

where H is the interparticle spacing.

In 2006, Guo et al. [50] considered the effect of particle diameter on viscosity and developed Batchelor's model for low concentrations:

$$\frac{\mu_{nf}}{\mu_f} = (1 + 2.5\varphi + 6.5 \varphi^2) (1 + 350 \varphi / r_p) \quad (60)$$

In their study, Avsec and Oblak [50] offered shear viscosity as:

$$\mu_r = \frac{\mu_{nf}}{\mu_f} = 1 + (2.5\varphi_e) + (2.5\varphi_e)^2 + (2.5\varphi_e)^3 + (2.5\varphi_e)^4 + \dots \quad (61)$$

They used the Ward equation and included the fact that the nanolayer was affected by changing volume concentration with effective volume concentration, which was named the renewed Ward equation.

Nguyen, Desgranges, Falanis, Roy, Maré, Boucher and Angue Mintsa [45] discussed the effects of temperature, particle size and concentration on nanofluid viscosity. They measured Al₂O₃-water viscosity for two different particle sizes (36 and 47 nm) at room temperature to nearly 75 °C. They proposed two correlations to determine the viscosity ratio in Al₂O₃-water with particle sizes of 36 and 47 nm respectively as:

$$\mu_r = \frac{\mu_{nf}}{\mu_f} = (1 + 0.025\varphi + 0.015 \varphi^2) \quad (62)$$

$$\mu_r = \frac{\mu_{nf}}{\mu_f} = 0.904 e^{0.1483\varphi} \quad (63)$$

Lee, Hwang, Jang, Lee, Kim, Choi and Choi [51] performed some experimental analyses for understanding the behaviour of Al₂O₃-water nanofluid in very low volume concentrations (0.01 to 0.3 volume percentage). The thermal conductivity and viscosity of this nanofluid were measured in their experiments. The experimental data has been compared with available models and previous experimental results. An oscillation viscometer was used to measure the viscosity as a function of temperature and volume concentration. The experimental results showed the non-linear behaviour of nanofluid against the volume concentration. Lee et al. [51] stated that this behaviour implies that some particle-particle interactions invalidate Einstein's model.

Murshed, Leong and Yang [52] studied the thermal conductivity and viscosity of nanofluids theoretically and experimentally. They stated that the classic models could not predict enhanced thermal conductivity at the time because the effects of particle size, distribution and interfacial layer were not included. Thus, they assumed that nanofluids include three component particles, as well as a liquid and interfacial layer that includes the effects of the interfacial layer on thermal conductivity and viscosity.

To calculate the thickness of nanolayer, the model of Hashimoto et al. [36] was employed. A nanolayer thickness of 1 and 2 nm was used for spherical and carbon nanotubes respectively. Comparisons between their experimental results and available models showed that the models underpredict the shear viscosity. They concluded that the clusters and surface adsorption could be the reason for this difference, and these two factors can increase the hydraulic diameter of particles and result in higher viscosity. They also stated that the nature of the particle surface, ionic strength of the base fluid, surfactants, pH values, interparticle potentials, such as repulsive (electric double-layer force) and attractive (Van der Waals force) forces, may play a significant role in altering the viscosity of nanofluids

Masoumi, Sohrabi and Behzadmehr [53] introduced a model for calculating the effective viscosity of nanofluids in which Brownian motion is considered.

$$\mu_{eff} = \mu_f + \mu_{app} \quad (64)$$

The μ_{app} is apparent viscosity and shows the effects of nanoparticles on the viscosity of nanofluids.

$$\mu_{eff} = \mu_f + \frac{\rho_p V_B d_p^2}{72CH}, \quad (65)$$

where C is the correction factor and was determined from experimental data associated with Al₂O₃-water nanofluid. The equation's limitation is $\varphi < -b/a$. However, the effect of the solid-liquid interface was not considered in the model of Masoumi et al. [53].

Hosseini, Moghadassi and Henneke [54] presented a model for predicting the viscosity of nanofluids. In their empirical model, nanofluid viscosity is a function of the base fluid's viscosity, particle volume fraction, particle size, properties of the surfactant layer, and temperature as:

$$\frac{\mu_{nf}}{\mu_f} = \exp \left[m + \alpha \left(\frac{T}{T_0} \right) + \varkappa(\varphi_h) + \varrho \left(\frac{d_p}{1+s} \right) \right], \quad (66)$$

where φ_h is hydrodynamic volume fraction.

$$\varphi_h = \varphi \left[\frac{d_p + 2s}{d_p} \right]^3, \quad (67)$$

where m is a factor that depends on the system's properties (like the solid nanoparticles, the base fluid and their interactions), while α , κ , and ϱ are empirical constants that were determined from experimental data.

Yang, Du, Ding, Cheng and Jun [49] studied the effects of the surfactant monolayer and interfacial nanolayer on nanofluid viscosity. They calculated the equivalent volume concentration of particles by adding these two layer thicknesses to nanoparticle radii and putting a new volume concentration into Einstein's model.

$$\varphi_{new} = \varphi \left[\frac{r_p + t_l + s}{r_p} \right]^3 \quad (68)$$

$$s = \frac{1}{\sqrt{3}} \left[\frac{4M_w}{\rho_f N_A} \right]^{1/3} \quad (69)$$

For the nanolayer thickness, Yang et al. [49] used the model of Hashimoto et al. [36] and a nanolayer thickness of 1 nm.

$$\mu_r = \frac{\mu_{nf}}{\mu_f} = \left(1 + 2.5 \left[\frac{r_p + t_l + s}{r_p} \right]^3 \right) \varphi \quad (70)$$

2.5. Nanofluid density

Not much research has been conducted on density as one of the physical properties of the nanofluids. However, density plays a major role in the application of nanofluids. In a number of studies, including Buongiorno [55], Polidori, Fohanno and Nguyen [56], Ogut [57], Kumar, Prasad and Banerjee [58], Alloui, Quiet, Vasseur and Reggi [59], Kuppalapalle [60], Ryzhkov and Minakov [61], Minea [62], Zhang, Diao, Zhao and Zhang [63], Azimi and Kalbasi [64], Inakov, Lobasov, Guzei, Pryazhnikov and Ya Rudyak [65], Hassan [66], Cianfrini, Corcione, Habib and Quintino [67], Hemmat Esfe, Saedodin and Mahmoodi [68], Pang, Jung and Tae Kang [69], Hemmat Esfe, Saedodin, Mahian and Wongwises [70], Maddah, Alizadeh, Ghasemi and Rafidah

Wan Alwi [71], Pang, Won Lee and Tae Kan [72], Abed, Alghoul, Sopian, Mohammed, Majdi and Al-Shamani [73], Hassan and Harmand [74] and Najah Al-Shamani, Sopian, Mohammed, Mat, Hafidz Ruslan and Abed [75], the classic formula for a conventional solid-liquid mixture has been used to calculate nanofluids density, which does not consider the nanolayer:

$$\rho_{nf} = \varphi \rho_p + (1 - \varphi)\rho_f \quad (71)$$

In fact, the nanolayer [23] is an approved layer between the base fluid and the nanoparticle. Thus, this layer needs to be considered in nanofluid density calculations.

2.6. Nanofluid's specific heat capacity

Cooling is one of the most important challenges faced by numerous industrial sectors. On the other hand, it is known that the knowledge of specific heat capacity is very important in determining other heat transfer properties in the study of nanofluid performance in a thermal installation. Thus, accurate c_p values are necessary in energy balances.

Specific heat is one of the major factors that affect the fluid's heat transfer characteristics. So, in the case of applying nanofluids in industry, knowing nanofluids' specific heat capacity is one of the challenges.

In the absence of enough experimental data, different equations have been used in literature to predict the specific heat capacities of nanofluids.

The model that has been used in some studies, including Parametthanuwat, Bhuwakietkumjohn, Rittidech and Ding [76] and Pak and Cho [77], is derived from a classic formula for measuring a conventional solid-liquid mixture, and is based on the concepts of mixing theory for ideal gas mixtures [78].

$$C_{p,nf} = \varphi C_{p,p} + (1 - \varphi)C_{p,f} \quad (72)$$

Equation 72 is approximately correct only for dilute suspensions for which density differences between nanofluid and base fluids are small [78].

Subsequently, Xuan and Roetzel [79] modified this correlation by assuming thermal equilibrium between the nanoscale solid particles and the liquid phase by rewriting the above equation to include the density. Several authors, including Vajjha and Das [80], Zhou, Wang, Peng, Du and Yang [81] and Bergman [82], used the following model based on the assumption of thermal equilibrium between nanoparticles and the surrounding base fluid, which is more accurate and fitted better experimental results.

$$\rho_{nf}c_{p,nf} = \varphi\rho_p c_{p,p} + (1 - \varphi)\rho_f c_{p,f}, \quad (73)$$

in which nanofluid density was calculated by using Equation 71.

Some authors, including Starace, Gomez, Wang, Pradhan and Glatzmaier [83] and Teng and Hung [84], predict isobaric-specific heat capacities by using the nanoparticle mass concentration:

$$c_{p,nf} = m_p c_{p,p} + (1 - m_p)c_{p,f} \quad (74)$$

However, since solids typically exhibit inferior specific heat capacity in relation to liquids, nanofluids are also expected to present lower heat capacities than their corresponding base fluids. Based on existing experimental and theoretical results, it is concluded that nanofluids' specific heat decreases as the nanoparticle concentration increases. Nevertheless, some studies found that isobaric heat capacity increases with an increase in the concentration of nanoparticles, which can be attributed to the addition of dispersants into the dispersions, as pointed out by Sharul et al. [78] This phenomenon could also be attributed to the formation of chain-like structures between the base fluid and nanoparticles, as suggested by Shin et al. From the literature review, it is concluded that more research is necessary to determine the volume concentration and temperature dependences on nanofluid heat capacities [78].

Therefore, from the studies presented in this chapter and sections 1.1 and 1.2, it can be concluded that there is a lack of research on nanolayer properties.

In the next chapters of this study, experiments that measure the density of four different types of nanofluids are explained in detail. Therefore, the results have been compared with the density of nanofluid, calculated from the mixture linear model, which has been used in many studies on nanofluid density. A new model has also been presented to calculate nanofluid density based on an examination of the nanolayer.

2.7 Conclusion

The literature shows that there are many available correlations on which to model nanofluid thermal conductivity and viscosity, but only a few of them considered the nanolayer in their calculations. On the other hand, there is just one linear equation to calculate density, and only a few to calculate the specific heat capacity of nanofluids. None of them considered the effect of the nanolayer.

In most of the thermal conductivity and viscosity correlations in which the effects of the nanolayer are considered, the thickness and thermal conductivity of the nanolayer are not validated. Therefore, they are selected in such a way that they match the experimental data. Consequently, more research is required to understand the nanolayer's characteristics for using these characteristics in nanofluid correlations.

CHAPTER 3: EXPERIMENTAL MEASUREMENT

3.1. Introduction

This chapter discusses the experimental work related to nanofluid density measurement. Four different nanofluids were prepared in different volume fractions ranging from 1 to 6%. Subsequently, density measurements were taken in a temperature range of 10° to 40 °C.

3.2. Nanofluid density measurement

A two-step method was used for preparing nanofluids. A Radwag AS220-R2 scale with a 0.1 mg readability and 0.2 mg accuracy and a Dispensette Organic dispenser with a 0.01 ml readability and an accuracy of 0.005 ml were used to prepare the nanofluids. (See Figure 3 and Figure 4.)

The Radwag AS220-R2 scale was used to measure the required nanopowder for each sample with a specific volume fraction. A dispenser was used to measure the required volume of base fluid for each sample.

For preparing the water-based EG fluid with a volume fraction of 60% EG and 40% water, a Radwag scale was used to measure the required amount of each fluid based on its density at room temperature. The mixture of these two measured fluids results in a single fluid with 60% EG and 40% water.



Figure 3: Radwag AS220-R2 scale with a readability of 0.1 mg and an accuracy of 0.2 mg

Four different kinds of nanofluids – SiO₂-water, SiO_x-EG-water, CuO-glycerol and MgO-glycerol – were prepared for density measurement experiments. (See Table 1.) The nanofluids were selected based on the experience in our laboratory, and the nanofluids were used which were reported more stable.

Deionised water, EG and glycerol, with the respective densities of 0.99704, 1.115 and 1.261 gr/cm³ at 25 °C, were obtained from Merck South Africa.

After scaling the required nanopowder and base fluid for each sample, a sonicator, Q700 QSonica (In Figure 5), (20 kHz, 700 W) was used to prepare a homogenous nanofluid with as little agglomeration as possible. The nanofluid mixtures were stirred and sonicated continuously for one to two hours with a 2 kJ/ml energy density and different amplitudes (70 to 90%), depending on the base fluid and volume fraction. For a more viscous base fluid like glycerol and a higher volume fraction, the sonication duration was longer with a 90% amplitude. To keep samples at the desired temperature, they were placed in a thermostatic bath during sonication, depicted in Figure 6.

The nanofluids were prepared in different volume fractions – 1, 2, 4 and 8%. In figures 7 and 8 the nanofluid mixtures at 4% ZnO-glycerol and 4% SiO₂-water are shown.

All the samples were prepared on the same day of density measurement so that as little settlement as possible occurs. The density of each kind of nanofluid was measured by a DDM 2911 digital density meter (Figure 9), produced by Rudolph Research Analytical.

Table 1: Nanopowder properties

Nanoparticles	Average Particle size (nm)	Density (gr/cm ³)	Company name
SiO ₂	80	2.4	Nanostructured and Amorphous Materials
SiO _x	20	2.4	Nanostructured and Amorphous Materials
CuO	40	6.4	Nanostructured and Amorphous Materials
MgO	40	3.58	Nanostructured and Amorphous Materials



Figure 4: Dispensette Organic dispenser with a readability of 0.01 ml and an accuracy of 0.005 ml



Figure 5: Q700 QSonica sonicator



Figure 6: Hielscher sonicator and Lauda thermostatic bath



Figure 7: ZnO-glycerol 4% nanofluid



Figure 8: SiO₂-water 4% nanofluid



Figure 9: Rudolph Research Analytical DDM 2911 digital density meter

Before measuring the density, the density meter was calibrated with air and deionised water according to its manual. After measuring the density of every two samples, the density of the air and deionised water was measured to make sure that the tube is clean and the device is calibrated to reduce experimental errors.

For the measurement process, the sample was injected into a tube in the density meter using a syringe and the density was measured at 10, 20, 30 and 40°C. Each sample were measures 4 times and if the measures were closed enough, the average amount have been used. Table 2 shows all the samples that were prepared and measured at different temperatures.

Table 2: Nanofluid samples and measuring ranges

Nanoparticle	Base fluid	Volume fractions	Temperature (°C)
SiO ₂	Water	1, 2, 4, 6	10, 20, 30, 40
SiO _x	EG-water	2, 4, 6	10, 20, 30, 40
CuO	Glycerol	1, 2, 4, 6	10, 20, 30, 40

After completion of the measurement, the tube inside the density meter was washed with deionised water and acetone, and dried with an air pump assembled inside the density meter.

3.3. Density measurement uncertainty analysis

The linear formula for the density of the solid-liquid mixture has been used for uncertainty analysis as indicated below:

$$\rho_{nf} = \rho_p \varphi + \rho_f (1 - \varphi) \quad (75)$$

The ρ_p is constant so the uncertainty of density is:

$$\delta \rho_{nf} = \left[\left(\frac{\partial \rho_{nf}}{\partial \varphi} \delta \varphi \right)^2 + \left(\frac{\partial \rho_{nf}}{\partial \rho_f} \delta \rho_f \right)^2 \right]^{1/2} \quad (76)$$

From equations 75 and 76:

$$\delta \rho_{nf} = \left[((\rho_p - \rho_f) \delta \varphi)^2 + ((1 - \varphi) \delta \rho_f)^2 \right]^{1/2} \quad (77)$$

The correlation for calculating the volume fraction is:

$$\varphi = \frac{V_p}{V_f + V_p} \quad (78)$$

The volume fraction uncertainty is as follows:

$$\delta \varphi = \left[\left(\frac{\partial \varphi}{\partial V_f} \delta V_f \right)^2 + \left(\frac{\partial \varphi}{\partial V_p} \delta V_p \right)^2 \right]^{1/2} \quad (79)$$

From equations 78 and 79:

$$\delta \varphi = \left[\left(\frac{V_p}{(V_f + V_p)^2} \delta V_f \right)^2 + \left(\frac{1}{(V_f + V_p)^2} \delta V_f \right)^2 \right]^{1/2} \quad (80)$$

The formula for base fluid density is:

$$\rho_f = \frac{m_f}{V_f} \quad (81)$$

The density uncertainty will be:

$$\delta\rho_f = \left[\left(\frac{\partial\rho_f}{\partial m_f} \delta m_f \right)^2 + \left(\frac{\partial\rho_f}{\partial V_f} \delta V_f \right)^2 \right]^{1/2} \quad (82)$$

$$\delta\rho_f = \left[\left(\frac{1}{V_f} \delta m_f \right)^2 + \left(\frac{m_f}{V_f^2} \delta V_f \right)^2 \right]^{1/2} \quad (83)$$

For nanoparticles, the density is constant and equal to the amount indicated by the manufacturer, and the volume of the nanoparticles could be calculated from the density formula:

$$V_p = \frac{m_p}{\rho_p} \quad (84)$$

$$\delta V_p = \left[\left(\frac{\partial V_p}{\partial m_p} \delta m_p \right)^2 \right]^{1/2} \quad (85)$$

$$\delta V_p = \left[\left(\frac{1}{\rho_p} \delta m_p \right)^2 \right]^{1/2} \quad (86)$$

An analytical balance with a readability of 0.1 mg and an accuracy of 0.2 mg, and a volume measuring device with a readability of 0.01 ml and an accuracy of 0.005 ml was used to calculate the uncertainty for the four nanofluids that were used in the experiments with different volume fractions at a range of temperatures. The results show that the maximum uncertainty is ± 0.000157 gr/ml. The uncertainty for each sample at each measuring condition is shown in Table A1 and Table A2 in Appendix A.

Same analysis has been done for equation 98 which will be introduced later in Chapter 4 for nanofluid density. The uncertainty analyses have been presented in the appendix A.

3.4. Conclusion

In the experimental part of this study, the densities of four different nanofluids (SiO₂-water, SiO_x-EG-water, CuO-glycerol and MgO-glycerol) were experimentally investigated. Sonication was used to prepare these nanofluids in two steps.

The density of these nanofluids have been measured using a DDM 2911 digital density meter. The densities are in the range of 1, 2, 4 and 6% volume fraction between 10 and 40 °C.

The uncertainty of experimental measures for each sample at each measuring condition were also calculated, which were in the range of 0.00011 to 0.00089 gr/ml.

CHAPTER 4: THEORETICAL ANALYSIS AND MODEL DEVELOPMENT

4.1 Introduction

Rapid progress in the application of nanofluids in technology has created a demand for the comprehensive understanding of nanofluid properties. Table 3 and Table 4 summarise the most common expression for the thermal conductivity and viscosity of nanofluids. As shown in the tables, most of these models are functions of volume fraction, base fluid thermal conductivity and particle thermal conductivity, and the effect of the nanolayer has not been taken into consideration. Consequently, the thermo-physical properties of the nanolayer and the way this layer affects the thermo-physical properties of the nanofluid needs to be investigated.

In the first section of this chapter, the effects of the thickness and thermal conductivity of the nanolayer on effective the thermal conductivity and viscosity of nanofluids, and consequently on heat transfer, are discussed.

The effects of different nanolayer thicknesses and thermal conductivity on effective thermal conductivity in the models of Yu and Choi [26], Xue and Xu [29], Xie et al. [30] and Feng et al. [35] have been analysed. The models of Avsec and Oblak [50] and Yang et al. [49] were used to conduct the same analysis of nanofluid viscosity. The results of these analyses will be presented in the next section.

In the second section of this chapter, nanofluid density and the effects of nanolayer density and thickness on nanofluid density is theoretically investigated.

In most of the studies on the calculation of nanofluid density, a classic formula for solid-liquid mixture is used. In this study, theoretical analysis and experimental results were used to develop a new model to calculate nanofluid density.

In the third section, the specific heat capacity of nanofluids is discussed and the effects of utilising the developed density formula instead of a classic formula for solid-liquid mixtures is shown.

Table 3: Most common expressions for the thermal conductivity of nanofluids

Model	Remarks	Researcher/ year
$k_{Maxwell} = \frac{k_p + 2k_f + 2(k_p - k_f)\varphi}{k_p + 2k_f - (k_p - k_f)\varphi} k_f$	Only particle and fluid thermal conductivity and volume fraction are considered.	Maxwell (1873) [17]
$k_{eff} = (3\varphi - 1) + [3(1 - \varphi) - 1]k_f + \sqrt{\Delta}$ $\sqrt{\Delta} = (3\varphi - 1)^2 k_p^2 + [3(1 - \varphi) - 1]^2 k_f^2 + 2[(2 + 9\varphi)]k_p k_f$	Only particle and fluid thermal conductivity, as well as volume fraction, are considered. It is valid for higher volume fractions.	Bruggeman (1935) [18]
$\frac{k_{eff}}{k_f} = \frac{\varepsilon_p + (\tau - 1) - (\tau - 1)(1 - \varepsilon_p)\varphi}{\varepsilon_p + (\tau - 1) + (1 - \varepsilon_p)\varphi}$	Volume shape factor is added to the model.	Hamilton and Crosser (1962) [19]
$\frac{k_{eff}}{k_f} = 1 + 3\partial\varphi + (3\partial^2 + \frac{3\partial^2}{4} + \frac{9\partial^3}{16} \frac{\varepsilon_p + 2}{2\varepsilon_p + 3})\varphi^2$ $\partial = \frac{\varepsilon_p - 1}{\varepsilon_p + 2}$	The interactions between pairs of spheres are considered.	Jeffrey (1973) [20]
$\frac{k_{eff}}{k_f} = 1 + \frac{3(\varepsilon_p - 1)}{(\varepsilon_p + 2) - (\varepsilon_p - 1)\varphi} [\varphi + f(\varepsilon_p)\varphi^2 + 0(\varphi^3)]$	The particle and fluid thermal conductivity and volume fraction are considered.	Davis (1986) [21]
$\frac{k_{eff}}{k_f} = 1 + \varepsilon_p\varphi + \partial\varphi^2$	The particle and fluid thermal conductivity and volume fraction are considered.	Lu and Lin (1996) [18]
$k_{eff} = \frac{k_{pe} + 2k_f + 2(k_{pe} - k_f)(1 + \gamma)^3\varphi}{k_{pe} + 2k_f - (k_{pe} - k_f)(1 + \gamma)^3\varphi} k_f$	The nanolayer thickness and its thermal conductivity are considered.	Yu and Choi (2003) [25]

Chapter 4: Theoretical analysis and model development

Model	Remarks	Researcher/ year
$(1 - \varphi_e) \frac{k_{eff} - k_f}{2k_{eff} + k_f} + \varphi_e \frac{(k_{eff} - k_l)(2k_l + k_p) - \alpha(k_p - k_l)(2k_l + k_{eff})}{(2k_{eff} + k_l)(2k_l + k_p) + 2\alpha(k_p - k_l)(k_l - k_{eff})} = 0$	The nanolayer thickness and its thermal conductivity are considered.	Xue and Xu (2005) [29]
$\frac{k_{eff} - k_f}{k_f} = 3\theta\varphi_e + \frac{3\theta^2\varphi_e^2}{1 - \theta\varphi_e}$ $\theta = \frac{\vartheta_{lf}[(1+\gamma)^3 - (\vartheta_{pl}/\vartheta_{fl})]}{(1+\gamma)^3 + 2\vartheta_{lf}\vartheta_{pl}}$	The effect of particle size, nanolayer thickness, volume fraction and thermal conductivity ratio of the particle to the base fluid on enhanced thermal conductivity are considered.	Xie et al. (2005) [30]
$k_{eff} = k_f \left[1 + F(Pe) + 3\theta\varphi_e + \frac{3\theta^2\varphi_e^2}{1 - \theta\varphi_e} \right]$	The nanolayer thickness and its thermal conductivity are considered.	Yajie et al. (2005) [32]
$k_{eff} = \left\{ k_f \frac{\varphi\epsilon(k_p - \epsilon k_f)[2\delta_1^3 - \delta^3 + 1] + (k_p + 2\epsilon k_f)\delta_1^3[\varphi\delta^3(\epsilon - 1) + 1]}{\delta_1^3(k_p + 2\epsilon k_f) - (k_p - \epsilon k_f)\varphi[\delta_1^3 + \delta^3 - 1]} \right\}$	The volume fraction, thickness and thermal conductivity of the interfacial layer are considered.	Leong et al. (2006) [33]
$k_{eff} = (1 - \varphi_e)k_{non-agg} + \varphi_e k_{agg}$ $k_{agg} = \left[\left(1 - \frac{3}{2}\varphi_e \right) k_f + \frac{3k_f}{\omega} \varphi_e \left[\frac{1}{\omega} \ln \frac{(r_p + t_l)}{(r_p + t_l)(1 - \omega)} - 1 \right] \right]$	The effects of the nanolayer and nanoparticle aggregation are considered.	Feng et al. (2007) [35]
$\left(1 - \frac{\varphi}{\alpha} \right) \frac{k_{eff} - k_f}{2k_{eff} + k_f} + \frac{\varphi}{\alpha} \frac{(k_{eff} - k_l)(2k_l + k_p) - \alpha(k_p - k_l)(2k_l + k_{eff})}{(2k_{eff} + k_l)(2k_l + k_p) + 2\alpha(k_p - k_l)(k_l - k_{eff})} = 0$	The effects of nanolayer thickness and its thermal conductivity have been considered.	Ghosh and Mukherjee (2013) [42]

Table 4: Most common expressions for the viscosity of nanofluids

Model	Remarks	Researcher/ year
$\frac{\mu_{nf}}{\mu_f} = (1 + 2.5\varphi)$	It is valid for low volume concentrations.	Einstein (1906) [45].
$\frac{\mu_{nf}}{\mu_f} = \frac{1}{(1-\varphi)^{2.5}}$	It is valid for volume concentration up to 4%.	Brikman (1952) in Nguyen et al. [45]
$\frac{\mu_{nf}}{\mu_f} = \frac{9}{8} \left[\frac{(\varphi/\varphi_m)^{1/3}}{1-(\varphi/\varphi_m)^{1/3}} \right]$	The expression is limited when the volume concentration approaches φ_m .	Frankei and Acrivos (1967) [46]
$\frac{\mu_{nf}}{\mu_f} = \left[1 + 2.5\varphi + \frac{25}{4} \varphi^2 + O(\varphi^3) \right]$	The expression is proposed based on the Taylor series. It is applicable for spherical particles in dilute systems.	Lundgren (1972) [45]
$\frac{\mu_{nf}}{\mu_f} = (1 + 2.5\varphi + 6.5 \varphi^2)$	The effects of Brownian motion on viscosity is considered.	Batchelor (1977) [47]
$\frac{\mu_{nf}}{\mu_f} = 1 + 2.5\varphi + 4.5 \left[1/\left(\frac{H}{r_p}\right) \left(2 + \frac{H}{r_p} \right) \left(1 + \frac{H}{r_p} \right)^2 \right]$	The inter-particle spacing is considered.	Graham (1981) [48]
$\frac{\mu_{nf}}{\mu_f} = (1 + 2.5\varphi + 6.5 \varphi^2)(1 + 350 \varphi/r_p)$	The influence of particle diameter on viscosity is considered.	Guo et al. (2006) [50]
$\frac{\mu_{nf}}{\mu_f} = 1 + (2.5\varphi_e) + (2.5\varphi_e)^2 + (2.5\varphi_e)^3 + (2.5\varphi_e)^4 + \dots$	The effects of the nanolayer on the viscosity equation by modifying the Ward equation and applying an equivalent volume fraction.	Avsec and Oblak (2007) [50]
$\frac{\mu_{nf}}{\mu_f} = (1 + 0.025\varphi + 0.015 \varphi^2),$ $r_p=36$ $\frac{\mu_{nf}}{\mu_f} = 0.904 e^{0.1483\varphi}, r_p=47$	The empirical models for Al ₂ O ₃ -water nanofluid.	Nguyen et al. (2008) [45]
$\mu_{eff} = \mu_f + \frac{\rho_p V_B d_p^2}{72CH}$	The effects of the properties of nanoparticles on the viscosity are considered.	Masoumi et al. (2009) [53]
$\frac{\mu_{nf}}{\mu_f} = \exp \left[m + \alpha \left(\frac{T}{T_0} \right) + \beta(\varphi_n) + \gamma \left(\frac{d_p}{1+s} \right) \right]$	The empirical model is a function of the viscosity of the base liquid, particle volume fraction, particle size, properties of the surfactant layer and temperature.	Hosseini et al. (2010) [54]
$\mu_r = \frac{\mu_{nf}}{\mu_f} = (1 + 2.5 \left[\frac{r_p+t_l+s}{r_p} \right]^3 \varphi)$	The effects of the surfactant monolayer and interfacial nanolayer on nanofluid viscosity are considered.	Yang et al. (2012) [49]

4.2. The effects of the nanolayer on the nanofluid properties and heat transfer

The thermal conductivity ratio of the model of Yu and Choi [25] is calculated for an Al₂O₃-water nanofluid, differing nanolayer thicknesses (1 and 2 nm), a volume fraction range of 1 to 6%, a nanoparticle size of 10 nm, and different nanolayer thermal conductivities. As shown in Figure 10a, the effective thermal conductivity enhancement changes from 23 to 33% in different nanolayer thicknesses for 6% volume fraction.

Same analyses have been performed on the model presented by Xue and Xu [29] for Al₂O₃-water nanofluid. They used the nanolayer thickness and thermal conductivity of the nanolayer, 3 nm and 5 Wm⁻¹ K⁻¹ respectively. As shown in Figure 10b, the thermal conductivity increased from 28 to 54% in 6% volume fraction of nanoparticles.

The model of Xie et al. [30] was also chosen for performing these analyses. These researchers assumed the thermal conductivity of the nanolayer in the intermediate physical state between nanoparticle and base fluid with a linear distribution.

In terms of the different nanolayer thicknesses shown in Figure 11a, in the case of 6% volume fraction of Al₂O₃ in water, effective thermal conductivity enhancement increases from 20 to 44%.

The result for the model of Feng et al. [35] is shown in Figure 11b; the thermal conductivity enhancement has increased by 7%.

As indicated in Figure 12a, the viscosity of Al₂O₃-water nanofluid is calculated for 10 nm spherical particles and a volume fraction range of 1 to 6% when the model of Avsec and Oblak [50] is used. In the 6% volume fraction, the viscosity increases by 21% for a nanolayer thickness equal to 0.5 nm, whereas it increases by 48% when the thickness of the nanolayer is 3 nm.

From the results of these analyses, which have been done on several effective thermal conductivity models, it can be concluded that nanolayer properties like thickness and thermal conductivity impact on the calculated effective thermal conductivity of nanofluids. Thus, more studies are necessary to develop models for these factors.

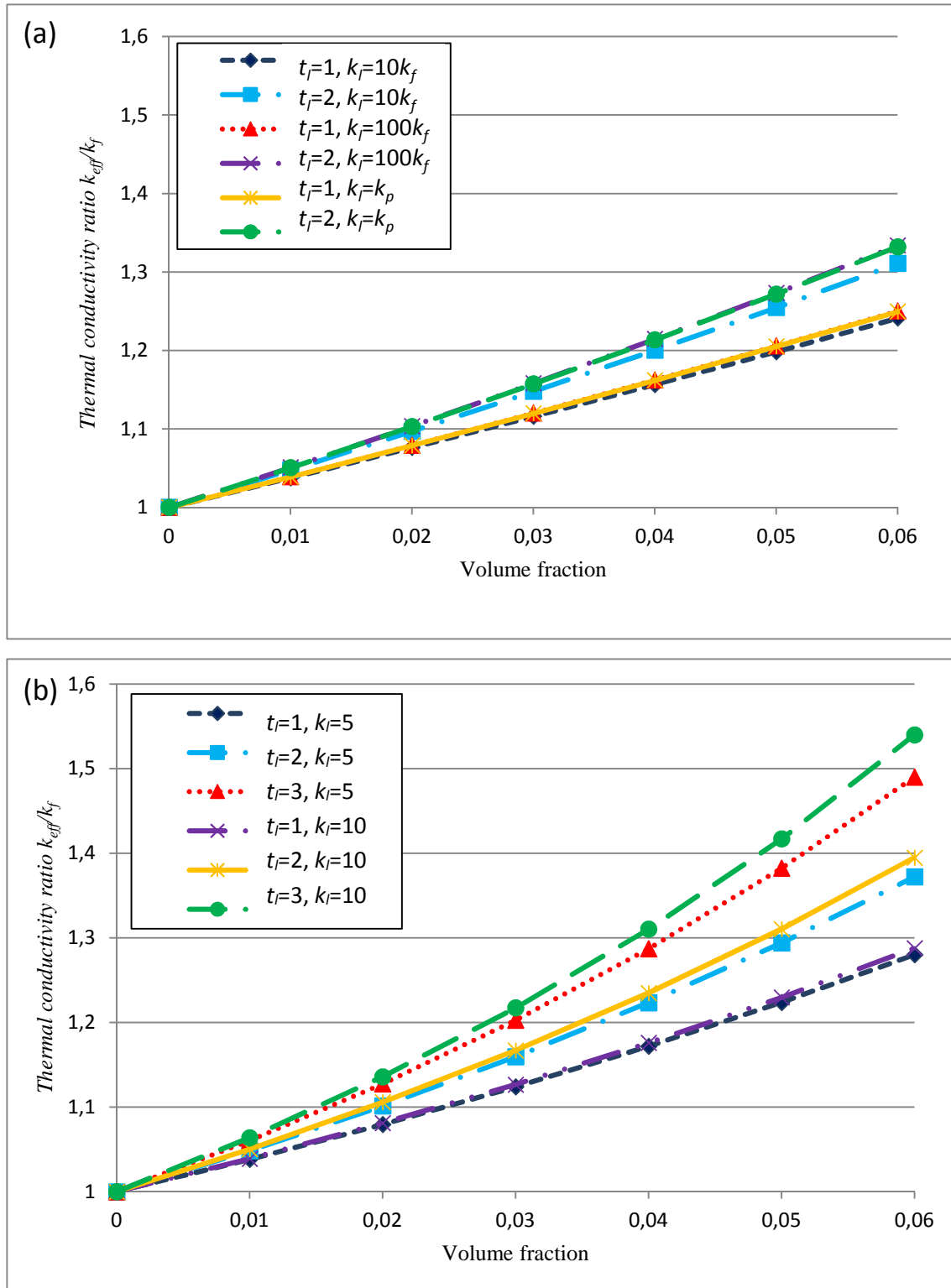


Figure 10: (a) The thermal conductivity ratio of an Al₂O₃-water nanofluid, according to the Yu and Choi [25] model ($k_r = 0.604$, $k_p = 46$, $r_p = 10$). (b) The thermal conductivity ratio of an Al₂O₃-water nanofluid, according to the model of Xue and Xu [29] ($k_r = 0.604$, $k_p = 46$, $r_p = 10$).

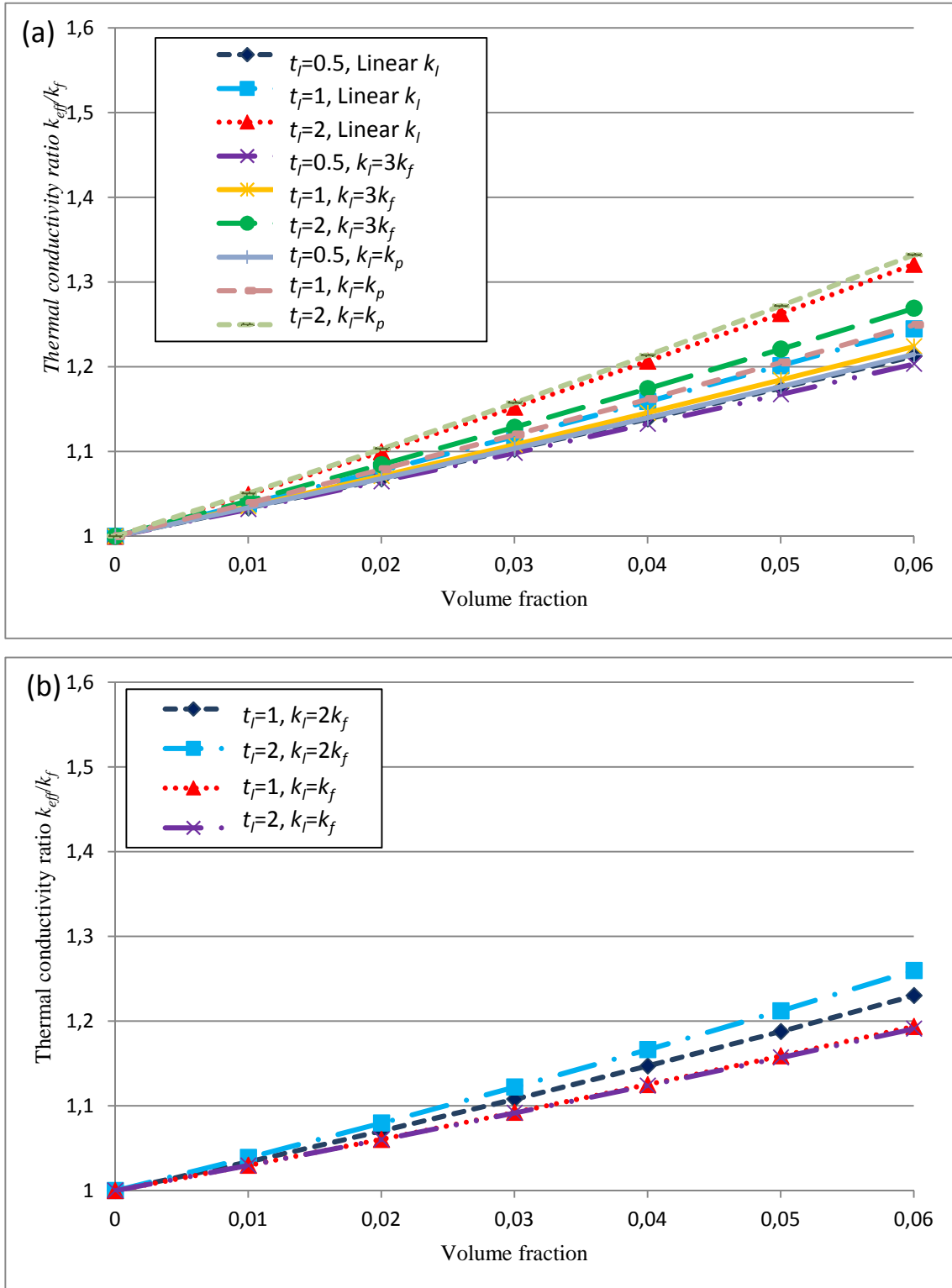


Figure 11: (a) The thermal conductivity ratio of an Al_2O_3 -water nanofluid, according to the model of Xie et al. [30] ($k_f = 0.604$, $k_p = 46$, $r_p = 10$). (b) The thermal conductivity ratio of an Al_2O_3 -water nanofluid according to the model of Feng et al. [35] ($k_f = 0.604$, $k_p = 46$, $r_p = 10$).

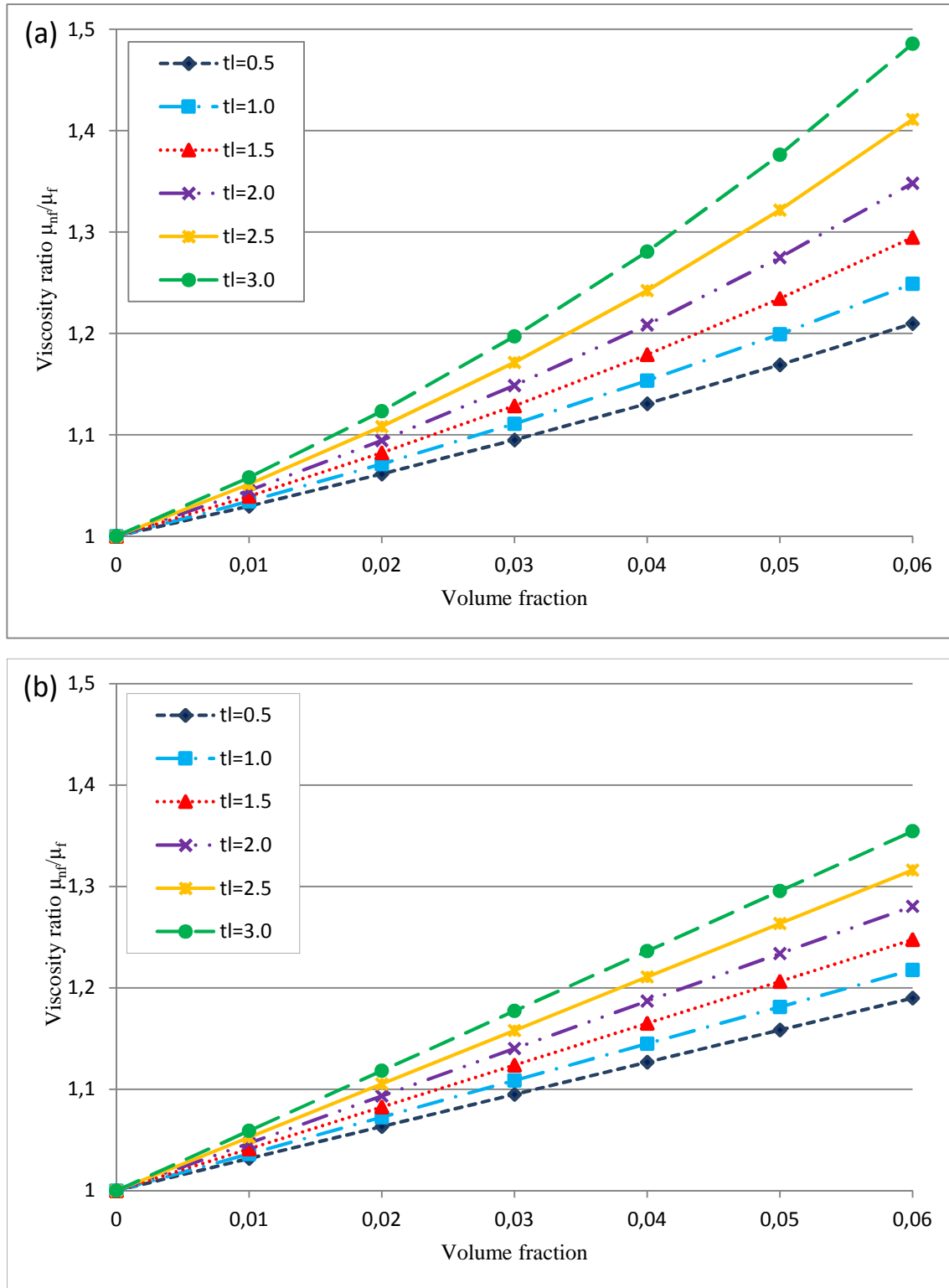


Figure 12: (a) The viscosity ratio of an Al_2O_3 -water nanofluid according to the model of Avsec and Oblak [50]. (b) The viscosity ratio of an Al_2O_3 -water nanofluid according to the model of Yang et al. [49].

In most studies, the nanolayer thickness value is selected or assumed by the authors.

Tillman and Hill [44] attempted to derive an equation to determine nanolayer thickness. A mathematical procedure was developed to determine the nanolayer thickness for any thermal conductivity profile. It was assumed that the nanolayer's thermal conductivity is known. Then, by solving the thermal conductivity equation in a solid-liquid interface, the nanolayer thickness is derived.

The mathematic analysis was done for an Al₂O₃-EG nanofluid, which indicates that the nanolayer thickness is 19% of the nanoparticle radius. Results for CuO-H₂O with the same analysis showed the ratio of the radius of the outer interface to the inner interface of the nanolayer, δ , which is equal to 1.22. Tillman and Hill [44] tested their model for $k_f < 1 \text{ W m}^{-1} \text{ K}^{-1}$ and various equilibrium constants. They concluded that the nanolayer thickness for all nanofluids is in the range of 19 to 22% of the nanoparticle radius. The effects of bonding between the nanoparticle and the base fluid were not considered in their model. There is also no evidence of the accuracy of the equation that was used to measure the thermal conductivity of nanolayer.

In the case of forced convection, the Nusselt and Reynolds numbers, and in the case of natural convection, Grashof or Reyleigh numbers, are dimensionless numbers that have been used to design engineering systems. They will be influenced by the effective thermal conductivity and viscosity of the heat transfer fluids.

$$\text{Nu} = \frac{hL_c}{k_{eff}} \quad (87)$$

$$\text{Re} = \frac{\rho_{nf}VL_c}{\mu_{nf}} \quad (88)$$

$$\text{Gr}_L = \frac{g\beta\rho_{nf}^2(T_s - T_\infty)L_c^3}{\mu_{nf}^2} \quad (89)$$

$$\text{Ra}_L = \text{Gr}_L\text{Pr} \quad (90)$$

The ranges of effective thermal conductivity enhancement and viscosity ratio for nanofluids are 1.20 to 1.44 and 1.19 to 1.48 respectively. If these two extremes are used to calculate each dimensionless number, they will vary over a wide range.

There will be a 20% difference in the calculated Nusselt number, 24% in the Reynolds number, 54% in the Grashof number and 49% in the Rayleigh number when two extremes of k_{eff} and μ_{nf} are used in their formulas.

It is clear that the nanolayer is one of the key factors that must be considered in the evaluation of nanofluids' effective thermal conductivity and viscosity. Unfortunately, most of the available models for determining nanofluids' effective thermal conductivity and viscosity do not include the nanolayer. On the other hand, the ones that consider the nanolayer are not accurate for the prediction of unknown values. Therefore, these uncertainties can produce at least a 20% difference in the calculation of the Nusselt number, as well as a 24% difference in the calculation of the Reynolds number, a 54% difference in the calculation of the Grashof number and a 49% difference in the calculation of the Rayleigh number. Consequently, the authors can conclude that the existing models for determining nanofluids' effective thermal conductivity and viscosity cause errors in thermal system design when nanofluids are used. Therefore, more investigation is necessary in this field.

4.3. Model development for measuring the density of nanofluids

In this section, the influence of the nanolayer's density and thickness on nanofluid density is discussed.

In most of the studies on calculating nanofluid density, a classic formula for a solid-liquid mixture model is used:

$$\rho_{nf} = \varphi \rho_p + (1 - \varphi)\rho_f \quad (91)$$

Equation 91 considers the nanoparticle and base fluid densities and the nanofluid's volume fraction.

However, the effects of nanolayer are not considered in this model and it is known that the formation of this layer could affect the thermo-physical properties of nanofluids.

By using the fact that nanofluids consist of base fluids, nanoparticles and nanolayers, and the correlation of density for mixtures, the process could be started by the following correlation:

$$\rho_{nf} = \varphi_p \rho_p + \varphi_f \rho_f + \varphi_l \rho_l \quad (92)$$

From the volume fraction definition:

$$\varphi_l = \frac{V_l}{V_{nf}} \quad (93)$$

$$\varphi_p = \frac{V_p}{V_{nf}} \quad (94)$$

By using equations 93 and 94:

$$\varphi_l = \frac{V_l}{V_p} \varphi_p \quad (95)$$

For spherical nanoparticles:

$$V_l = \frac{4}{3} \pi (r_o^3 - r_i^3) = \frac{4}{3} \pi r_i^3 (\delta^3 - 1) \quad (96)$$

So:

$$\varphi_l = \frac{V_l}{V_p} \varphi_p = (\delta^3 - 1) \varphi_p \quad (97)$$

Therefore, the model below can be used to determine the nanofluid density:

$$\rho_{nf} = \varphi \rho_p + (1 - \delta^3 \varphi) \rho_f + (\delta^3 - 1) \varphi \rho_l \quad (98)$$

This correlation considers nanoparticle and base fluid densities, nanoparticle size and volume fraction, as well as nanolayer thickness and density. If Equation 98 is to be used, the nanolayer density and thickness are required. According to the literature review conducted in Chapter 2, the nanolayer thickness range used by different authors in other studies is 0.5-3 nm, as presented in Table 5. The nanolayer has been ignored in most of the literature for calculating nanofluid density.

Consequently, by modifying Equation 98 in such a way that experimental results could be used, a correlation that can be used for nanofluid density is derived without knowing the nanolayer thickness and density:

$$\rho_{nf} = \varphi \rho_p + \left(1 - \left(\frac{r_{p+t_l}}{r_p}\right)^3 \varphi\right) \rho_f + \left(\left(\frac{r_{p+t_l}}{r_p}\right)^3 - 1\right) \varphi \rho_l \quad (99)$$

$$r_{po} = r_p + t_l \quad (100)$$

$$\rho_{nf} = \varphi \rho_p + \left(\frac{r_p^3 - r_{po}^3 \varphi}{r_p^3}\right) \rho_f + [(r_{po}^3 - r_p^3) \rho_l] \frac{\varphi}{r_p^3} \quad (101)$$

Table 5: Nanolayer thickness ranges were used in some studies

Nanofluid type	Nanolayer thickness range	Author/year
CuO-EG	$t_l = 1$ nm	Yu and Choi (2003)
	$t_l = 2$ nm	[25]
Al ₂ O ₃ -water	$t_l = 3$ nm	Xue and Xu (2005) [29]
CuO-water		
CuO-EG		
Al ₂ O ₃ -water	$t_l = 0.5$ nm	Xie et al. (2005) [30]
CuO-water	$t_l = 1$ nm	
Cu-EG	$t_l = 2$ nm	
Al ₂ O ₃ -water	$t_l = 1$ nm	Yajie et al. (2005) [32]
CuO-EG	$t_l = 2$ nm	
Cu-EG	$t_l = 3$ nm	
Al ₂ O ₃ -water	$t_l = 1$ nm	Leong et al. (2006) [33]
Al ₂ O ₃ -EG		
CuO-water		
Cu-EG		
Al ₂ O ₃ -water	$t_l = 1$ nm	Feng et al. (2007) [35]
CuO-water		
CuO-EG		
Al ₂ O ₃ -EG		
Al ₂ O ₃ -water	$* t_l = \frac{1}{\sqrt{3}} \left[\frac{4M_w}{\rho_f N_A} \right]^{1/3}$	Ghosh and Mukherjee
CuO-water		(2013) [42]
CuO-EG		*Calculated thicknesses are less
Al ₂ O ₃ -EG		than 1 nm.

4.4. Conclusion

It is clear that the nanolayer is one of the key factors that must be considered for the evaluation of the effective thermal conductivity and viscosity of nanofluids. Unfortunately, most of the available models to determine nanofluids' effective thermal conductivity and viscosity do not include the nanolayer. On the other hand, the models that consider the nanolayer are not accurate for the prediction of unknown values. Therefore, these uncertainties can produce at least a 20% difference in the calculation of the Nusselt number, as well as a 24% difference in the calculation of the Reynolds

number, a 54% difference in the calculation of the Grashof number and a 49% difference in the calculation of the Rayleigh number. Consequently, the existing models for determining nanofluids' thermal conductivity and viscosity cause error in thermal system design when using nanofluids. Therefore, more investigation is necessary in this field.

In section 4.2, a correlation for nanofluid density has been developed by performing a theoretical analysis on the mixture density formula. The unknowns in this correlation could be derived from the experimental results that have been presented in Chapter 3.

CHAPTER 5: RESULTS AND DISCUSSIONS

5.1. Introduction

This chapter deals with the results of the density measurement experiments, and discusses nanofluid density and specific heat capacity.

5.2. Nanofluid density results and discussion

Four different kinds of nanofluids were used for density measurement experiments: SiO₂-water, SiO_x-EG-water, CuO-glycerol and MgO-glycerol.

A comparison of test results shows deviation from the linear model for solid-liquid mixtures that different authors have used to calculate density. An uncertainty analysis was performed, and these deviations are bigger than the density measurement uncertainty range. As is clear in the linear model, the nanolayer effect has not been considered in the nanofluid density model, which could be the reason for these deviations.

Thus, Equation 101 should be used to calculate nanofluid density, instead of the solid-liquid mixture model to consider nanolayer effects.

$$\rho_{nf} = \varphi \rho_p + \left(\frac{r_p^3 - r_{po}^3 \varphi}{r_p^3} \right) \rho_f + [(r_{po}^3 - r_p^3) \rho_l] \frac{\varphi}{r_p^3} \quad (101)$$

The exact figures for nanolayer thickness and density are unknown, so the experimental results should be utilised:

$$A = r_{po}^3 \quad (102)$$

$$B = (r_{po}^3 - r_p^3) \rho_l \quad (103)$$

$$\rho_{nf} = \varphi \rho_p + \frac{(r_p^3 - A\varphi)}{r_p^3} \rho_f + B \frac{\varphi}{r_p^3} \quad (104)$$

A and B are constants which have been used for more simplicity, with values as shown in Table 6. A is dependent to nanoparticle size and B is dependent on the base fluid and nanoparticle size.

Table 6: Nanofluid density model constants

Nanofluid	A (cm ³)	B (gr)
SiO ₂ -water	7,15E-17	4,65E-19
SiO _x -EG-water	1,52E-18	4,67E-19
MgO-glycerol	9,94E-18	1,22E-18
CuO-glycerol	9,94E-18	1,22E-18

Graphs and figures related to these analyses have been presented below.

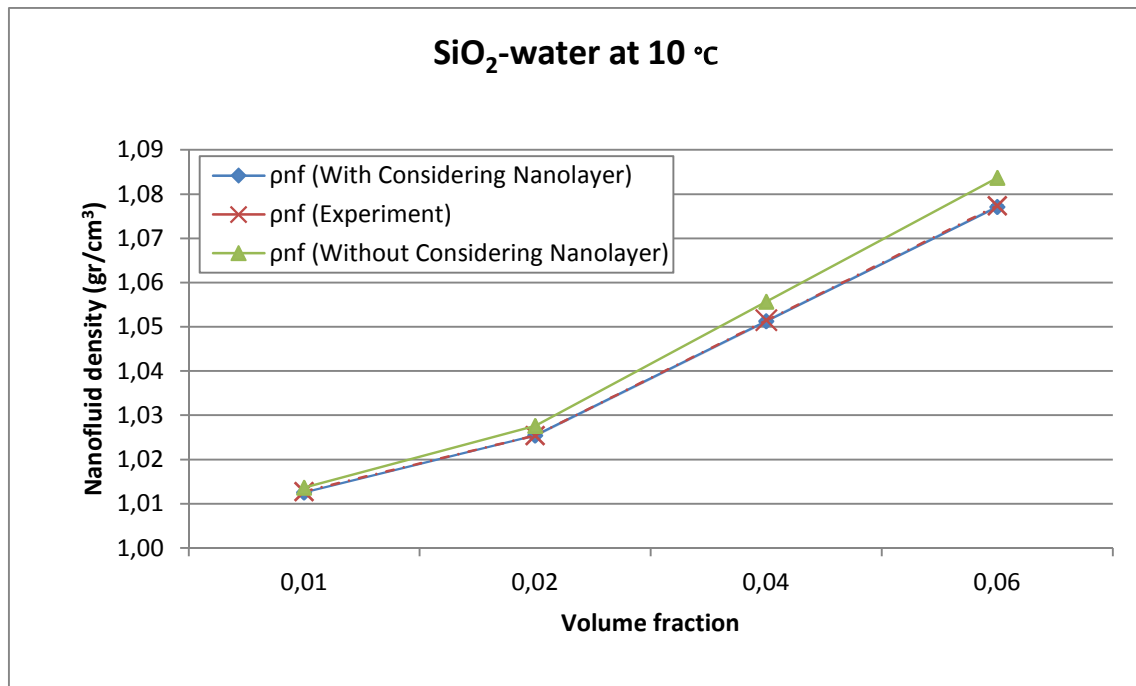


Figure 13: The nanofluid density of SiO₂-water at 10 °C

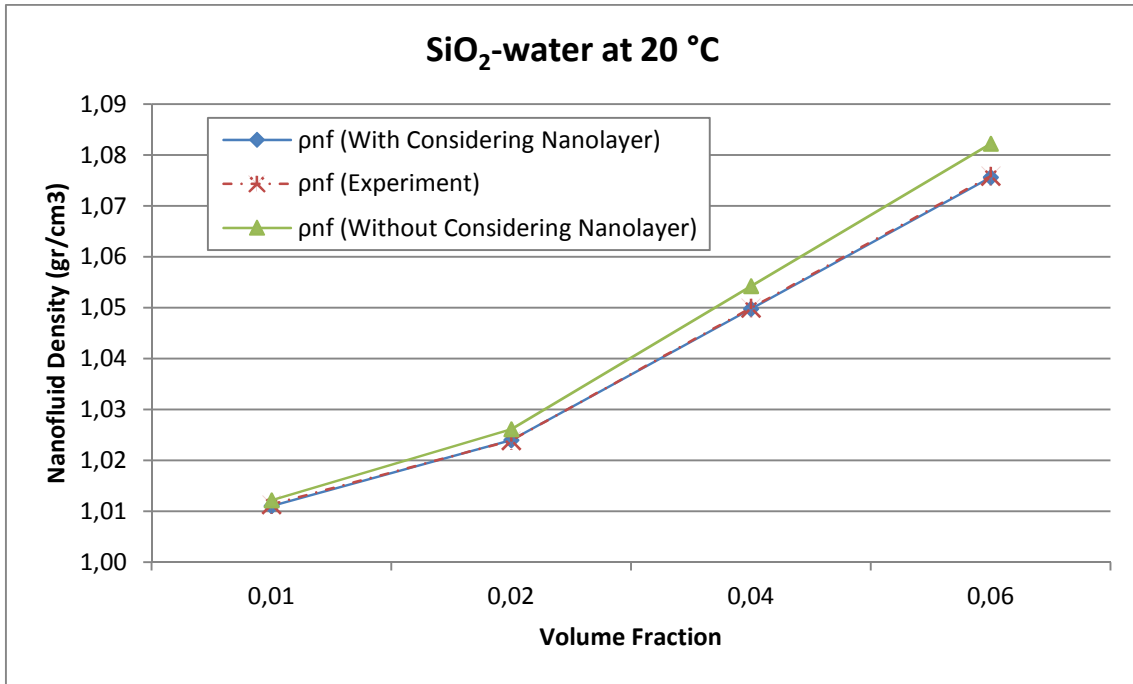


Figure 14: The nanofluid density of SiO₂-water at 20 °C

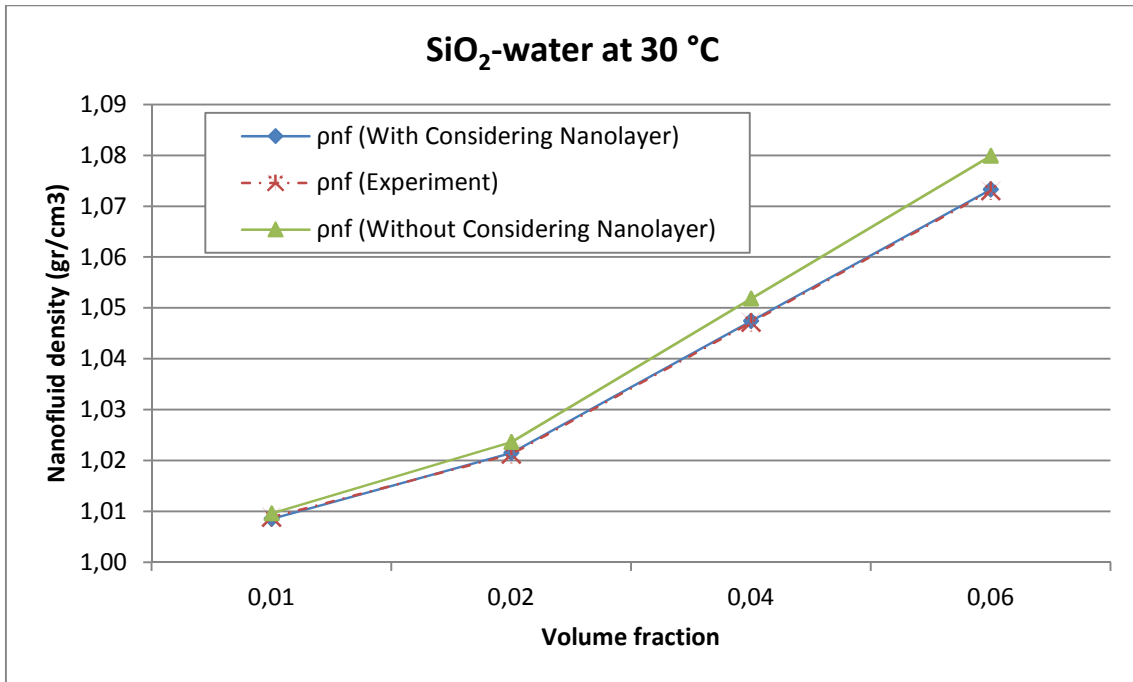


Figure 15: The nanofluid density of SiO₂-water at 30 °C

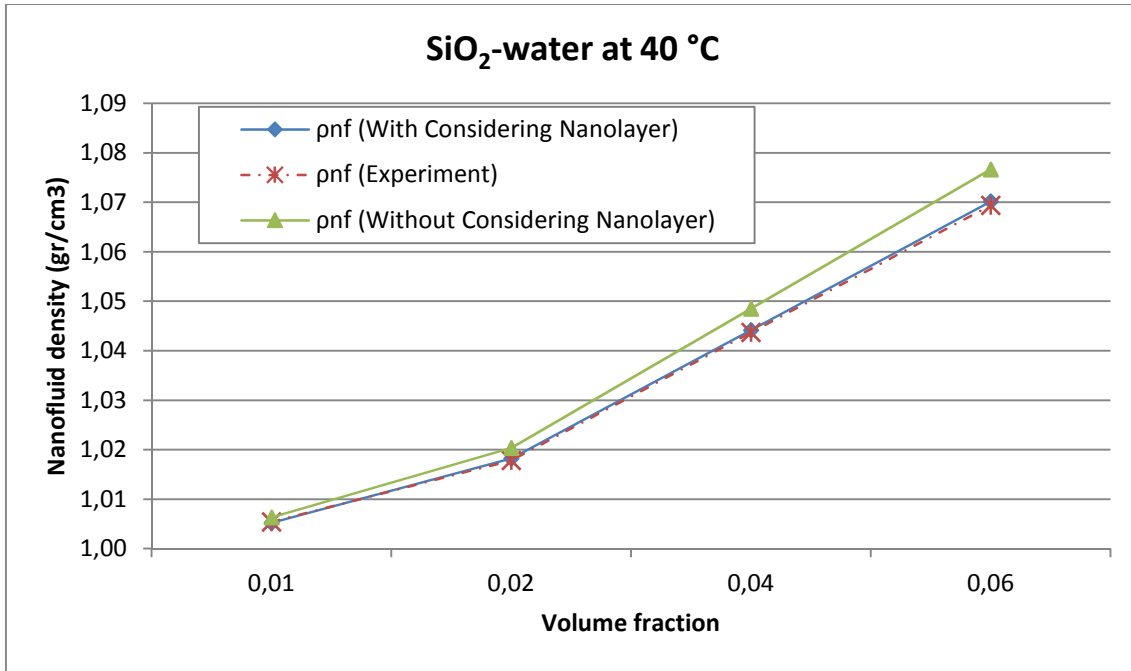


Figure 16: The nanofluid density of SiO₂-water at 40 °C

SiO₂-water

Table 7: The nanofluid density of SiO₂-water

Temp.	ρ_f	ρ_p	ϕ	r_p	ρ_{nf} (considering the nanolayer)	ρ_{nf} (experiment)	ρ_{nf} (without considering the nanolayer)
10 °C	0.999665	2.4	0.01	40	1.01257	1.01283	1.01367
10 °C	0.999665	2.4	0.02	40	1.02548	1.02550	1.02767
10 °C	0.999665	2.4	0.04	40	1.05130	1.05149	1.05571
10 °C	0.999665	2.4	0.06	40	1.07712	1.07742	1.08372
20 °C	0.99814	2.4	0.01	40	1.01107	1.01140	1.01216
20 °C	0.99814	2.4	0.02	40	1.02399	1.02393	1.02618
20 °C	0.99814	2.4	0.04	40	1.04984	1.05001	1.05427
20 °C	0.99814	2.4	0.06	40	1.07569	1.07593	1.08231
30 °C	0.995605	2.4	0.01	40	1.00856	1.00889	1.00965
30 °C	0.995605	2.4	0.02	40	1.02151	1.02129	1.02369
30 °C	0.995605	2.4	0.04	40	1.04742	1.04720	1.05182
30 °C	0.995605	2.4	0.06	40	1.07333	1.07306	1.07991
40 °C	0.99225	2.4	0.01	40	1.00524	1.00545	1.00633
40 °C	0.99225	2.4	0.02	40	1.01823	1.01788	1.02041
40 °C	0.99225	2.4	0.04	40	1.04422	1.04378	1.04852
40 °C	0.99225	2.4	0.06	40	1.07020	1.06946	1.07668

The error bars have been added to experimental results curve in SiO_x-EG-Water nanofluid, and because of the small values compared to graph data they are not visible. (Uncertainty analysis data have been presented in Appendix A)

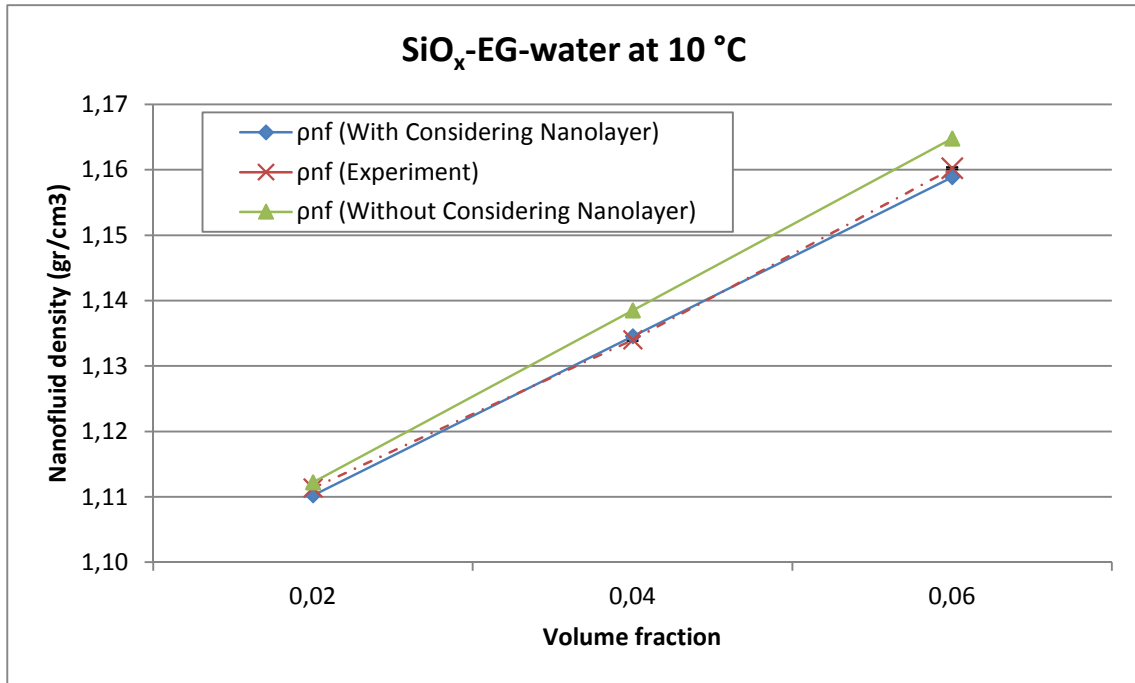


Figure 17: The nanofluid density of SiO_x-EG-water at 10 °C

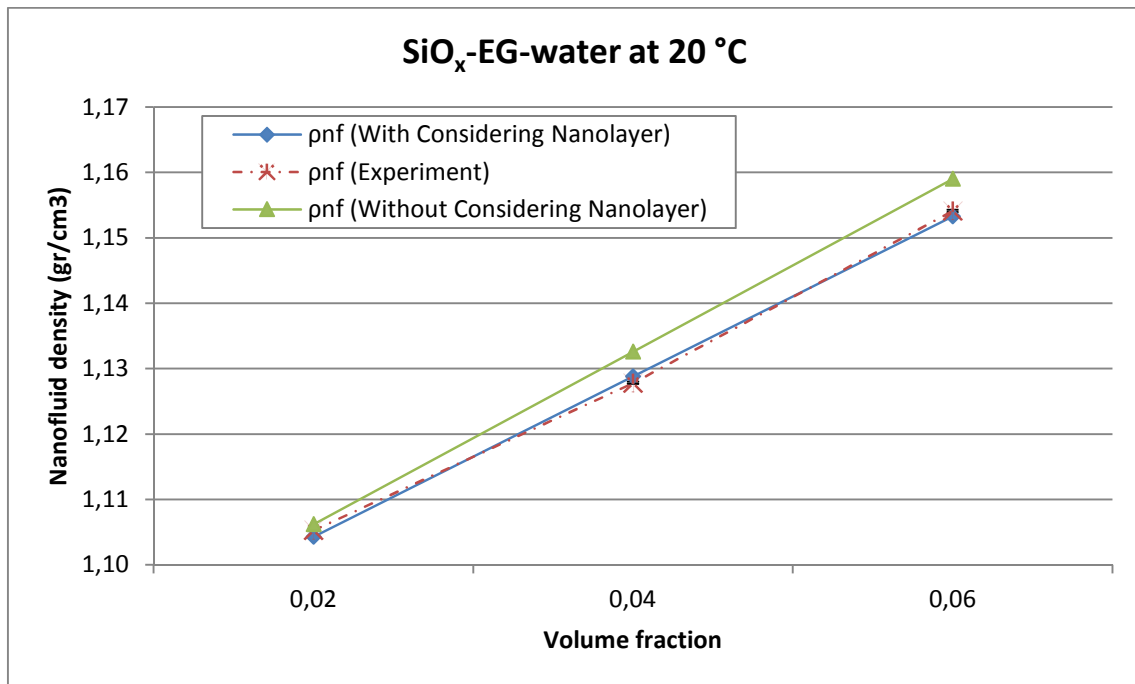


Figure 18: The nanofluid density of SiO_x-EG-water at 20 °C

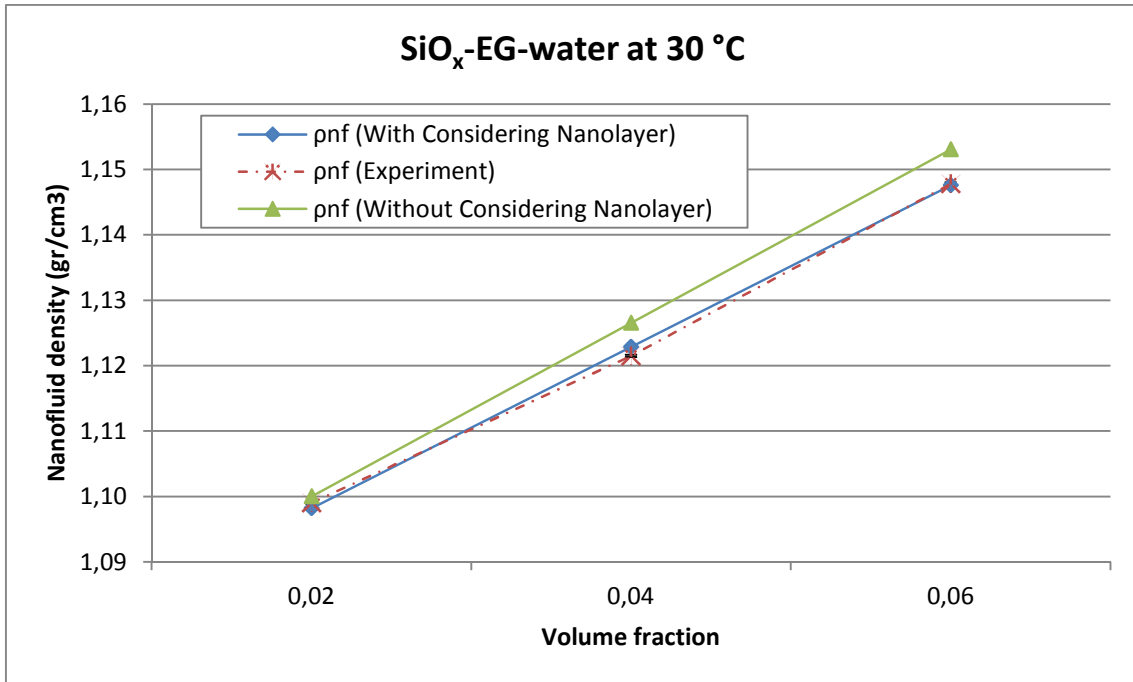


Figure 19: The nanofluid density of SiO_x-EG-water at 30 °C

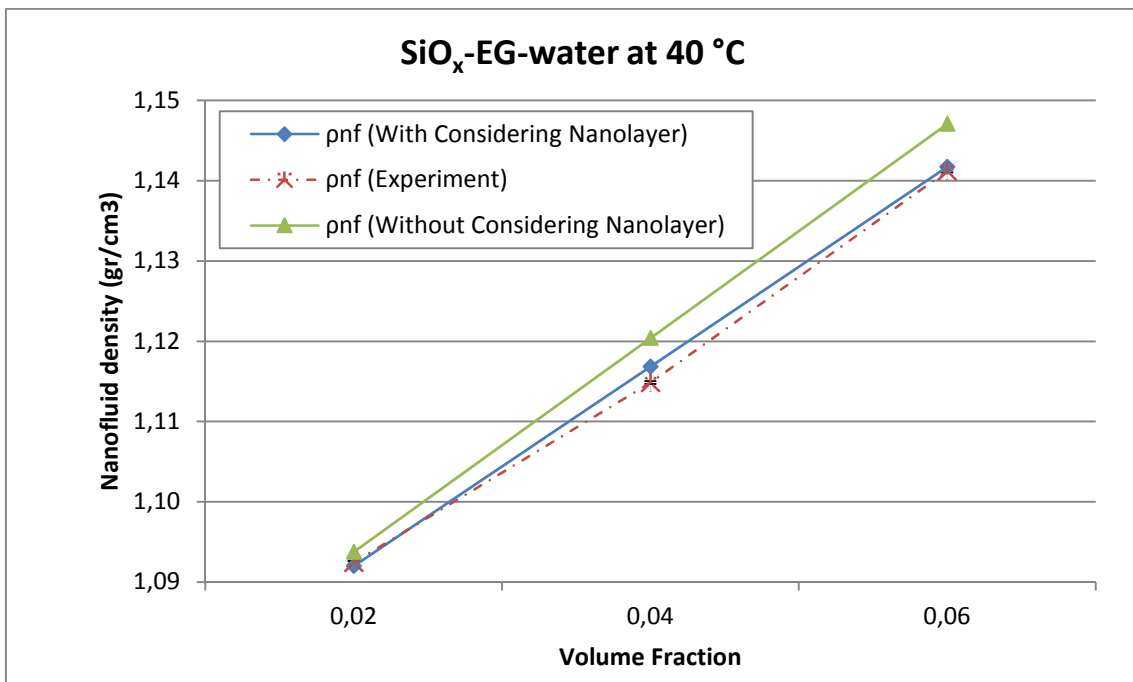


Figure 20: The nanofluid density of SiO_x-EG-water at 40 °C

SiO_x-EG-water

Table 8: The nanofluid density of SiO_x-EG-water

Temperature	ρ_f	ρ_p	φ	r_p	ρ_{nf} (considering the nanolayer)	ρ_{nf} (experiment)	ρ_{nf} (without considering the nanolayer)
10 °C	1.08595	2.4	0.02	10	1.11026	1.11136	1.11223
10 °C	1.08595	2.4	0.04	10	1.13458	1.13402	1.13851
10 °C	1.08595	2.4	0.06	10	1.15889	1.16022	1.16479
20 °C	1.07982	2.4	0.02	10	1.10432	1.10531	1.10622
20 °C	1.07982	2.4	0.04	10	1.12882	1.12784	1.13263
20 °C	1.07982	2.4	0.06	10	1.15332	1.15413	1.15903
30 °C	1.073505	2.4	0.02	10	1.09820	1.09905	1.10003
30 °C	1.073505	2.4	0.04	10	1.12289	1.12151	1.12656
30 °C	1.073505	2.4	0.06	10	1.14758	1.14786	1.15309
40 °C	1.067115	2.4	0.02	10	1.09200	1.09246	1.09377
40 °C	1.067115	2.4	0.04	10	1.11689	1.11486	1.12043
40 °C	1.067115	2.4	0.06	10	1.14178	1.14123	1.14709

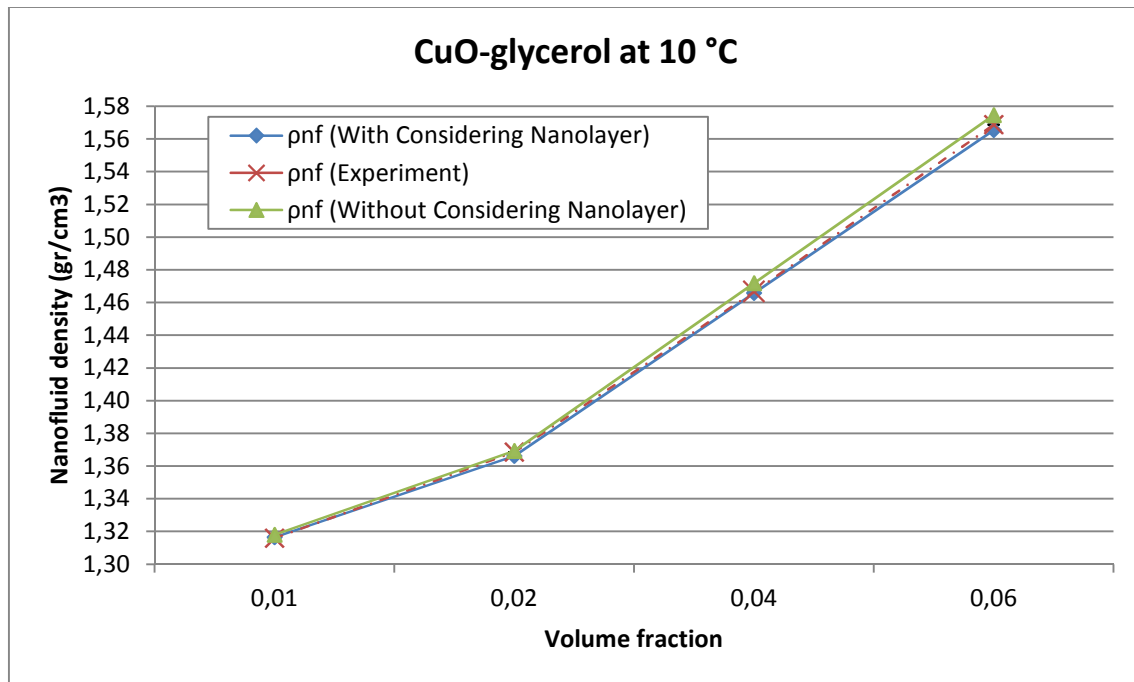


Figure 21: The nanofluid density of CuO-glycerol at 10 °C

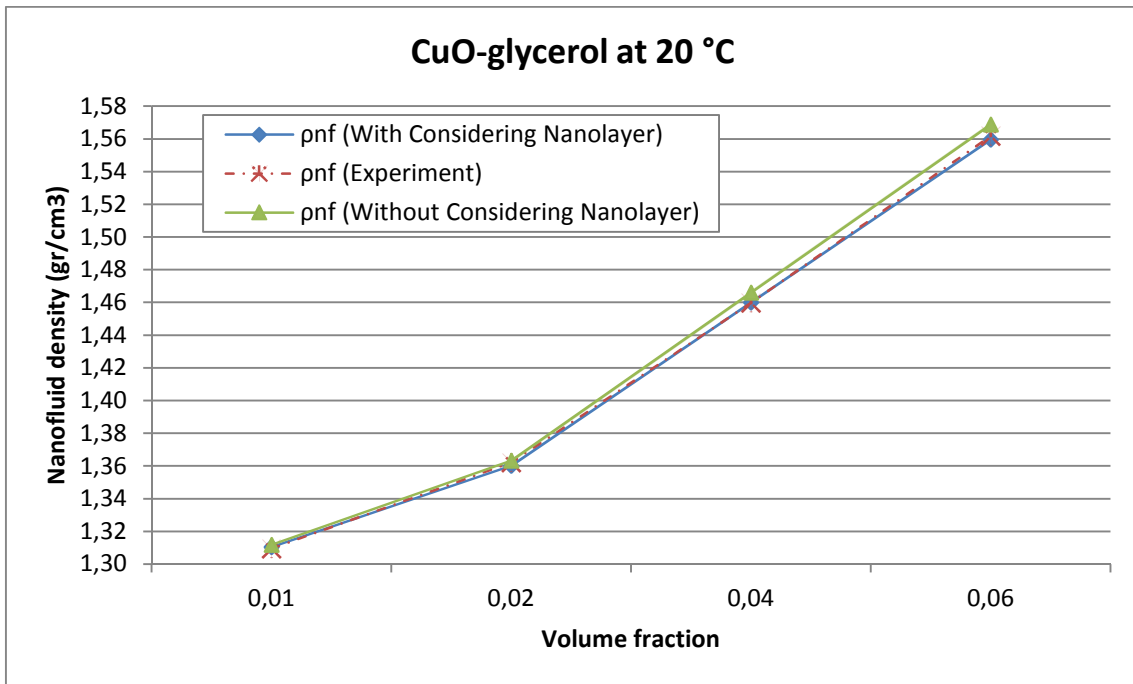


Figure 22: The nanofluid density of CuO-glycerol at 20 °C

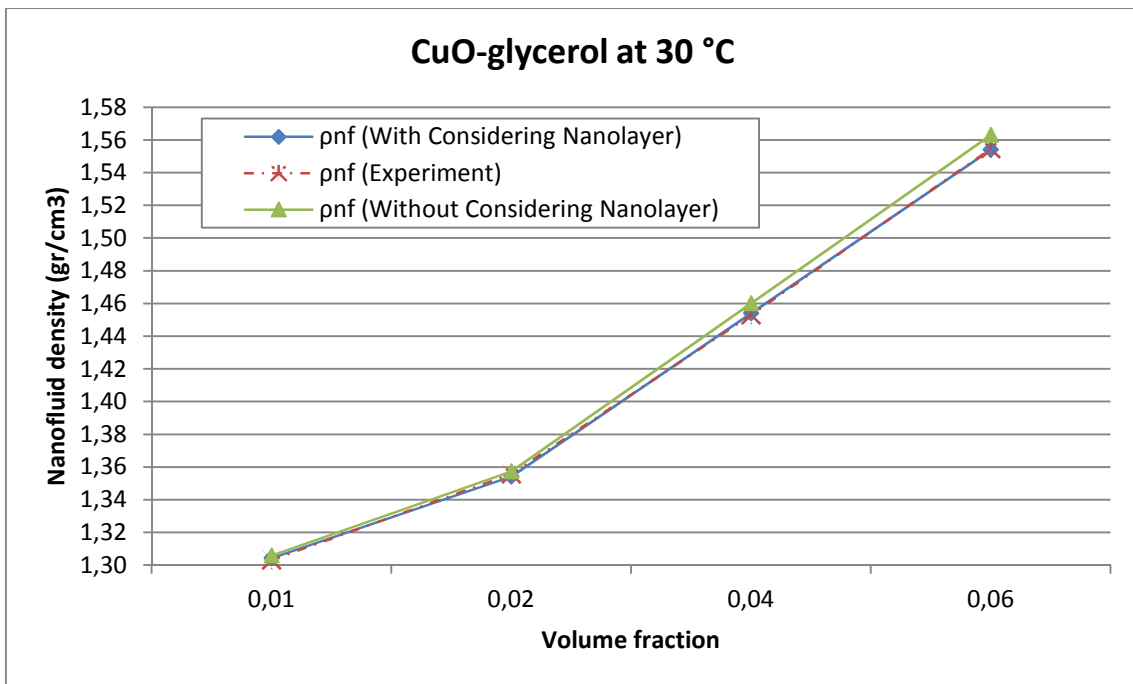


Figure 23: The nanofluid density of CuO-glycerol at 30 °C

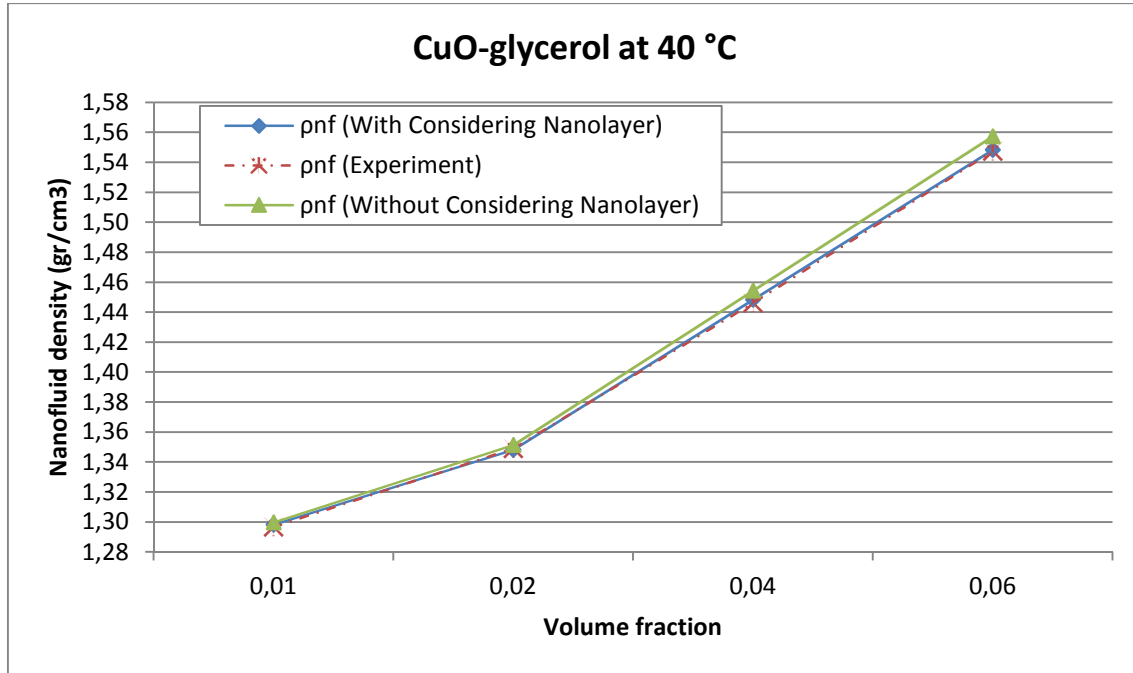


Figure 24: The nanofluid density of CuO-glycerol at 40 °C

CuO-glycerol

Table 9: The nanofluid density of CuO-glycerol

Temperature	ρ_f	ρ_p	φ	r_p	ρ_{nf} (considering the nanolayer)	ρ_{nf} (experiment)	ρ_{nf} (without considering the nanolayer)
10 °C	1.26673	6.4	0.01	20	1.31652	1.31588	1.31806
10 °C	1.26673	6.4	0.02	20	1.36630	1.36869	1.36940
10 °C	1.26673	6.4	0.04	20	1.46588	1.46673	1.47206
10 °C	1.26673	6.4	0.06	20	1.56545	1.56885	1.57473
20 °C	1.26061	6.4	0.01	20	1.31047	1.30959	1.31200
20 °C	1.26061	6.4	0.02	20	1.36034	1.36229	1.36340
20 °C	1.26061	6.4	0.04	20	1.46006	1.45993	1.46619
20 °C	1.26061	6.4	0.06	20	1.55979	1.56181	1.56897
30 °C	1.254395	6.4	0.01	20	1.30434	1.30319	1.30585
30 °C	1.254395	6.4	0.02	20	1.35428	1.35583	1.35731
30 °C	1.254395	6.4	0.04	20	1.45416	1.45305	1.46022
30 °C	1.254395	6.4	0.06	20	1.55404	1.55474	1.56313
40 °C	1.248265	6.4	0.01	20	1.29828	1.29681	1.29978
40 °C	1.248265	6.4	0.02	20	1.34830	1.34912	1.35130
40 °C	1.248265	6.4	0.04	20	1.44833	1.44631	1.45433
40 °C	1.248265	6.4	0.06	20	1.54836	1.54746	1.55737

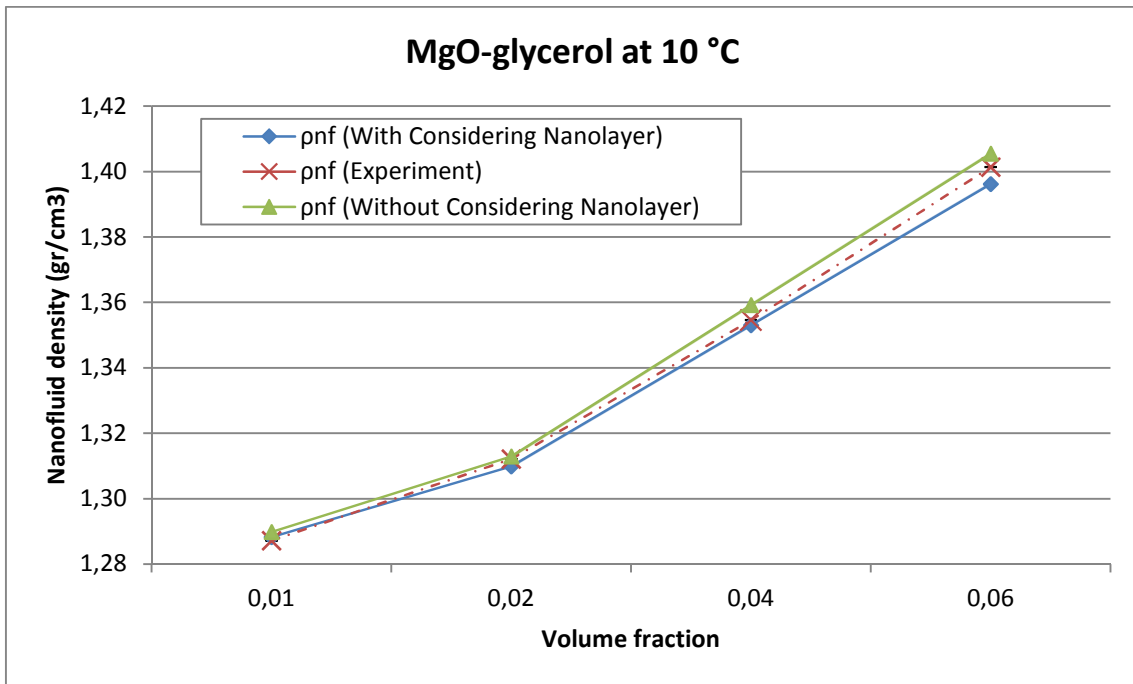


Figure 25: The nanofluid density of MgO-glycerol at 10 °C

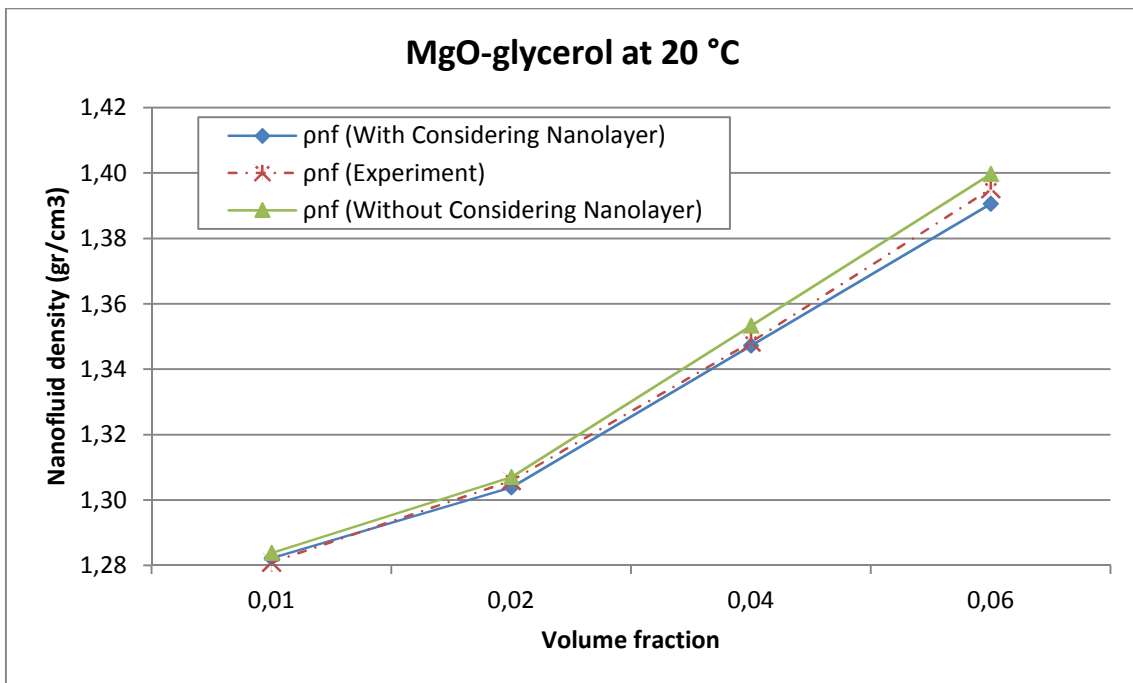


Figure 26: The nanofluid density of MgO-glycerol at 20 °C

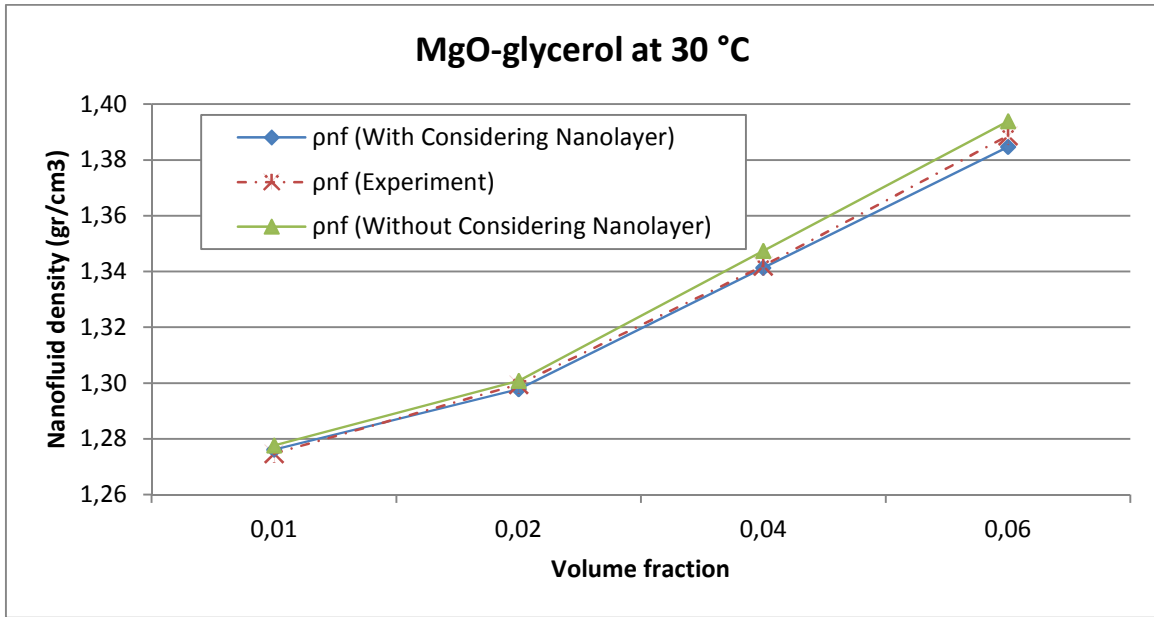


Figure 27: The nanofluid density of MgO-glycerol at 30 °C

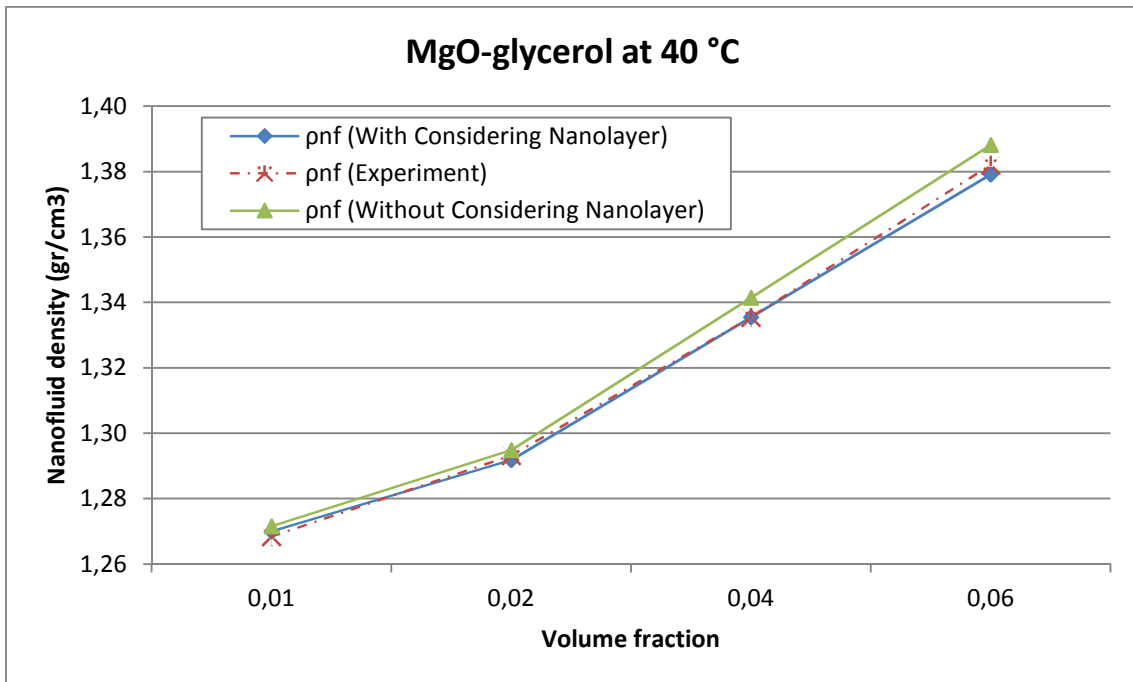


Figure 28: The nanofluid density of MgO-glycerol at 40 °C

MgO-glycerol

Table 10: The nanofluid density of MgO-glycerol

Temp.	ρ_f	ρ_p	ϕ	r_p	ρ_{nf} (considering the nanolayer)	ρ_{nf} (experiment)	ρ_{nf} (without considering the nanolayer)
10 °C	1.26673	3.58	0.01	20	1.28832	1.28724	1.28986
10 °C	1.26673	3.58	0.02	20	1.30990	1.31221	1.31300
10 °C	1.26673	3.58	0.04	20	1.35308	1.35462	1.35926
10 °C	1.26673	3.58	0.06	20	1.39625	1.40148	1.40553
20 °C	1.26061	3.58	0.01	20	1.28227	1.28105	1.28380
20 °C	1.26061	3.58	0.02	20	1.30394	1.30598	1.30700
20 °C	1.26061	3.58	0.04	20	1.34726	1.34838	1.35339
20 °C	1.26061	3.58	0.06	20	1.39059	1.39518	1.39977
30 °C	1.254395	3.58	0.01	20	1.27614	1.27476	1.27765
30 °C	1.254395	3.58	0.02	20	1.29788	1.29965	1.28986
30 °C	1.254395	3.58	0.04	20	1.34136	1.34209	1.31300
30 °C	1.254395	3.58	0.06	20	1.38484	1.38881	1.35926
40 °C	1.248265	3.58	0.01	20	1.27008	1.26852	1.40553
40 °C	1.248265	3.58	0.02	20	1.29190	1.29325	1.28380
40 °C	1.248265	3.58	0.04	20	1.33553	1.33554	1.30700
40 °C	1.248265	3.58	0.06	20	1.37916	1.38217	1.35339

As Graphs show, all four nanofluids have same behaviour as volume fraction increase, the effects of nanolayer on the resultant density increases, so the variance between experiment and traditional linear model increase.

In terms of base fluids, this variance is less when the base fluid is Glycerol. In case of nanofluids with water or EG-Water, the variances between densities increase.

Change in temperature doesn't have a visible effect on density differences between three different densities in a sample.

The fluid density model could also be used as a base formula to develop a model for nanofluid density:

$$\rho_{nf} = \frac{m_p + m_f}{V_p + V_f + V_l}, \quad (105)$$

where m_p and V_f are the amount of material that was used to test each sample. V_p and m_f could also be calculated from properties of nanoparticles and base fluid at experiment temperature. Nanofluid density is the experiment result. Nanolayer thickness could be calculated as follows:

$$V_p = n \left(\frac{4}{3} \pi r_p^3 \right) \quad (106)$$

$$V_p + V_l = n \left(\frac{4}{3} \pi (r_p + t_l)^3 \right) \quad (107)$$

Nanolayer thickness for each sample at each temperature will be calculated by substituting n from Equation 106 to Equation 107. Tables 11 to 13 show the results of this method for SiO₂-water, SiO_x-EG-water, CuO-glycerol and MgO-glycerol respectively. The average nanolayer thickness for each type of nanofluid has been presented in the tables, ranging from 0.5 to 1.5 nm (Average of 1.04 nm). Comparing the results shows that nanolayer thickness is mostly dependent on the base fluid type.

Table 11: The results of nanolayer thickness calculations for SiO₂-water nanofluid

T (°C)	φ	ρ_f	ρ_p	r_p	ρ_{nf}	M_p	M_f	V_p	V_f	V_l	t_l (nm)	Ave. t_l
10	0,01	0,99967	2,4	40	1,01283	0,9697	39,9866	0,4040	40	0,0334	1,0745	at 10°C: 1,25
10	0,02	0,99967	2,4	40	1,02550	1,9592	39,9866	0,8163	40	0,0866	1,3678	
10	0,04	0,99967	2,4	40	1,05149	4,0000	39,9866	1,6667	40	0,1662	1,2875	
10	0,06	0,99967	2,4	40	1,07742	6,1277	39,9866	2,5532	40	0,2474	1,2526	
20	0,01	0,99814	2,4	40	1,01140	0,9697	39,9256	0,4040	40	0,0305	0,9823	at 20°C: 1,24
20	0,02	0,99814	2,4	40	1,02393	1,9592	39,9256	0,8163	40	0,0896	1,4126	
20	0,04	0,99814	2,4	40	1,05001	4,0000	39,9256	1,6667	40	0,1670	1,2940	
20	0,06	0,99814	2,4	40	1,07593	6,1277	39,9256	2,5532	40	0,2500	1,2652	
30	0,01	0,99561	2,4	40	1,00889	0,9697	39,8242	0,4040	40	0,0306	0,9852	at 30°C: 1,32
30	0,02	0,99561	2,4	40	1,02129	1,9592	39,8242	0,8163	40	0,0960	1,5108	
30	0,04	0,99561	2,4	40	1,04720	4,0000	39,8242	1,6667	40	0,1823	1,4080	
30	0,06	0,99561	2,4	40	1,07306	6,1277	39,8242	2,5532	40	0,2702	1,3640	
40	0,01	0,99225	2,4	40	1,00545	0,9697	39,6900	0,4040	40	0,0353	1,1314	at 40°C: 1,41
40	0,02	0,99225	2,4	40	1,01788	1,9592	39,6900	0,8163	40	0,1015	1,5928	
40	0,04	0,99225	2,4	40	1,04378	4,0000	39,6900	1,6667	40	0,1910	1,4732	
40	0,06	0,99225	2,4	40	1,06946	6,1277	39,6900	2,5532	40	0,2889	1,4550	

Table 12: The results of nanolayer thickness calculations for SiO_x-EG-water nanofluid

T (°C)	φ	ρ_f	ρ_p	r_p	ρ_{nf}	M_p	M_f	V_p	V_f	V_l	t_l (nm)	Ave. t_l
10	0,02	1,08595	2,4	10	1,11136	1,95918	43,43800	0,81633	40	0,03199	0,12895	at 10°C: 1,1
10	0,04	1,08595	2,4	10	1,13402	4,00000	43,43800	1,66667	40	0,16505	0,31976	
10	0,06	1,16022	2,4	10	1,16022	6,12766	46,40880	2,55319	40	2,72827	2,74159	
20	0,02	1,07982	2,4	10	1,10531	1,95918	43,19280	0,81633	40	0,03374	0,13590	at 20°C: 1,1
20	0,04	1,07982	2,4	10	1,12784	4,00000	43,19280	1,66667	40	0,17704	0,34224	
20	0,06	1,15413	2,4	10	1,15413	6,12766	46,16520	2,55319	40	2,75614	2,76396	
30	0,02	1,07351	2,4	10	1,09905	1,95918	42,94020	0,81633	40	0,03676	0,14792	at 30°C: 1,1
30	0,04	1,07351	2,4	10	1,12151	4,00000	42,94020	1,66667	40	0,18798	0,36266	
30	0,06	1,14786	2,4	10	1,14786	6,12766	45,91440	2,55319	40	2,78514	2,78716	
40	0,02	1,06712	2,4	10	1,09246	1,95918	42,68460	0,81633	40	0,04923	0,19712	at 40°C: 1,1
40	0,04	1,06712	2,4	10	1,11486	4,00000	42,68460	1,66667	40	0,20819	0,40015	
40	0,06	1,14123	2,4	10	1,14123	6,12766	45,64920	2,55319	40	2,81616	2,81187	

Table 13: The results of nanolayer thickness calculations for CuO-glycerol nanofluid

T (°C)	φ	ρ_f	ρ_p	r_p	ρ_{nf}	M_p	M_f	V_p	V_f	V_l	t_l (nm)	Ave. t_l
10	0,01	1,26673	6,4	20	1,31588	2,58586	50,66920	0,40404	40	0,06702	1,04976	at 10°C: 0,55
10	0,02	1,26673	6,4	20	1,36869	5,22449	50,66920	0,81633	40	0,02119	0,17154	
10	0,04	1,26673	6,4	20	1,46673	10,66667	50,66920	1,66667	40	0,15144	0,58827	
10	0,06	1,26673	6,4	20	1,56885	16,34043	50,66920	2,55319	40	0,15938	0,40780	
20	0,01	1,26061	6,4	20	1,30959	2,58586	50,42440	0,40404	40	0,07463	1,16250	at 20°C: 0,65
20	0,02	1,26061	6,4	20	1,36229	5,22449	50,42440	0,81633	40	0,03334	0,26866	
20	0,04	1,26061	6,4	20	1,45993	10,66667	50,42440	1,66667	40	0,17868	0,69060	
20	0,06	1,26061	6,4	20	1,56181	16,34043	50,42440	2,55319	40	0,19531	0,49750	
30	0,01	1,25440	6,4	20	1,30319	2,58586	50,17580	0,40404	40	0,08266	1,28017	at 30°C: 0,75
30	0,02	1,25440	6,4	20	1,35583	5,22449	50,17580	0,81633	40	0,04462	0,35793	
30	0,04	1,25440	6,4	20	1,45305	10,66667	50,17580	1,66667	40	0,20558	0,79065	
30	0,06	1,25440	6,4	20	1,55474	16,34043	50,17580	2,55319	40	0,22981	0,58290	
40	0,01	1,24827	6,4	20	1,29681	2,58586	49,93060	0,40404	40	0,09261	1,42421	at 40°C: 0,88
40	0,02	1,24827	6,4	20	1,34912	5,22449	49,93060	0,81633	40	0,06610	0,52584	
40	0,04	1,24827	6,4	20	1,44631	10,66667	49,93060	1,66667	40	0,23117	0,88496	
40	0,06	1,24827	6,4	20	1,54746	16,34043	49,93060	2,55319	40	0,27249	0,68759	

5.3. Nanofluids' isobaric specific heat capacity results and discussions

In this section, the nanofluid density model and the model for specific heat capacity for nanofluids have been combined, and the results have been compared with experimental data. As shown in Section 2.6, nanofluids' specific heat capacity is as follows:

$$c_{p,nf} = \frac{\varphi \rho_p c_{p,p} + (1-\varphi) \rho_f c_{p,f}}{\rho_{nf}} \quad (108)$$

$$\rho_{nf} = \varphi \rho_p + \frac{(r_p^3 - A\varphi)}{r_p^3} \rho_f + B \frac{\varphi}{r_p^3} \quad (109)$$

$$c_{p,nf} = \frac{\varphi \rho_p c_{p,p} + (1-\varphi) \rho_f c_{p,f}}{\varphi \rho_p + \frac{(r_p^3 - A\varphi)}{r_p^3} \rho_f + B \frac{\varphi}{r_p^3}} \quad (110)$$

Substituting the nanofluid density from Equation 109 into Equation 108 will result in a more accurate specific heat capacity value.

Vajjha and Das [80] performed some experiments for measuring the specific heat capacity of three different nanofluids. They used experimental results and theoretical analysis to derive a model to calculate the specific heat capacity:

$$\frac{c_{p,nf}}{c_{p,f}} = \frac{\left((AT) + B \left(\frac{c_{p,p}}{c_{p,f}} \right) \right)}{(C + \varphi)}, \quad (111)$$

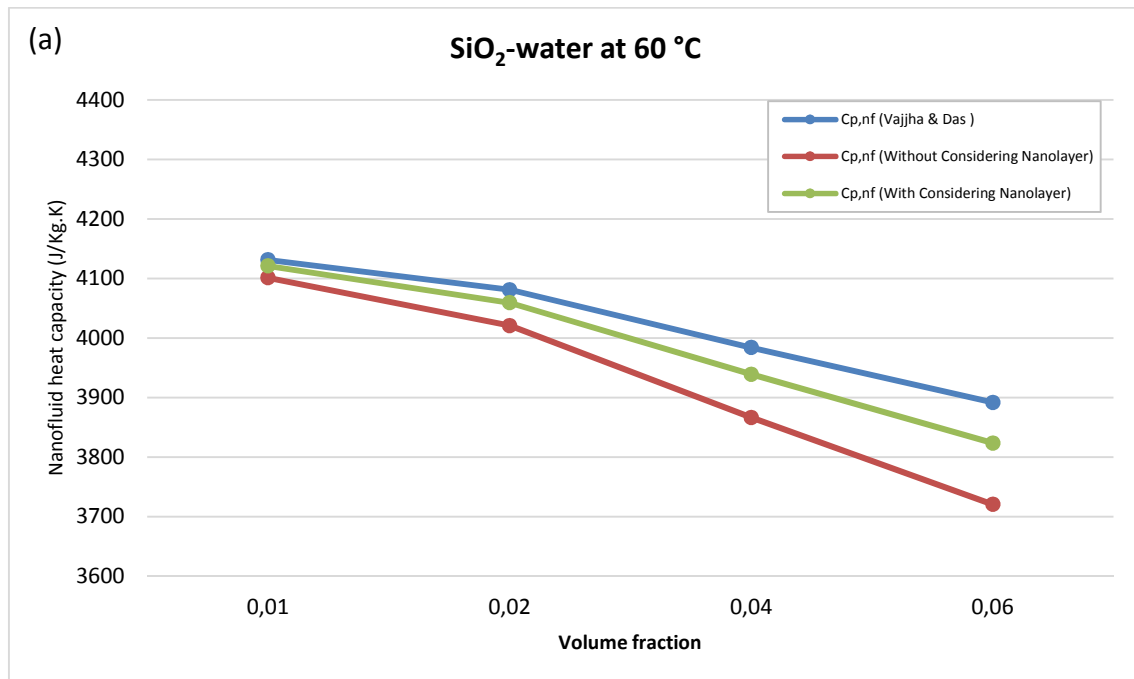
where SiO₂-water nanofluid A = 0.001769, B = 1.1937 and C = 0.8021.

This equation is applicable for the SiO₂ nanofluid in the temperature range of 315 K < T < 363 K for volumetric concentrations in the range of 0 < φ ≤ 0.1.

Comparing the SiO₂ -water nanofluid's specific heat capacities calculated from Equation 108, Equation 110 and the equation that resulted from the experiments of Vajjha and Das show the results from the equation, which consider that the effects of the nanolayer are closer to experimental data.

Table 14: Specific heat capacity of SiO₂ nanofluid in a volume fraction ranging from 1 to 6%, at temperatures of 60, 70 and 80 °C

Temp.	ϕ	r_p	T ('K)	$c_{p,p}$	$c_{p,f}$	$c_{p,nf}$ (Vajjha and Das)	$c_{p,nf}$ (without considering the nanolayer)	$c_{p,nf}$ (considering the nanolayer)
60 °C	0.01	10	333.15	745.00	4184.3	4132	4102	4121
60 °C	0.02	10	333.15	745.00	4184.3	4081	4021	4060
60 °C	0.04	10	333.15	745.00	4184.3	3984	3867	3939
60 °C	0.06	10	333.15	745.00	4184.3	3892	3721	3824
70 °C	0.01	10	343.15	745.00	4189.5	4227	4106	4126
70 °C	0.02	10	343.15	745.00	4189.5	4175	4025	4064
70 °C	0.04	10	343.15	745.00	4189.5	4076	3870	3943
70 °C	0.06	10	343.15	745.00	4189.5	3982	3723	3826
80 °C	0.01	10	353.15	745.00	4196.3	4323	4112	4132
80 °C	0.02	10	353.15	745.00	4196.3	4271	4031	4069
80 °C	0.04	10	353.15	745.00	4196.3	4169	3874	3947
80 °C	0.06	10	353.15	745.00	4196.3	4072	3726	3829



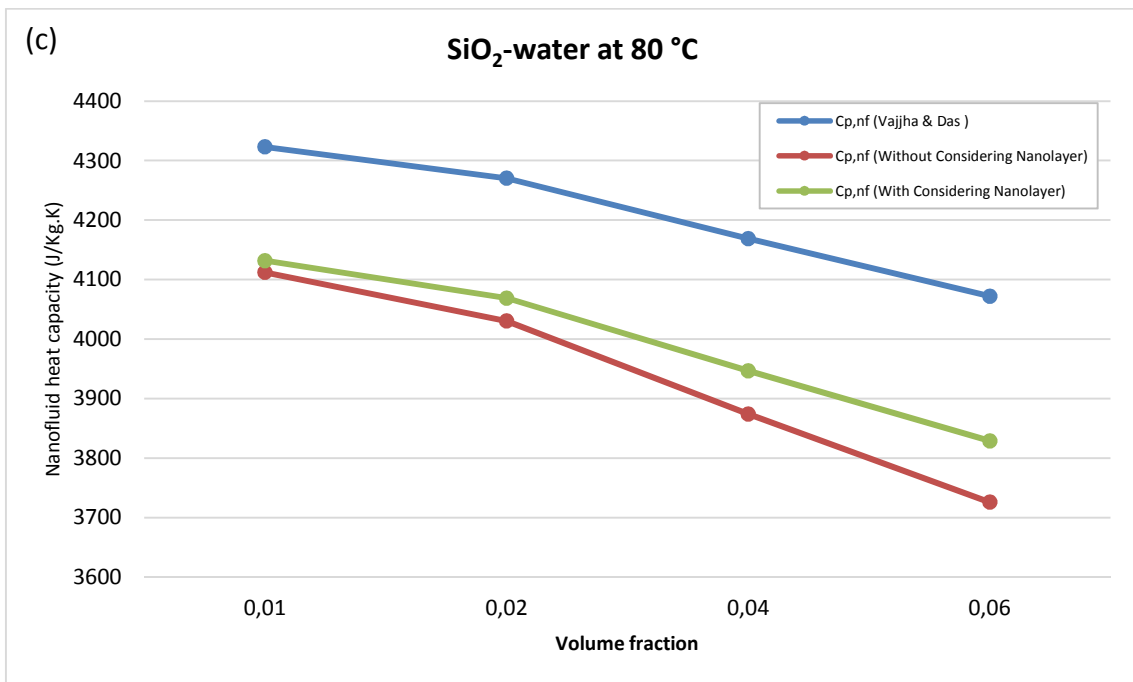
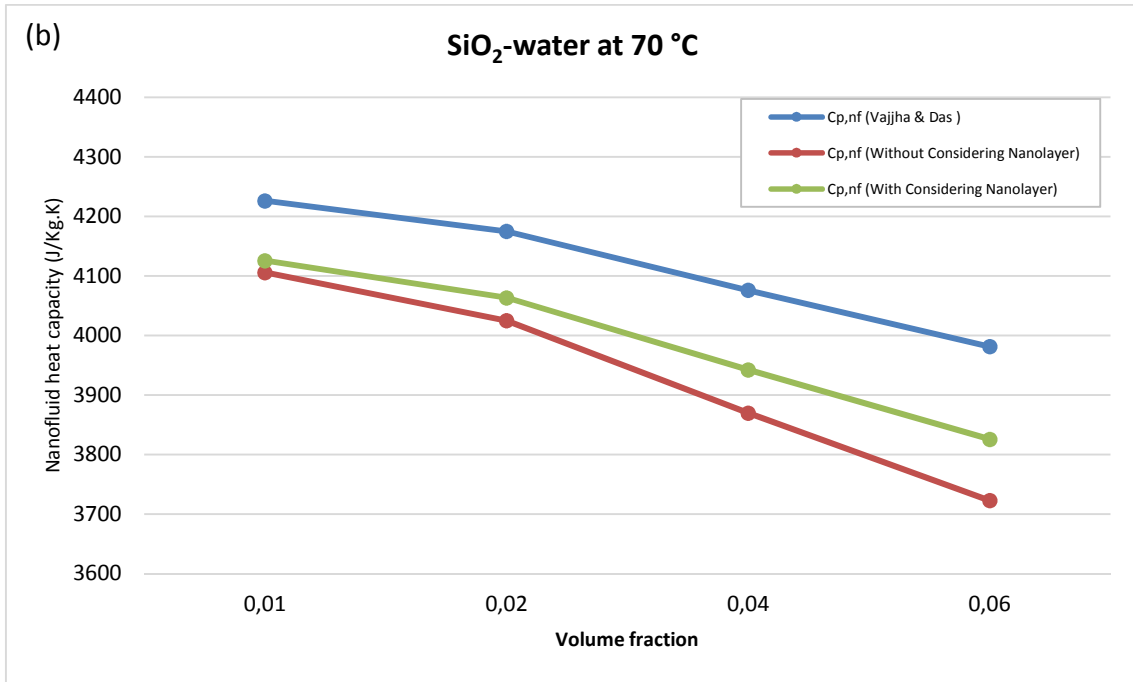


Figure 29a-c: The specific heat capacity of SiO₂-water in the range of a volume fraction of 1 to 6%, at temperatures 60, 70 and 80 °C

Another approach is to consider the nanolayer's specific heat capacity in calculations. Murshed, Leong and Yang [85] presented a model for the specific heat capacity of equivalent nanoparticles, as indicated below:

$$c_{p,e} = \frac{1}{(1+\gamma)^3} c_{p,p} + \left(1 - \frac{1}{(1+\gamma)^3}\right) \left\{ \frac{3c_{p,p}}{pb'^3} (2t^2 + 2b'r_p t + b'^2 r_p^2) - \frac{3c_{p,f}}{pb'^3} [t^2(2 + 2b' + b'^2) + b'r_p(b'r_p + 2b't + 2t)] \right\}, \quad (112)$$

where $p = (3r_p^2 + 3r_p t + t^2)$, $b = \ln(\rho_p/\rho_f)$, and $b' = \ln(c_{p,p}/c_{p,f})$

By inserting $c_{p,e}$ instead of $c_{p,p}$ in Equation 110, the result is closer to experimental data, as presented in Table 15, which means that the effects of the nanolayer on the nanofluids' specific heat capacity requires further study.

Table 15: The specific heat capacity of equivalent SiO₂ nanoparticles in water from Equation 112

Temp.	ρ_f	ρ_p	r_p	γ	$c_{p,p}$	$c_{p,f}$	p	b	b'	$c_{p,e}$
50 °C	0.9923	2.4	10	0.15	745	4180.6	347.25	0.88	-1.72	1198.18
60 °C	0.9832	2.4	10	0.15	746	4184.3	347.25	0.89	-1.72	1199.58
70 °C	0.9775	2.4	10	0.15	747	4189.5	347.25	0.90	-1.72	1201.14
80 °C	0.9718	2.4	10	0.15	748	4196.3	347.25	0.90	-1.72	1202.88

5.4. Conclusion

In the first section of this chapter, the nanofluid density is discussed. By utilising the experimental data presented in Chapter 3 and the developed model in Chapter 4, the proposed model is analysed. Therefore, the experimental density data is compared with the presented model and the mixture density model. The comparisons show that the developed model gives a more accurate result (closer to the experimental data).

In section 5.3, nanofluids' specific heat capacity is investigated theoretically. Two figures that resulted from the specific heat capacity model have been compared with available experimental data for SiO₂-water nanofluids. One of the figures is calculated using the mixture density formula, so nanolayer effects are ignored in the calculations. The other figure is calculated using the developed model for nanofluid density, which considers the nanolayer effects. The comparisons show that the nanolayer could affect

nanofluids' specific heat capacity and, by considering the effects, more accurate results for performing engineering designs can be obtained.

Table 16: The specific heat capacity of SiO₂-water comparisons

Temp.	ϕ	r_p	$c_{p,p}$	$c_{p,f}$	$c_{p,e}$	$c_{p,nf}$ (Vajjh a and Das)	Without considering the nanolayer		Considering the nanolayer in pnf		Considering the nanolayer in pnf and Cp	
							$c_{p,nf}$	Variance	$c_{p,nf}$	Variance	$c_{p,nf}$	Variance
50 °C	0.01	10	745.0	4180.6	1198.0	4038	4098	1.50%	4118	1.99%	4129	2.26%
50 °C	0.02	10	745.0	4180.6	1198.0	3989	4018	0.74%	4057	1.71%	4078	2.25%
50 °C	0.04	10	745.0	4180.6	1198.0	3894	3865	-0.75%	3937	1.12%	3980	2.20%
50 °C	0.06	10	745.0	4180.6	1198.0	3804	3719	-2.22%	3822	0.49%	3885	2.13%
60 °C	0.01	10	745.0	4184.3	1200.0	4132	4102	-0.73%	4121	-0.25%	4132	0.02%
60 °C	0.02	10	745.0	4184.3	1200.0	4081	4021	-1.48%	4060	-0.53%	4081	0.00%
60 °C	0.04	10	745.0	4184.3	1200.0	3984	3867	-2.95%	3939	-1.13%	3982	-0.05%
60 °C	0.06	10	745.0	4184.3	1200.0	3892	3721	-4.40%	3824	-1.76%	3887	-0.14%
70 °C	0.01	10	745.0	4189.5	1201.0	4227	4106	-2.85%	4126	-2.38%	4137	-2.12%
70 °C	0.02	10	745.0	4189.5	1201.0	4175	4025	-3.60%	4064	-2.67%	4086	-2.15%
70 °C	0.04	10	745.0	4189.5	1201.0	4076	3870	-5.06%	3943	-3.28%	3986	-2.22%
70 °C	0.06	10	745.0	4189.5	1201.0	3982	3723	-6.50%	3826	-3.91%	3889	-2.32%
80 °C	0.01	10	745.0	4196.3	1203.0	4323	4112	-4.88%	4132	-4.42%	4143	-4.16%
80 °C	0.02	10	745.0	4196.3	1203.0	4271	4031	-5.62%	4069	-4.71%	4091	-4.19%
80 °C	0.04	10	745.0	4196.3	1203.0	4169	3874	-7.07%	3947	-5.33%	3991	-4.28%
80 °C	0.06	10	745.0	4196.3	1203.0	4072	3726	-8.50%	3829	-5.97%	3893	-4.40%

CHAPTER 6: CONCLUSION

6.1. Summary

It is clear that the nanolayer is one of the key factors to be considered for the evaluation of effective thermal conductivity, effective viscosity, density and specific heat capacity of nanofluids. Unfortunately, most of the available models for nanofluids' effective thermal conductivity and viscosity do not include the effects of the nanolayer or are not accurate enough to be used as a basis for other studies.

In the case of nanofluid density, the presented model in this study could give accurate results for the four nanofluids that have been used in the experiments.

When the density model is used to calculate nanofluids' specific heat capacity, the results more closely resemble the available experimental results.

6.2. Conclusions

Literature shows that there are many available correlations to model for nanofluid thermal conductivity and viscosity, but only a small number of them considered the nanolayer in the calculations. On the other hand, there is just one linear equation for calculating density and a few for calculating the specific heat capacity of nanofluids. None of them considered the effect of the nanolayer.

In most of the thermal conductivity and viscosity correlations where the effects of the nanolayer are considered, its thickness and thermal conductivity are not validated. Therefore, they were selected in such a way that they match experimental data. Consequently, more research is required to understand nanolayer characteristics in order to use them in nanofluid correlations.

In the experimental part of this study, nanofluid density was experimentally investigated for four different nanofluids. A two-step sonication method was used to prepare these nanofluids.

The density of the nanofluids (SiO₂-water, SiO_x-EG-water, CuO-glycerol and MgO-glycerol) has been measured using a DDM 2911 digital density meter. The measurements were taken in the range of 1 to 6% of volume fraction and 10°C to 40°C.

The uncertainty of experimental measures for each sample at each measuring condition have also been calculated, which were in the range of 0.00011 gr/ml to 0.00089 gr/ml, as shown in Table A1 and Table A2 in Appendix A.

It is clear that the nanolayer is one of the key factors that must be considered for the evaluation of the effective thermal conductivity and viscosity of nanofluids. Unfortunately, most of the available models to calculate nanofluids' effective thermal conductivity and viscosity do not include the nanolayer. On the other hand, the ones that consider the nanolayer are not accurate for predicting unknown values. Therefore, these uncertainties can produce at least a 20% difference in the calculation of the Nusselt number, as well as a 24% difference in the calculation of the Reynolds number, a 54% difference in the calculation of the Grashof number and a 49% difference in the calculation of the Rayleigh number. Consequently, existing models for calculating the thermal conductivity and viscosity of nanofluids cause error in the design of thermal systems using nanofluids. Therefore, more investigation is necessary in this field.

In section 4.2, a correlation for nanofluid density is developed by performing a theoretical analysis of the mixture density formula. The unknowns in this correlation could be derived from the experimental results that are presented in Chapter 3.

In the first section of Chapter 5, the nanofluid density is discussed. By utilising the experimental data presented in Chapter 3 and the developed model in Chapter 4, the unknowns of the model are analysed and the number is presented for each nanofluid.

Subsequently, the nanofluid densities from experiments, presented models and mixture density models are drawn and compared. This comparison shows that the densities that resulted from the developed model are closer to the experimental data.

In Chapter 5, the nanofluids' specific heat capacity is theoretically investigated. The two figures that resulted from a specific heat capacity model are compared with the available experimental data for a SiO₂-water nanofluid. One of the figures is calculated using the mixture density formula, so nanolayer effects are ignored in the calculations. The other figure is calculated using a developed model for nanofluid density that considers nanolayer effects. The comparisons show that the nanolayer could affect the nanofluids' specific heat capacity. In this way, more accurate results for performing engineering designs by considering the effects can be obtained.

The following conclusions were drawn for nanofluid density: Firstly, the density of the nanolayer is between void and base fluid densities. Secondly, the nanolayer density changes gradually from void to base fluid. Thirdly, by using experimental results and theoretical work, a model has been developed to calculate the density of the nanofluids that are used in the experiment.

REFERENCES

- [1] S. Choi, "Enhancing thermal conductivity of fluids with nanoparticles", *Development and Applications of Non-Newtonian Flows*, pp. 99–105, 1995.
- [2] M. Sharifpur and T. Ntumba, "Parametric analysis of effective thermal conductivity models for nanofluids", in *Proceedings of the ASME 2012 International Mechanical Engineering Congress and Exposition*, Houston, 2012.
- [3] J. Meyer, P. Nwosu, M. Sharifpur and T. Ntumba, "Parametric analysis of effective viscosity models for nanofluids", in *Proceedings of the the ASME 2012 International Mechanical Engineering Congress and Exposition*, Houston, 2012.
- [4] J.Q. Broughton and F.F. Abraham, "A comparison of the fcc (111) and (100) crystal-melt interfaces by molecular dynamics simulation", *Chemical Physics Letters*, pp. 456–459, 1980.
- [5] J.R. Henderson and F. van Swol, "On the interface between a fluid and a planar wall theory and simulations of a hard sphere fluid at a hard wall", *Molecular Physics*, pp. 991–1010, 1984.
- [6] P.A. Thompson and M.O. Robbins, "Shear flow near solids: epitaxial order and flow boundary conditions", *Physical Review A*, pp. 6830–6837, 1990.
- [7] Q. Han and J. Hunt, "Particle pushing: the attachment of particles on the solid-liquid interface during fluid flow", *Journal of Crystal Growth*, pp. 406–413, 1994.
- [8] X-Y. Liu, P. Bennema, L. Meijer and M. Couto, "Ordering of paraffin-like molecules at the solid-fluid interface", *Chemical Physics Letters* 220, pp. 53–58, 1994.
- [9] Y. Teramoto and K. Nakanishi, "Molecular orientation in fluids near solid-liquid interface as studied by the density functional method", *Journal of Molecular Liquid*, pp. 281–284, 1995.
- [10] R. Steitz, C. Braun, P. Lang, G. Reiss and G. Findenegg, "Preordering phenomena of complex fluids Preordering phenomena of complex fluids at solid/liquid interfaces", *Physica B*, pp. 377–379, 1997.

- [11] W.J. Huisman, J.F. Peters, J.W. Derks, D.L. Abernathy and J.F. van der Veen, "A new x-ray diffraction method for structural investigations of solid-liquid Interfaces", *Review of Scientific Instruments* 68(11), pp. 4169–4176, 1997.
- [12] W.J. Huisman and J.F. van der Veen, "Modelling the atomic density across a solid-liquid interface", *Surface Science*, pp. 866–870, 1998.
- [13] A. Doerr, M. Tolan, T. Seydel and W. Press, "The interface structure of thin liquid hexane films", *Physica B*, pp. 263–268, 1998.
- [14] C-J. Yu, A. G. Richter, A. Datta, M.K. Durbin and P. Dutta, "Observation of molecular layering in thin liquid films using X-ray reflectivity", *Physical Review Letters*, pp. 2326–2329, 1999.
- [15] C-J. Yu, A. Richter, A. Datta, M. Durbin and P. Dutta, "Molecular layering in a liquid on a solid substrate an X-ray reflectivity study", *Physica B*, pp. 31–16, 2000.
- [16] C-J. Yu, A.G. Richter, J. Kmetko, S.W. Dugan, A. Datta and P. Dutta, "Structure of interfacial liquids: X-ray scattering studies", *Physical Review E, Volume 63*, 021205, pp. 021205-1–021205-2, 2001.
- [17] J.C. Maxwell, *A treatise on electricity and magnetism*, Oxford: Oxford University Press, pp. 435–441, 1873.
- [18] S.K. Das and S. Choi, "A review of heat transfer in nanofluids", *Advances in Heat Transfer*, pp. 81–197, 2009.
- [19] R. Hamilton and O. Crosser, "Thermal conductivity of heterogeneous two-component systems", *I&EC Fundamentals*, pp. 187–191, 1962.
- [20] D. Jeffrey, "Conduction through a random suspension of spheres," *Proceeding of the Royal Society of London A* 335, pp. 355–367, 1973.
- [21] R. Davis, "The effective thermal conductivity of a composite material with spherical inclusions", *International Journal of Thermophysics*, 7 (3), pp. 609–620, 1986.
- [22] J.A. Eastman, S.U.S. Choi, S. Li, W. Yu and L.J. Thompson, "Anomalously increased effective thermal conductivities of ethylene glycol-based nanofluids containing copper nanoparticles", *Applied Physics Letters*, 78 (6), 2001.

- [23] P. Keblinski, S. Phillpot, S. Choi and J. Eastman, "Mechanisms of heat flow in suspensions of nano-sized particles (nanofluids)", *International Journal of Heat and Mass Transfer*, pp. 855–863, 2002.
- [24] Q-Z. Xue, "Model for effective thermal conductivity of nanofluids", *Physics Letters A* 307, pp. 313–317, 2003.
- [25] W. Yu and S. Choi, "The role of interfacial layers in the enhanced thermal conductivity of nanofluids a renovated Maxwell mode," *Journal of Nanoparticle Research*, pp. 167–171, 2003.
- [26] W. Yu and S. Choi, "The role of interfacial layers in the enhanced thermal conductivity of nanofluids a renovated Hamilton-Crosser model", *Journal of Nanoparticle Research*, pp. 355–361, 2004.
- [27] L. Xue, P. Keblinski, S. Phillpot and S. Choi, "Effect of liquid layering at the liquid-solid interface on thermal transport", *International Journal of Heat and Mass Transfer*, pp. 4277–4284, 2004.
- [28] S.P. Jang and S. Choi, "Role of Brownian motion in the enhanced thermal conductivity of nanofluids", *Applied Physics Letters*, 2004.
- [29] Q. Xue and W-M. Xu, "A model of thermal conductivity of nanofluids with interfacial shells" *Materials Chemistry and Physics*, pp. 298–301, 2005.
- [30] H. Xie, M. Fujii and X. Zhang, "Effect of interfacial nanolayer on the effective thermal", *International Journal of Heat and Mass Transfer*, pp. 2926–2932, 2005.
- [31] S-Y. Lu, "Critical interfacial characteristics for effective conductivities of isotropic composites containing spherical inclusions", *Journal of Applied Physics*, pp. 5215–5219, 1995.
- [32] R. Yajie, H. Xie and A. Cai, "Effective thermal conductivity of nanofluids containing spherical nanoparticles", *Journal of Physics D: Applied Physics*, pp. 3958–3961, 2005.
- [33] K. Leong, C. Yang and S. Murshed, "A model for the thermal conductivity of nanofluids – the effect of interfacial layer", *Journal of Nanoparticle Research*, pp. 245–254, 2006.

- [34] J. Sabbaghzadeh and S. Ebrahimi, "Effective thermal conductivity of nanofluids containing cylindrical nanoparticles", *International Journal of Nanoscience*, pp. 45–49, 2007.
- [35] Y. Feng, Y. Boming, P. Xu and M. Zou, "The effective thermal conductivity of nanofluids based on nanolayer and aggregation of nanoparticles", *Applied Physics*, pp. 3164–3171, 2007.
- [36] T. Hashimoto, M. Fujimura and H. Kawai, "Domain-boundary structure of styreneisoprene block co-polymer films cast from solutions", *Macromolecules*, pp. 660–669, 1980.
- [37] Z. Li, Y. Gong, M. Pu, D. Wu, Y. Sun, J. Wang, Y. Liu and B. Dong, "Determination of interfacial layer thickness of a pseudo two-phase system by extension of the Debye equation", *Applied Physics*, pp. 2085–2088, 2001.
- [38] M. Kole and T. Dey, "Role of interfacial layer and clustering on the effective thermal conductivity of CuO-gear oil nanofluids", *Experimental Thermal and Fluid Science*, pp. 1490–1495, 2011.
- [39] M. Hari, S.A. Joseph, S. Mathewa, B. Nithyaja, V. Nampoori and P. Radhakrishnan, "Thermal diffusivity of nanofluids composed of rod-shaped silver nanoparticles", *International Journal of Thermal Sciences*, pp. 188–194, 2013.
- [40] M. Kole and T. Dey, "Enhanced thermophysical properties of copper nanoparticles dispersed in gear oil", *Applied Thermal Engineering*, 56, pp. 45–53, 2013.
- [41] H. Chen, Y. Ding, Y. He and C. Tan, "Rheological behaviour of ethylene glycol based titania nanofluids", *Chemical Physics Letters*, 444, pp. 333–337, 2007.
- [42] S.K. Ghosh and P. Mukherjee, "Mathematical modelling of thermal conductivity for nanofluid considering interfacial nano-layer", *Heat Mass Transfer*, pp. 595–600, 2013.
- [43] B-X. Wang, L-P. Zhou and X-F. Peng, "A fractal model for predicting the effective thermal conductivity of liquid with suspension of nanoparticles", *International Journal of Heat and Mass Transfer*, 46, pp. 2665–2672, 2003.

- [44] P. Tillman and J.M. Hill, "Determination of nanolayer thickness for a nanofluid", *International Communications in Heat and Mass Transfer*, pp. 399–407, 2007.
- [45] C. Nguyen, F. Desgranges, N. Galanis, G. Roy, T. Maré, S. Boucher and H. Angue Mintsa, "Viscosity data for Al₂O₃-water nanofluid-hysteresis is heat transfer enhancement using nanofluids reliable?", *International Journal of Thermal Sciences*, 47, pp. 103–111, 2008.
- [46] N. Frankei and A. Acrivos, "On the viscosity of a concentrated suspension of solid spheres", *Chemical Engineering Science*, pp. 847–853, 1967.
- [47] G. Batchelor, "The effect of Brownian motion on the bulk stress in a suspension of spherical particles", *Journal of Fluid Mechanics*, pp. 97–117, 1977.
- [48] A.L. Graham, "On the viscosity of suspensions of solid spheres", *Applied Scientific Research*, 37, pp. 275–286, 1981.
- [49] L. Yang, K. Du, Y.H. Ding, B. Cheng and Y. Jun, "Viscosity-prediction models of ammonia water nanofluids based on various dispersion types", *Powder Technology*, pp. 210–218, 2012.
- [50] J. Avsec and M. Oblak, "The calculation of thermal conductivity, viscosity and thermodynamic properties for nanofluids on the basis of statistical nanomechanics", *International Journal of Heat and Mass Transfer*, 50, pp. 4331–4341, 2007.
- [51] J-H. Lee, K.S. Hwang, S.P. Jang, B.H. Lee, J.H. Kim, S.U. Choi and C.J. Choi, "Effective viscosities and thermal conductivities of aqueous nanofluids containing low volume concentrations of Al₂O₃ nanoparticles", *International Journal of Heat and Mass Transfer*, 51, pp. 2651–2656, 2008.
- [52] S. Murshed, K. Leong and C. Yang, "Investigations of thermal conductivity and viscosity of nanofluids", *International Journal of Thermal Sciences*, 47, pp. 560–568, 2008.
- [53] N. Masoumi, N. Sohrabi and A. Behzadmehr, "A new model for calculating the effective viscosity of nanofluids", *Journal of Physics D: Applied Physics*, 42, pp. 055501 (6pp), 2009.

- [54] S.M. Hosseini, A.R. Moghadassi and D.E. Henneke, "A new dimensionless group model for determining the viscosity of nanofluids", *Journal of Thermal Analysis Calorim*, pp. 873–877, 2010.
- [55] J. Buongiorno, "Convective transport in nanofluids", *Journal of Heat Transfer*, pp. 240–250, 2006.
- [56] G. Polidori, S. Fohanno and C. Nguyen, "A note on heat transfer modelling of Newtonian nanofluids in laminar free convection", *International Journal of Thermal Sciences*, pp. 739–744, 2007.
- [57] E.. Ogut, "Natural convection of water-based nanofluids in an inclined enclosure with a heat source", *International Journal of Thermal Sciences*, pp. 2063–2073, 2009.
- [58] S. Kumar, S.K. Prasad and J. Banerjee, "Analysis of flow and thermal field in nanofluid using a single phase thermal dispersion model", *Applied Mathematical Modelling*, pp. 573–592, 2010.
- [59] Z. Alloui, J. Guet, P. Vasseur and M. Reggi, "Natural convection of nanofluids in a shallow rectangular enclosure heated from the side", *The Canadian Journal of Chemical Engineering*, pp. 69–78, 2012.
- [60] V. Kuppalapalle, "The effect of variable viscosity on the flow and heat transfer of a viscous Ag-water and Cu-water nanofluids", *Journal of Hydrodynamics*, pp. 1–9, 2013.
- [61] I.I. Ryzhkov and A.V. Minakov, "The effect of nanoparticle diffusion and thermophoresis on convective heat transfer of nanofluid in a circular tube", *International Journal of Heat and Mass Transfer*, pp. 956–969, 2014.
- [62] A.A. Minea, "Uncertainties in modeling thermal conductivity of laminar forced convection heat transfer with water alumina nanofluids", *International Journal of Heat and Mass Transfer*, pp. 78–84, 2014.
- [63] J. Zhang, Y. Diao, Y. Zhao and Y. Zhang, "Experimental study of TiO₂–water nanofluid flow and heat transfer characteristics in a multiport minichannel flat tube", *International Journal of Heat and Mass Transfer*, pp. 628–638, 2014.

- [64] S.S. Azimi and M. Kalbasi, "Numerical study of dynamic thermal conductivity of nanofluid in the forced convective heat transfer", *Applied Mathematical Modelling*, pp. 1373–1384, 2014.
- [65] A. Inakov, A. Lobasov, D. Guzei, M. Pryazhnikov and V. Ya Rudyak, "The experimental and theoretical study of laminar forced convection of nanofluids in the round channel", *Applied Thermal Engineering*, pp. 1–9, 2014.
- [66] H. Hassan, "Heat transfer of Cu–water nanofluid in an enclosure with a heat sink and discrete heat source", *European Journal of Mechanics B/Fluids*, pp. 72–83, 2014.
- [67] C. Cianfrini, M. Corcione, E. Habib and A. Quintino, "Buoyancy-induced convection in Al_2O_3 /water nanofluids from an enclosed heater", *European Journal of Mechanics B/Fluids*, pp. 123–134, 2014.
- [68] M. Hemmat Esfe, S. Saedodin and M. Mahmoodi, "Experimental studies on the convective heat transfer performance and thermophysical properties of MgO–water nanofluid under turbulent flow", *Experimental Thermal and Fluid Science*, pp. 68–78, 2014.
- [69] C. Pang, J-Y. Jung and Y. Tae Kang, "Aggregation based model for heat conduction mechanism in nanofluids", *International Journal of Heat and Mass Transfer*, pp. 392–399, 2014.
- [70] M. Hemmat Esfe, S. Saedodin, O. Mahian and S. Wongwises, "Heat transfer characteristics and pressure drop of COOH-functionalized DWCNTs/water nanofluid in turbulent flow at low concentrations", *International Journal of Heat and Mass Transfer*, pp. 186–194, 2014.
- [71] H. Maddah, M. Alizadeh, N. Ghasemi and S. Rafidah Wan Alwi, "Experimental study of Al_2O_3 /water nanofluid turbulent heat transfer enhancement in the horizontal double pipes fitted with modified twisted tapes", *International Journal of Heat and Mass Transfer*, pp. 1042–1054, 2014.
- [72] C. Pang, J. Won Lee and Y. Tae Kan, "Review on combined heat and mass transfer characteristics in nanofluids", *International Journal of Thermal Sciences*, pp. 49–67, 2015.

- [73] A.M. Abed, M. Alghoul, K. Sopian, H. Mohammed, H.S. Majdi and A.N. Al-Shamani, "Design characteristics of corrugated trapezoidal plate heat exchangers using nanofluids", *Chemical Engineering and Processing*, pp. 88–103, 2015.
- [74] H. Hassan and S. Harmand, "Effect of using nanofluids on the performance of rotating heat pipe", *Applied Mathematical Modelling*, 2015.
- [75] A. Najah Al-Shamani, K. Sopian, H. Mohammed, S. Mat, M. Hafidz Ruslan and A.M. Abed, "Enhancement heat transfer characteristics in the channel with Trapezoidal rib-groove using nanofluids", *Case Studies in Thermal Engineering*, pp. 48–58, 2015.
- [76] T. Parametthanuwat, N. Bhuwakietkumjohn, S. Rittidech and Y. Ding, "Experimental investigation on thermal properties of silver nanofluids", *International Journal of Heat and Fluid Flow*, pp. 80–90, 2015.
- [77] B. Pak and Y. Cho, "Hydrodynamic and heat transfer study of dispersed fluids with submicron metallic oxide particles", *Experimental Heat Transfer*, pp. 171–150, 1998.
- [78] D. Cabaleiro, C. Gracia-Fernández, J. Legido and L. Lugo, "Specific heat of metal oxide nanofluids at high concentrations for heat transfer", *International Journal of Heat and Mass Transfer*, pp. 872–879, 2015.
- [79] Y. Xuan and W. Roetzel, "Conceptions for heat transfer correlations of nanofluids", *International Journal of Heat and Mass Transfer*, 43 (2000) 3701±3707, pp. 3701–3707, 2000.
- [80] R. Vajjha and D. Das, "Specific heat measurement of three nanofluids and development of new correlations", *Journal of Heat Transfer*, pp. 071601 (1–7), 2009.
- [81] L. Zhou, B. Wang, X. Peng, X. Du and Y. Yang, "On the specific heat capacity of CuO nanofluid", *Advances in Mechanical Engineering*, pp. 172085, 2010.
- [82] T. Bergman, "Effect of reduced specific heats of nanofluids on single phase, laminar internal forced convection", *International Journal of Heat and Mass Transfer*, pp. 1240–1244, 2009.

- [83] A. Starace, J. Gomez, J. Wang, S. Pradhan and G. Glatzmaier, "Nanofluid heat capacities", *Journal of Applied Physics*, 110, pp. 124323, 2011.
- [84] T.P. Teng and Y.H. Hung, "Estimation and experimental study of the density and specific heat for alumina nanofluid", *Journal of Experimental Nanoscience*, pp. 707–718, 2014.
- [85] S. Murshed, K. Leong and C. Yang, "A combined model for the effective thermal conductivity of nanofluids", *Applied Thermal Engineering*, pp. 2477–2483, 2009.
- [86] N. Sohrabi, N. Masoumi, A. Behzadmehr and S. Sarvari, "A simple analytical model for calculating the effective thermal conductivity of nanofluids", *Heat Transfer – Asian Research*, pp. 141–150, 2010.
- [87] H. Fu and L. Gao, "Effect of interfacial nanolayer on thermophoresis in nanofluids", *International Journal of Thermal Sciences*, pp. 61–66, 2012.
- [88] P.K. Namburu, D.P. Kulkarni, D. Misra and D.K. Das, "Viscosity of copper oxide nanoparticles dispersed in ethylene glycol and water mixture", *Experimental Thermal and Fluid Science*, 32, pp. 397–402, 2007.
- [89] S. Van Kao, L.E. Nielsen and C.T. Hill, "Rheology of concentrated suspensions of spheres I. Effect of the liquid-solid interface", *Journal of Colloid and Interface Science*, 53 (3), pp. 358–366, 1974.

Appendix A: Nanofluid Density Uncertainty Analysis

A – 1: Uncertainty Analysis Results Tables

Table A1: Uncertainty analysis data

Nano fluid type	T (°c)	ϕ	δV (ml)	δm (gr)	δV_p (ml)	$\delta \phi$	$\delta \rho_f$ (gr/ml)	$\delta \rho_{nf}$ (gr/ml)
SiO _x -EG-water	10	0.01	0.005	0.0002	8.3333E-05	1.2386E-06	0.00013584	0.00013449
SiO _x -EG-water	20	0.01	0.005	0.0002	8.3333E-05	1.2386E-06	0.00013507	0.00013373
SiO _x -EG-water	30	0.01	0.005	0.0002	8.3333E-05	1.2386E-06	0.00013428	0.00013295
SiO _x -EG-water	40	0.01	0.005	0.0002	8.3333E-05	1.2386E-06	0.00013348	0.00013216
SiO _x -EG-water	10	0.02	0.005	0.0002	8.3333E-05	2.4505E-06	0.00013584	0.00013316
SiO _x -EG-water	20	0.02	0.005	0.0002	8.3333E-05	2.4505E-06	0.00013502	0.00013236
SiO _x -EG-water	30	0.02	0.005	0.0002	8.3333E-05	2.4505E-06	0.00013428	0.00013164
SiO _x -EG-water	40	0.02	0.005	0.0002	8.3333E-05	2.4505E-06	0.00013348	0.00013085
SiO _x -EG-water	10	0.04	0.005	0.0002	8.3333E-05	4.8002E-06	0.00013584	0.00013055
SiO _x -EG-water	20	0.04	0.005	0.0002	8.3333E-05	4.8002E-06	0.00013507	0.000130
SiO _x -EG-water	30	0.04	0.005	0.0002	8.3333E-05	4.8002E-06	0.00013428	0.00012907
SiO _x -EG-water	40	0.04	0.005	0.0002	8.3333E-05	4.8002E-06	0.00013348	0.0001283
SiO _x -EG-water	10	0.06	0.005	0.0002	8.3333E-05	7.0502E-06	0.00013584	0.00012802
SiO _x -EG-water	20	0.06	0.005	0.0002	8.3333E-05	7.0502E-06	0.00013507	0.00012731
SiO _x -EG-water	30	0.06	0.005	0.0002	8.3333E-05	7.0502E-06	0.00013428	0.00012657
SiO _x -EG-water	40	0.06	0.005	0.0002	8.3333E-05	7.0502E-06	0.00013348	0.00012583
SiO ₂ -water	10	0.01	0.005	0.0002	8.3333E-05	1.2386E-06	0.00012506	0.00012382
SiO ₂ -water	20	0.01	0.005	0.0002	8.3333E-05	1.2386E-06	0.00012487	0.00012363
SiO ₂ -water	30	0.01	0.005	0.0002	8.3333E-05	1.2386E-06	0.00012455	0.00012332
SiO ₂ -water	40	0.01	0.005	0.0002	8.3333E-05	1.2386E-06	0.00012413	0.0001229
SiO ₂ -water	10	0.02	0.005	0.0002	8.3333E-05	2.4505E-06	0.00012506	0.0001226
SiO ₂ -water	20	0.02	0.005	0.0002	8.3333E-05	2.4505E-06	0.00012487	0.00012242
SiO ₂ -water	30	0.02	0.005	0.0002	8.3333E-05	2.4505E-06	0.00012455	0.00012211
SiO ₂ -water	40	0.02	0.005	0.0002	8.3333E-05	2.4505E-06	0.00012413	0.0001217
SiO ₂ -water	10	0.04	0.005	0.0002	8.3333E-05	4.8002E-06	0.00012506	0.00012024
SiO ₂ -water	20	0.04	0.005	0.0002	8.3333E-05	4.8002E-06	0.00012487	0.00012006
SiO ₂ -water	30	0.04	0.005	0.0002	8.3333E-05	4.8002E-06	0.00012455	0.00011976
SiO ₂ -water	40	0.04	0.005	0.0002	8.3333E-05	4.8002E-06	0.00012413	0.00011936
SiO ₂ -water	10	0.06	0.005	0.0002	8.3333E-05	7.0502E-06	0.00012506	0.00011797
SiO ₂ -water	20	0.06	0.005	0.0002	8.3333E-05	7.0502E-06	0.00012487	0.00011779
SiO ₂ -water	30	0.06	0.005	0.0002	8.3333E-05	7.0502E-06	0.00012455	0.0001175
SiO ₂ -water	40	0.06	0.005	0.0002	8.3333E-05	7.0502E-06	0.00012413	0.00011711

Appendix A: Uncertainty analysis result tables

Table A2: Uncertainty analysis data

Nano fluid type	T (°c)	ϕ	δV (ml)	δm (gr)	δV_p (ml)	$\delta \phi$	$\delta \rho_f$ (gr/ml)	$\delta \rho_{nf}$ (gr/ml)
MgO-glycerol	10	0.01	0.005	0.0002	5.5866E-05	1.238E-06	0.00015842	0.00015686
MgO-glycerol	20	0.01	0.005	0.0002	5.5866E-05	1.238E-06	0.00015766	0.00015611
MgO-glycerol	30	0.01	0.005	0.0002	5.5866E-05	1.238E-06	0.00015688	0.00015534
MgO-glycerol	40	0.01	0.005	0.0002	5.5866E-05	1.238E-06	0.00015611	0.00015458
MgO-glycerol	10	0.02	0.005	0.0002	5.5866E-05	2.4502E-06	0.00015842	0.00015536
MgO-glycerol	20	0.02	0.005	0.0002	5.5866E-05	2.4502E-06	0.00015766	0.00015461
MgO-glycerol	30	0.02	0.005	0.0002	5.5866E-05	2.4502E-06	0.00015688	0.00015385
MgO-glycerol	40	0.02	0.005	0.0002	5.5866E-05	2.4502E-06	0.00015611	0.0001531
MgO-glycerol	10	0.04	0.005	0.0002	5.5866E-05	4.8001E-06	0.00015842	0.00015249
MgO-glycerol	20	0.04	0.005	0.0002	5.5866E-05	4.8001E-06	0.00015766	0.00015176
MgO-glycerol	30	0.04	0.005	0.0002	5.5866E-05	4.8001E-06	0.00015688	0.00015102
MgO-glycerol	40	0.04	0.005	0.0002	5.5866E-05	4.8001E-06	0.00015611	0.00015029
MgO-glycerol	10	0.06	0.005	0.0002	5.5866E-05	7.0501E-06	0.00015842	0.00014981
MgO-glycerol	20	0.06	0.005	0.0002	5.5866E-05	7.0501E-06	0.00015766	0.0001491
MgO-glycerol	30	0.06	0.005	0.0002	5.5866E-05	7.0501E-06	0.00015688	0.00014837
MgO-glycerol	40	0.06	0.005	0.0002	5.5866E-05	7.0501E-06	0.00015611	0.00014766
CuO-glycerol	10	0.01	0.005	0.0002	0.00003125	1.2376E-06	0.00015842	0.00015696
CuO-glycerol	20	0.01	0.005	0.0002	0.00003125	1.2376E-06	0.00015766	0.00015621
CuO-glycerol	30	0.01	0.005	0.0002	0.00003125	1.2376E-06	0.00015688	0.00015544
CuO-glycerol	40	0.01	0.005	0.0002	0.00003125	1.2376E-06	0.00015611	0.00015468
CuO-glycerol	10	0.02	0.005	0.0002	0.00003125	2.4501E-06	0.00015842	0.00015576
CuO-glycerol	20	0.02	0.005	0.0002	0.00003125	2.4501E-06	0.00015766	0.00015501
CuO-glycerol	30	0.02	0.005	0.0002	0.00003125	2.4501E-06	0.00015688	0.00015426
CuO-glycerol	40	0.02	0.005	0.0002	0.00003125	2.4501E-06	0.00015611	0.00015351
CuO-glycerol	10	0.04	0.005	0.0002	0.00003125	4.8E-06	0.00015842	0.00015407
CuO-glycerol	20	0.04	0.005	0.0002	0.00003125	4.8E-06	0.00015766	0.00015335
CuO-glycerol	30	0.04	0.005	0.0002	0.00003125	4.8E-06	0.00015688	0.00015262
CuO-glycerol	40	0.04	0.005	0.0002	0.00003125	4.8E-06	0.00015611	0.0001519
CuO-glycerol	10	0.06	0.005	0.0002	0.00003125	7.05E-06	0.00015842	0.00015325
CuO-glycerol	20	0.06	0.005	0.0002	0.00003125	7.05E-06	0.00015766	0.00015256
CuO-glycerol	30	0.06	0.005	0.0002	0.00003125	7.05E-06	0.00015688	0.00015186
CuO-glycerol	40	0.06	0.005	0.0002	0.00003125	7.05E-06	0.00015611	0.00015117

A – 2: Uncertainty Analysis – Equation 98

Equation 98 has been presented in chapter 4, which consider nanolayer effects in calculation of nanofluid density.

$$\rho_{nf} = \varphi \rho_p + (1 - \delta^3 \varphi) \rho_f + (\delta^3 - 1) \varphi \rho_l \quad (98)$$

And in the same chapter the results from same model have been compared with traditional linear model and experimental data. Hence, uncertainty analysis has been performed for this new model as:

$$\delta \rho_{nf} = \left[\left(\frac{\partial \rho_{nf}}{\partial \varphi} \delta \varphi \right)^2 + \left(\frac{\partial \rho_{nf}}{\partial \rho_f} \delta \rho_f \right)^2 + \left(\frac{\partial \rho_{nf}}{\partial \rho_l} \delta \rho_l \right)^2 \right]^{1/2} \quad (113)$$

From equations 98 and 113:

$$\delta \rho_{nf} = \left[((\rho_p - \delta^3 \rho_f + (\delta^3 - 1) \rho_l) \delta \varphi)^2 + ((1 - \delta^3 \varphi) \delta \rho_f)^2 + ((\delta^3 - 1) \varphi \delta \rho_l)^2 \right]^{1/2} \quad (114)$$

The correlation for calculating the volume fraction is:

$$\varphi = \frac{V_p}{V_f + V_p} \quad (78)$$

The volume fraction uncertainty is as follows:

$$\delta \varphi = \left[\left(\frac{\partial \varphi}{\partial V_f} \delta V_f \right)^2 + \left(\frac{\partial \varphi}{\partial V_p} \delta V_p \right)^2 \right]^{1/2} \quad (79)$$

From equations 78 and 79:

$$\delta \varphi = \left[\left(\frac{V_p}{(V_f + V_p)^2} \delta V_f \right)^2 + \left(\frac{1}{(V_f + V_p)^2} \delta V_p \right)^2 \right]^{1/2} \quad (80)$$

Appendix A: Uncertainty analysis result tables

The formula for base fluid density is:

$$\rho_f = \frac{m_f}{V_f} \quad (81)$$

The density uncertainty will be:

$$\delta\rho_f = \left[\left(\frac{\partial\rho_f}{\partial m_f} \delta m_f \right)^2 + \left(\frac{\partial\rho_f}{\partial V_f} \delta V_f \right)^2 \right]^{1/2} \quad (82)$$

$$\delta\rho_f = \left[\left(\frac{1}{V_f} \delta m_f \right)^2 + \left(\frac{m_f}{V_f^2} \delta V_f \right)^2 \right]^{1/2} \quad (83)$$

For nanoparticles, the density is constant and equal to the amount indicated by the manufacturer, and the volume of the nanoparticles could be calculated from the density formula:

$$V_p = \frac{m_p}{\rho_p} \quad (84)$$

$$\delta V_p = \left[\left(\frac{\partial V_p}{\partial m_p} \delta m_p \right)^2 \right]^{1/2} \quad (85)$$

$$\delta V_p = \left[\left(\frac{1}{\rho_p} \delta m_p \right)^2 \right]^{1/2} \quad (86)$$

The formula for base fluid density is:

$$\rho_l = \frac{m_l}{V_l} \quad (115)$$

The density uncertainty will be:

Appendix A: Uncertainty analysis result tables

$$\delta\rho_l = \left[\left(\frac{\partial\rho_l}{\partial m_l} \delta m_l \right)^2 + \left(\frac{\partial\rho_l}{\partial V_l} \delta V_l \right)^2 \right]^{1/2} \quad (116)$$

$$\delta\rho_l = \left[\left(\frac{1}{V_l} \delta m_l \right)^2 + \left(\frac{m_l}{V_l^2} \delta V_l \right)^2 \right]^{1/2} \quad (117)$$

$$V_l = \frac{4}{3}\pi(r_o^3 - r_i^3) = \frac{4}{3}\pi r_i^3(\delta^3 - 1) \quad (96)$$

So:

$$V_l = V_p(\delta^3 - 1) \quad (118)$$

By substituting ρ_p , ρ_f , ρ_l , ϕ , $\delta\rho_f$, $\delta\rho_l$ and $\delta\phi$ in equation 114 the uncertainty could be calculated for each sample. The results have been presented in Table A3. The results show that the maximum uncertainty is ± 0.000899 gr/ml.

Table A3: Uncertainty analysis data (Equation 98)

Nano Fluid Type	T (°c)	ϕ	ρ_p (gr/ml)	ρ_f (gr/ml)	m_p (gr)	V_p (ml)	m_f (gr)	V_f (ml)	m_l (gr)	V_l (ml)	δV (ml)	δm (gr)	δV_p (ml)	$\delta\phi$	$\delta\rho_f$ (gr/ml)	$\delta\rho_l$ (gr/ml)	$\delta\rho_{nf}$ (gr/ml)
SiO _x - EG Water	10	0.01	2.4	1.08595	0.96970	0.40404	43.438	40	0.188889	0.21212	0.005	0.0002	8.3333E-05	1.2386E-06	0.000136	0.170591	0.000899
SiO _x - EG Water	20	0.01	2.4	1.07982	0.96970	0.40404	43.1928	40	0.188889	0.21212	0.005	0.0002	8.3333E-05	1.2386E-06	0.000135	0.170591	0.000898
SiO _x - EG Water	30	0.01	2.4	1.07351	0.96970	0.40404	42.9402	40	0.188889	0.21212	0.005	0.0002	8.3333E-05	1.2386E-06	0.000134	0.170591	0.000898
SiO _x - EG Water	40	0.01	2.4	1.06712	0.96970	0.40404	42.6846	40	0.188889	0.21212	0.005	0.0002	8.3333E-05	1.2386E-06	0.000133	0.170591	0.000898
SiO _x - EG Water	10	0.02	2.4	1.08595	1.95918	0.81633	43.438	40	0.381633	0.42857	0.005	0.0002	8.3333E-05	2.4505E-06	0.000136	0.084434	0.000889
SiO _x - EG Water	20	0.02	2.4	1.07945	1.95918	0.81633	43.1778	40	0.381633	0.42857	0.005	0.0002	8.3333E-05	2.4505E-06	0.000135	0.084434	0.000889
SiO _x - EG Water	30	0.02	2.4	1.07351	1.95918	0.81633	42.9402	40	0.381633	0.42857	0.005	0.0002	8.3333E-05	2.4505E-06	0.000134	0.084434	0.000889
SiO _x - EG Water	40	0.02	2.4	1.06712	1.95918	0.81633	42.6846	40	0.381633	0.42857	0.005	0.0002	8.3333E-05	2.4505E-06	0.000133	0.084434	0.000889
SiO _x - EG Water	10	0.04	2.4	1.08595	4.00000	1.66667	43.438	40	0.779167	0.87500	0.005	0.0002	8.3333E-05	4.8002E-06	0.000136	0.041355	0.000871
SiO _x - EG Water	20	0.04	2.4	1.07982	4.00000	1.66667	43.1928	40	0.779167	0.87500	0.005	0.0002	8.3333E-05	4.8002E-06	0.000135	0.041355	0.000871
SiO _x - EG Water	30	0.04	2.4	1.07351	4.00000	1.66667	42.9402	40	0.779167	0.87500	0.005	0.0002	8.3333E-05	4.8002E-06	0.000134	0.041355	0.000871
SiO _x - EG Water	40	0.04	2.4	1.06712	4.00000	1.66667	42.6846	40	0.779167	0.87500	0.005	0.0002	8.3333E-05	4.8002E-06	0.000133	0.041355	0.000871
SiO _x - EG Water	10	0.06	2.4	1.08595	6.12766	2.55319	43.438	40	1.193617	1.34043	0.005	0.0002	8.3333E-05	7.0502E-06	0.000136	0.026996	0.000853
SiO _x - EG Water	20	0.06	2.4	1.07982	6.12766	2.55319	43.1928	40	1.193617	1.34043	0.005	0.0002	8.3333E-05	7.0502E-06	0.000135	0.026996	0.000853
SiO _x - EG Water	30	0.06	2.4	1.07351	6.12766	2.55319	42.9402	40	1.193617	1.34043	0.005	0.0002	8.3333E-05	7.0502E-06	0.000134	0.026996	0.000853

Appendix A: Uncertainty analysis result tables

Nano Fluid Type	T (°c)	ϕ	ρ_p (gr/ml)	ρ_f (gr/ml)	m_p (gr)	V_p (ml)	m_f (gr)	V_f (ml)	m_l (gr)	V_l (ml)	δV (ml)	δm (gr)	δV_p (ml)	$\delta \phi$	$\delta \rho_f$ (gr/ml)	$\delta \rho_l$ (gr/ml)	$\delta \rho_{nf}$ (gr/ml)
SiO _x - EG Water	40	0.06	2.4	1.06712	6.12766	2.55319	42.6846	40	1.193617	1.34043	0.005	0.0002	8.3333E-05	7.0502E-06	0.000133	0.026996	0.000853
SiO ₂ - Water	10	0.01	2.4	0.99967	0.96970	0.40404	39.9866	40	0.002936	0.04735	0.005	0.0002	8.3333E-05	1.2386E-06	0.000125	0.052922	0.000138
SiO ₂ - Water	20	0.01	2.4	0.99814	0.96970	0.40404	39.9256	40	0.002936	0.04735	0.005	0.0002	8.3333E-05	1.2386E-06	0.000125	0.052922	0.000138
SiO ₂ - Water	30	0.01	2.4	0.99561	0.96970	0.40404	39.8242	40	0.002936	0.04735	0.005	0.0002	8.3333E-05	1.2386E-06	0.000125	0.052922	0.000138
SiO ₂ - Water	40	0.01	2.4	0.99225	0.96970	0.40404	39.69	40	0.002936	0.04735	0.005	0.0002	8.3333E-05	1.2386E-06	0.000124	0.052922	0.000137
SiO ₂ - Water	10	0.02	2.4	0.99967	1.95918	0.81633	39.9866	40	0.005931	0.09566	0.005	0.0002	8.3333E-05	2.4505E-06	0.000125	0.026193	0.000137
SiO ₂ - Water	20	0.02	2.4	0.99814	1.95918	0.81633	39.9256	40	0.005931	0.09566	0.005	0.0002	8.3333E-05	2.4505E-06	0.000125	0.026193	0.000137
SiO ₂ - Water	30	0.02	2.4	0.99561	1.95918	0.81633	39.8242	40	0.005931	0.09566	0.005	0.0002	8.3333E-05	2.4505E-06	0.000125	0.026193	0.000136
SiO ₂ - Water	40	0.02	2.4	0.99225	1.95918	0.81633	39.69	40	0.005931	0.09566	0.005	0.0002	8.3333E-05	2.4505E-06	0.000124	0.026193	0.000136
SiO ₂ - Water	10	0.04	2.4	0.99967	4.00000	1.66667	39.9866	40	0.012109	0.19531	0.005	0.0002	8.3333E-05	4.8002E-06	0.000125	0.012829	0.000134
SiO ₂ - Water	20	0.04	2.4	0.99814	4.00000	1.66667	39.9256	40	0.012109	0.19531	0.005	0.0002	8.3333E-05	4.8002E-06	0.000125	0.012829	0.000134
SiO ₂ - Water	30	0.04	2.4	0.99561	4.00000	1.66667	39.8242	40	0.012109	0.19531	0.005	0.0002	8.3333E-05	4.8002E-06	0.000125	0.012829	0.000133
SiO ₂ - Water	40	0.04	2.4	0.99225	4.00000	1.66667	39.69	40	0.012109	0.19531	0.005	0.0002	8.3333E-05	4.8002E-06	0.000124	0.012829	0.000133
SiO ₂ - Water	10	0.06	2.4	0.99967	6.12766	2.55319	39.9866	40	0.018551	0.29920	0.005	0.0002	8.3333E-05	7.0502E-06	0.000125	0.008375	0.000131
SiO ₂ - Water	20	0.06	2.4	0.99814	6.12766	2.55319	39.9256	40	0.018551	0.29920	0.005	0.0002	8.3333E-05	7.0502E-06	0.000125	0.008375	0.000131

Appendix A: Uncertainty analysis result tables

Nano Fluid Type	T (°c)	ϕ	ρ_p (gr/ml)	ρ_f (gr/ml)	m_p (gr)	V_p (ml)	m_f (gr)	V_f (ml)	m_l (gr)	V_l (ml)	δV (ml)	δm (gr)	δV_p (ml)	$\delta\phi$	$\delta\rho_f$ (gr/ml)	$\delta\rho_l$ (gr/ml)	$\delta\rho_{nf}$ (gr/ml)
SiO ₂ - Water	30	0.06	2.4	0.99561	6.12766	2.55319	39.8242	40	0.018551	0.29920	0.005	0.0002	8.3333E-05	7.0502E-06	0.000125	0.008375	0.000131
SiO ₂ - Water	40	0.06	2.4	0.99225	6.12766	2.55319	39.69	40	0.018551	0.29920	0.005	0.0002	8.3333E-05	7.0502E-06	0.000124	0.008375	0.000130
MgO - Glycerol	10	0.01	3.58	1.26673	1.4465	0.40404	50.6692	40	0.061553	0.09785	0.005	0.0002	5.5866E-05	1.238E-06	0.000158	0.256908	0.000642
MgO - Glycerol	20	0.01	3.58	1.26061	1.4465	0.40404	50.4244	40	0.061553	0.09785	0.005	0.0002	5.5866E-05	1.238E-06	0.000158	0.256908	0.000642
MgO - Glycerol	30	0.01	3.58	1.25440	1.4465	0.40404	50.1758	40	0.061553	0.09785	0.005	0.0002	5.5866E-05	1.238E-06	0.000157	0.256908	0.000641
MgO - Glycerol	40	0.01	3.58	1.24827	1.4465	0.40404	49.9306	40	0.061553	0.09785	0.005	0.0002	5.5866E-05	1.238E-06	0.000156	0.256908	0.000641
MgO - Glycerol	10	0.02	3.58	1.26673	2.9224	0.81633	50.6692	40	0.124362	0.19770	0.005	0.0002	5.5866E-05	2.4502E-06	0.000158	0.127157	0.000635
MgO - Glycerol	20	0.02	3.58	1.26061	2.9224	0.81633	50.4244	40	0.124362	0.19770	0.005	0.0002	5.5866E-05	2.4502E-06	0.000158	0.127157	0.000635
MgO - Glycerol	30	0.02	3.58	1.25440	2.9224	0.81633	50.1758	40	0.124362	0.19770	0.005	0.0002	5.5866E-05	2.4502E-06	0.000157	0.127157	0.000635
MgO - Glycerol	40	0.02	3.58	1.24827	2.9224	0.81633	49.9306	40	0.124362	0.19770	0.005	0.0002	5.5866E-05	2.4502E-06	0.000156	0.127157	0.000635
MgO - Glycerol	10	0.04	3.58	1.26673	5.9667	1.66667	50.6692	40	0.253906	0.40365	0.005	0.0002	5.5866E-05	4.8001E-06	0.000158	0.062281	0.000622
MgO - Glycerol	20	0.04	3.58	1.26061	5.9667	1.66667	50.4244	40	0.253906	0.40365	0.005	0.0002	5.5866E-05	4.8001E-06	0.000158	0.062281	0.000622
MgO - Glycerol	30	0.04	3.58	1.25440	5.9667	1.66667	50.1758	40	0.253906	0.40365	0.005	0.0002	5.5866E-05	4.8001E-06	0.000157	0.062281	0.000622
MgO - Glycerol	40	0.04	3.58	1.24827	5.9667	1.66667	49.9306	40	0.253906	0.40365	0.005	0.0002	5.5866E-05	4.8001E-06	0.000156	0.062281	0.000622
MgO - Glycerol	10	0.06	3.58	1.26673	9.1404	2.55319	50.6692	40	0.388963	0.61835	0.005	0.0002	5.5866E-05	7.0501E-06	0.000158	0.040656	0.000609

Appendix A: Uncertainty analysis result tables

Nano Fluid Type	T (°c)	ϕ	ρ_p (gr/ml)	ρ_f (gr/ml)	m_p (gr)	V_p (ml)	m_f (gr)	V_f (ml)	m_l (gr)	V_l (ml)	δV (ml)	δm (gr)	δV_p (ml)	$\delta\phi$	$\delta\rho_f$ (gr/ml)	$\delta\rho_l$ (gr/ml)	$\delta\rho_{nf}$ (gr/ml)
MgO - Glycerol	20	0.06	3.58	1.26061	9.1404	2.55319	50.4244	40	0.388963	0.61835	0.005	0.0002	5.5866E-05	7.0501E-06	0.000158	0.040656	0.000609
MgO - Glycerol	30	0.06	3.58	1.25440	9.1404	2.55319	50.1758	40	0.388963	0.61835	0.005	0.0002	5.5866E-05	7.0501E-06	0.000157	0.040656	0.000609
MgO - Glycerol	40	0.06	3.58	1.24827	9.1404	2.55319	49.9306	40	0.388963	0.61835	0.005	0.0002	5.5866E-05	7.0501E-06	0.000156	0.040656	0.000609
CuO - Glycerol	10	0.01	6.4	1.26673	2.585859	0.40404	50.6692	40	0.061553	0.09785	0.005	0.0002	0.00003125	1.2376E-06	0.000158	0.256908	0.000642
CuO - Glycerol	20	0.01	6.4	1.26061	2.585859	0.40404	50.4244	40	0.061553	0.09785	0.005	0.0002	0.00003125	1.2376E-06	0.000158	0.256908	0.000642
CuO - Glycerol	30	0.01	6.4	1.25440	2.585859	0.40404	50.1758	40	0.061553	0.09785	0.005	0.0002	0.00003125	1.2376E-06	0.000157	0.256908	0.000642
CuO - Glycerol	40	0.01	6.4	1.24827	2.585859	0.40404	49.9306	40	0.061553	0.09785	0.005	0.0002	0.00003125	1.2376E-06	0.000156	0.256908	0.000641
CuO - Glycerol	10	0.02	6.4	1.26673	5.22449	0.81633	50.6692	40	0.124362	0.19770	0.005	0.0002	0.00003125	2.4501E-06	0.000158	0.127157	0.000635
CuO - Glycerol	20	0.02	6.4	1.26061	5.22449	0.81633	50.4244	40	0.124362	0.19770	0.005	0.0002	0.00003125	2.4501E-06	0.000158	0.127157	0.000635
CuO - Glycerol	30	0.02	6.4	1.25440	5.22449	0.81633	50.1758	40	0.124362	0.19770	0.005	0.0002	0.00003125	2.4501E-06	0.000157	0.127157	0.000635
CuO - Glycerol	40	0.02	6.4	1.24827	5.22449	0.81633	49.9306	40	0.124362	0.19770	0.005	0.0002	0.00003125	2.4501E-06	0.000156	0.127157	0.000635
CuO - Glycerol	10	0.04	6.4	1.26673	10.66667	1.66667	50.6692	40	0.253906	0.40365	0.005	0.0002	0.00003125	4.8E-06	0.000158	0.062281	0.000623
CuO - Glycerol	20	0.04	6.4	1.26061	10.66667	1.66667	50.4244	40	0.253906	0.40365	0.005	0.0002	0.00003125	4.8E-06	0.000158	0.062281	0.000623
CuO - Glycerol	30	0.04	6.4	1.25440	10.66667	1.66667	50.1758	40	0.253906	0.40365	0.005	0.0002	0.00003125	4.8E-06	0.000157	0.062281	0.000622
CuO - Glycerol	40	0.04	6.4	1.24827	10.66667	1.66667	49.9306	40	0.253906	0.40365	0.005	0.0002	0.00003125	4.8E-06	0.000156	0.062281	0.000622

Appendix A: Uncertainty analysis result tables

Nano Fluid Type	T (°c)	ϕ	ρ_p (gr/ml)	ρ_f (gr/ml)	m_p (gr)	V_p (ml)	m_f (gr)	V_f (ml)	m_l (gr)	V_l (ml)	δV (ml)	δm (gr)	δV_p (ml)	$\delta \phi$	$\delta \rho_f$ (gr/ml)	$\delta \rho_l$ (gr/ml)	$\delta \rho_{nf}$ (gr/ml)
CuO - Glycerol	10	0.06	6.4	1.26673	16.34043	2.55319	50.6692	40	0.388963	0.61835	0.005	0.0002	0.00003125	7.05E-06	0.000158	0.040656	0.000610
CuO - Glycerol	20	0.06	6.4	1.26061	16.34043	2.55319	50.4244	40	0.388963	0.61835	0.005	0.0002	0.00003125	7.05E-06	0.000158	0.040656	0.000610
CuO - Glycerol	30	0.06	6.4	1.25440	16.34043	2.55319	50.1758	40	0.388963	0.61835	0.005	0.0002	0.00003125	7.05E-06	0.000157	0.040656	0.000610
CuO - Glycerol	40	0.06	6.4	1.24827	16.34043	2.55319	49.9306	40	0.388963	0.61835	0.005	0.0002	0.00003125	7.05E-06	0.000156	0.040656	0.000610